SYNTHESIS AND CHARACTERIZATION OF
STA INCORPORATED MESOPOROUS MATERIALS AS CATALYSTS FOR
POLYETHYLENE PYROLYSIS

A THESIS SUBMITTED TO
THE GRADUATE SCHOOL OF NATURAL AND APPLIED SCIENCES
OF
MIDDLE EAST TECHNICAL UNIVERSITY

BY

NERİMAN KELEBEK

IN PARTIAL FULFILLMENT OF THE REQUIREMENTS
FOR
THE DEGREE OF MASTER OF SCIENCE
IN
CHEMICAL ENGINEERING

OCTOBER 2013

Approval of the thesis:

**SYNTHESIS AND CHARACTERIZATION OF
STA INCORPORATED MESOPOROUS MATERIALS AS CATALYSTS FOR
POLYETHYLENE PYROLYSIS**

Submitted by **NERİMAN KELEBEK** in partial fulfillment of the requirements for the degree of **Master of Science in Chemical Engineering Department, Middle East Technical University** by,

Prof. Dr. Canan Özgen   _____
Dean, Graduate School of **Natural and Applied Sciences**

Prof. Dr. Deniz Üner   _____
Head of Department, **Chemical Engineering**

Assoc. Prof. Dr. Naime Aslı Sezgi   _____
Supervisor, **Chemical Engineering Dept., METU**

Examining Committee Members:

Prof. Dr. Timur Doğu   _____
Chemical Engineering Dept., METU

Assoc. Prof. Dr. Naime Aslı Sezgi   _____
Chemical Engineering Dept., METU

Prof. Dr. Hayrettin Yücel   _____
Chemical Engineering Dept., METU

Prof. Dr. Göknur Bayram   _____
Chemical Engineering Dept., METU

Prof. Dr. Suna Balcı   _____
Chemical Engineering Dept., Gazi University

Date: 03.10.2013

I hereby declare that all the information in this document has been obtained and presented in accordance with academic rules and ethical conduct. I also declare that, as required by these rules and conduct, I have fully cited and referenced all material and results that are not original to this work.

Name, Last Name : NERİMAN KELEBEK

Signature   :

ABSTRACT

SYNTHESIS AND CHARACTERIZATION OF STA INCORPORATED MESOPOROUS MATERIALS AS CATALYSTS FOR POLYETHYLENE PYROLYSIS

KELEBEK, Neriman
M.Sc., Department of Chemical Engineering
Supervisor: Assoc. Prof. Dr. Naime Aslı SEZGİ

October 2013, 78 pages

Pyrolysis of polymers, which is a process for recovery of the waste polymer, has attracted great attention in recent years due to the high amount of plastic waste present in nature. However, degradation process requires high amount of external energy to break long chain of chemical bonds in the polymer. For this reason, suitable catalysts with strong acid sites are necessary. High surface area silica structured mesoporous materials with narrow pore size distributions are excellent catalysts for these reactions. However, these catalysts are synthesized with the incorporation of appropriate materials because they lack acid sites necessary for the pyrolysis reactions. Heteropoly acids having strong acid sites are good choice to load into these catalysts in order to increase their activity in the pyrolysis reactions.

Silicotungstic acid (STA) loaded MCM-41 catalysts were synthesized hydrothermally at a calcination temperature of 400 °C with the W to Si molar ratio of 0.25 and synthesis solution pH values of 1.2 and 1.4. X-ray diffraction analysis of the sample with pH value of 1.2 showed that this catalyst had an MCM-like structure. According to the nitrogen adsorption-desorption analysis, the synthesized MCM-41 catalysts were in the mesoporous diameter range and the adsorption-desorption branches reflected the typical Type IV isotherms. The surface area of the sample having pH value of 1.2 was 234.08 m^2/g. EDS results of this catalyst revealed that there was a good incorporation of STA into MCM-41 structure. DRIFTS analysis of this catalyst showed the existence of Bronsted acid sites in addition to Lewis acid sites with STA loading.

STA loaded SBA-15 catalyst was synthesized hydrothermally at a calcination temperature of 250 °C with the W to Si molar ratio of 0.1 in highly acidic synthesis solution. X-ray diffraction analysis of this catalyst showed that an ordered silica structure of SBA was obtained. According to the nitrogen adsorption-desorption analysis, the synthesized SBA-15 catalyst was in the mesoporous diameter range and reflected the typical Type IV isotherms. The surface area of this catalyst was 448.49 m^2/g which was higher than that of the synthesized STA loaded MCM-41 catalysts. EDS results of this catalyst showed that there was a low incorporation of STA into SBA-15 structure.

To test the activity of the synthesized catalysts, thermogravimetric analysis was performed under nitrogen atmosphere. Among the synthesized catalysts, STA loaded MCM-41 with pH value of 1.2 and STA incorporated SBA-15 catalysts showed good performance in the polyethylene degradation reaction. These catalysts reduced activation energy and degradation temperature significantly (From 130 kJ/mole to 53.4 kJ/mole and 59.3 kJ/mole, respectively). So the two catalysts were active catalysts for the polyethylene degradation reaction.

ÖZ

POLİETİLEN PİROLİZİ İÇİN KATALİZÖR OLARAK STA İÇERİKLİ MEZOGÖZENEKLİ MALZEMELERİN SENTEZİ VE KARAKTERİZASYONU

KELEBEK, Neriman
Yüksek Lisans, Kimya Mühendisliği Bölümü
Tez Yöneticisi: Doç. Dr. Naime Aslı SEZGİ

Ekim 2013, 78 sayfa

Atık polimerlerin geri dönüşümü için bir proses olan polimerlerin pirolizi, doğada çok miktarda plastik atığın mevcut olmasına bağlı olarak son yıllarda büyük ilgi toplamıştır. Ancak polimerin uzun zincirli kimyasal bağının kırılması için degredasyon prosesi dışarıdan yüksek miktarda enerji gerektirmektedir. Bu nedenle güçlü asit bölgeleri olan uygun katalizörler gereklidir. Yüzey alanı yüksek silika yapılı dar gözenek dağılımlı mezogözenekli malzemeler bu reaksiyonlar için mükemmel katalizörlerdir. Ancak piroliz reaksiyonları için gerekli olan asit bölgelerine sahip olmadıkları için, bu katalizörler uygun malzemelerin yüklenmesiyle sentezlenmektedir. Piroliz reaksiyonlarında katalizörün aktivitesini artırmak amacıyla güçlü asit bölgelerine sahip heteropoliasitler bu katalizörlere yüklemek için iyi bir seçimdir.

Silikatungstik asit (STA) yüklü MCM-41 katalizörleri, 400°C kalsinasyon sıcaklığında, 0,25'lik W/Si mol oranında, 1,2 ve 1,4 sentez çözeltisi pH değerlerinde hidrotermal olarak sentezlenmiştir. pH değeri 1,2 olan STA yüklü MCM-41 katalizörünün X-ışını kırınım analizi, bu katalizörün MCM-benzeri bir yapıya sahip olduğunu göstermiştir. Nitrojen adsorpsiyon-desorpsiyon analizine göre sentezlenen MCM-41 katalizörleri mezogözenek çap aralığındadır ve adsorpsiyon-desorpsiyon branşları karakteristik Tip IV izotermlerini yansıtmıştır. pH değeri 1,2 olan STA yüklü MCM-41 katalizörünün yüzey alanı 234,08 m^2/g'dır. Bu katalizörün EDS analizi, STA'nın MCM-41 yapısına katılımının yüksek olduğunu göstermiştir. DRIFTS analizi, STA eklenmesi ile bu katalizörün Lewis asit bölgelerine ek olarak Bronsted asit bölgeleri olduğunu göstermiştir.

STA yüklü SBA-15 katalizörü, 250 °C kalsinasyon sıcaklığında 0,1'lik W/Si mol oranında yüksek asidik sentez çözeltisinde hidrotermal yöntemle sentezlenmiştir. X-ışını kırınım analizi, STA yüklü SBA-15 malzemesinin düzenli silika yapısına sahip olduğunu göstermiştir. Nitrojen adsorpsiyon-desorpsiyon analiz sonuçlarına göre sentezlenen SBA-15 katalizörü mezogözenek çap aralığındadır ve karakteristik Tip IV izotermini yansıtmıştır. STA yüklü SBA-15 katalizörünün yüzey alanı 448,49 m^2/g olarak bulunmuş olup bu değer sentezlenen STA yüklü MCM-41 katalizörlerindeki yüzey alanı değerlerinden yüksektir. EDS analizi sonucu, STA'nın SBA-15 yapısına katılımının düşük oranda olduğunu göstermiştir.

Sentezlenen katalizörlerin aktivitesini test etmek için azot atmosferi ortamında termogravimetrik analizi gerçekleştirilmiştir. Sentezlenen katalizörler arasında, pH değeri 1,2 olan STA yüklü MCM-41 ve SBA-15 katalizörleri polietilen degradasyon reaksiyonunda iyi performans göstermiştir. Bu katalizörler aktivasyon enerjisi ve degradasyon sıcaklığını önemli ölçüde (130 kJ/mol'den 53,4 kJ/mol'e ve 59,3 kJ/mol'e) düşürmüştür. Bu nedenle, sentezlenen bu iki katalizör polietilen piroliz reaksiyonu için aktif katalizörlerdir.

Anahtar sözcükler: MCM-41, SBA-15, STA, piroliz, polietilen, aktivasyon enerjisi

To my dear family and friends…

ACKNOWLEDGEMENTS

TABLE OF CONTENTS

LIST OF TABLES

TABLES

LIST OF FIGURES

FIGURES

LIST OF SYMBOLS

A	Preexponential factor (min^{-1})
E	Activation energy of the reaction (kJ/mol)
n_i	Number of mole of component i
R	Gas constant (J/mol.K)
Si	Silica
Al	Aluminum
t	Time (min)
T	Temperature (K)
W	Tungsten
w	Weight (g)

Abbreviations

BET	Brunauer-Emmet-Teller
BJH	Barret-Joyner-Harrenda
DTA	Differential thermal analyis
EDS	Energy dispersive spectroscopy
EPA	US Environment Protection Agency
ETBE	Ethyl tert-buthylether
FSM-16	Folded sheet mesoporous silica
GC	Gas chromatograph
HDPE	High density polyethylene
HPA	Heteropoly acid
HSM	High silica modified material
HZSM-5	High silica modified zeolite
IUPAC	International Union of Pure and Applied Sciences
LCT	Liquid crystal templating mechanism
MCM-41	Mobile composition of matter
MPA	Molybdophophoric acid
MSU	Molecular sieve ultrastable catalyst
PE	Polyethylene
PP	Polypropylene
PS	Polystyrene
PMMA	Polymethylmetacrylate
STA	Silicotungstic acid
SAHA	Amorphous silica alumina
SBA-15	Santa Barbara amorphous type material
SEM	Scanning electron microscope
TEM	Transmission electron microscope
TPA	Tungstophosphoric acid
HUSY	Highly ultrastable Y zeolite
XRD	X-ray diffraction

CHAPTER 1

INTRODUCTION

Throughout the world plastic materials have been commonly preferred to be used in various industrial applications for a long time. The world's annual plastic material consumption has grown dramatically from around 5 million tonnes up to 100 million tonnes since 1950s [1]. This considerable increase in plastic use is mostly due to their properties like being lightweight, durable, resistant to chemicals and etc. [1]. Also they have a large range of usage area, low price, industrially high production capacity and simple processing properties. However, there is a major drawback of this common usage of plastic materials. This major drawback which makes the world suffer from it for years is the environmental pollution problem. Because of their structure, most of the plastics are not biologically degradable in nature and this situation leads to the accumulation of the plastic waste dramatically in nature. Deficiency for the control of this plastic waste triggers the increase of this plastic waste. On the other hand, some temporary solution methods for destroying plastic waste are generated. One of these solution methods is the incineration of plastic waste. In the incineration method, plastic waste can be destroyed up to a limit but it converts the environmental pollution problem to another form of it because highly toxic and hazardous burning products are emitted to the atmosphere with this method. One of the other solution methods is the landfilling of plastic waste. In the landfilling method, plastic waste is buried into the soil, so the waste can be destroyed but it also has a major drawback that the size of landfilling areas has become very limited day by day. It is not possible to exactly destroy the plastic waste without any harm to environment or livings with these solution methods. Because of these reasons, temporary solutions are not fully satisfactory, so a more permanent and useful way of destroying plastic waste has been generated to overcome most of the drawbacks. This permanent solution way is called as the "pyrolysis of plastic waste".

In the pyrolysis process, plastic materials decompose thermally up to their pyrolysis reaction products under inert atmospheric condition. In this process, the chemical bonds in the structure of the long-chained huge polymer need to be broken and the energy to break these bonds is provided by external heat. Aromatic organic compounds and olefins are obtained as pyrolysis products.

The pyrolysis process also has some drawbacks but it is possible to overcome these drawbacks with some suitable solution methods. One of the drawbacks is that, as it is a chemical degradation process, high energy is consumed during pyrolysis reaction so pyrolysis reaction requires high amount of activation energy. Another drawback is that the pyrolysis products may not have the required or desired properties, i.e. they may be in an extended carbon number interval, which means that the desired products may not be present in this obtained range specifically. On the other hand, the pyrolysis reaction activation energy can be decreased and the product distribution can be controlled by using suitable catalysts in the pyrolysis reaction.

Through studies done on pyrolysis, different solid catalysts have been used in the pyrolysis reaction. Solid catalysts are grouped as microporous, mesoporous and macroporous materials according to the size of their pore diameter. The functionality of the catalyst is one of the

most crutial parameters in the pyrolysis reaction for detecting the performance and suitability of the catalyst for the reaction. The reason of it is that if the material to be catalyzed is in a big size, it is difficult for it to pass from the pores of the catalyst and also it is difficult for the reaction to take place. In microporous catalysts, as polymeric materials are in big size, the catalysts either lose efficiency when these materials pass from the pores of the catalyst or the big size polymer can not pass from the active site of the catalyst and therefore no reaction takes place. Most studies on polymer pyrolysis reaction have been held using mesoporous catalysts because they have a high suitability for these kinds of reaction [2]. Among mesoporous solid catalysts the most two popular ones, which are Mobile Composition of Matter (MCM-41) and Santa Barbara amorphous type material (SBA-15) were selected to be synthesized and to be used in the pyrolysis reactions. These mesoporous catalysts have low catalytic activity themselves because they lack of suitable acid sites that are necessary for this reaction. In order to eliminate this inconsistency, heteropoly acids are incorporated into the structure of these catalysts because heteropoly acids generally have high acidic character to activate the catalyst in an extended manner. Among heteropoly acids, silicotungstic acid (STA) was selected as the incorporated heteropoly acid because of its high acidic property.

This study includes the hydrothermal synthesis of STA incorporated MCM-41 and SBA-15 catalysts, the characterization of these catalysts, the activity test of these cataysts in the polyethylene pyrolysis reaction using the thermal gravimetric analyser and determination of the kinetic parameters for the PE degradation reaction.

CHAPTER 2

POLYMERS

The word *polymer* is derived from two terms: *poly* has a meaning of *many* and *mer* is the abbreviation of the word *monomer* [1]. A polymer is a substance that is formed by the repetition of small and simple chemical units. In order to form three dimensional networks, the repetition of the chemical units can be linear, branched or interconnected. The repeating unit of the polymer is generally equivalent to the monomer or the starting material from which the polymer is formed. There are long sequences of one or more types of atoms or atom groups that are connected to each other in the structure of a polymer. The term plastic is used to describe a wide range of synthetic macromolecules so the words *polymer*, *plastic* and *macromolecule* can be used interchangeably [2, 3].

2.1 A Brief History of Polymers

Synthetic polymers or plastics were first discovered at the end of the 19th century. Natural materials that are based on cellulose were modified and plastics were obtained at that time. For example, cellulose nitrate was discovered and mostly used in the production of early movie films. In the 20th century, the atomic molecular nature of the matter was investigated in detail. At that time, Staudinger proved that plastics were made up of large single molecules and studies on plastics had developed faster based on this proof [1, 4].

Polystyrene and polyvinylchloride were developed by Interessen-Gemeinschaft (IG) Farben Industrie AG chemical company in Germany after the First World War. In 1930s, Wallace Carruthers created a synthetic plastic, which is nylon, by the chemical reaction of smaller molecules. The production of plastics had been grown increasingly by the broad diversity of materials which were used commonly in everyday life. The synthetic nylon fibre had been rapidly replaced with natural bristles by the time. By 1936 polymethylmethacrylate was produced to replace glass. Plexiglas was used during the Second World War to build aircraft canopies [1].
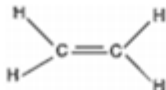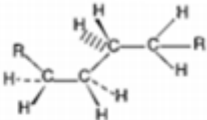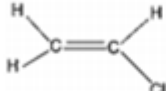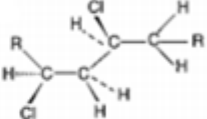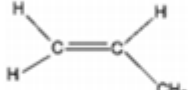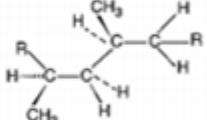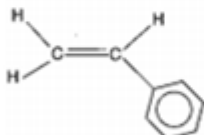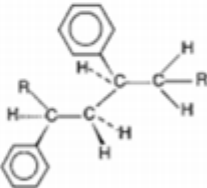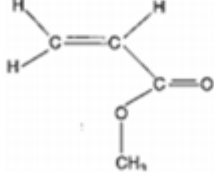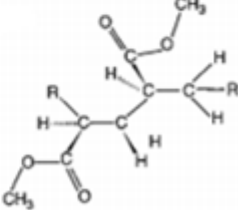
Polyethylene was discovered in 1933 by Gibson and Fawcett at Imperial Chemical Industries in England in which ethylene was subjected to 1400 atm of pressure at 170 °C [2]. Polyethyleneteraphthalate was developed by Whinfield and Dickson in 1941. Polypropylene was discovered in 1950s by Zeigler and Natta. Polycarbonate was developed by General Electric company in the 1970s [1, 5].

2.2 Properties and Usage of Polymers

Polymers can be rigid, flexible, brittle or elastic. Unlike metals and ceramics, change of temperature can convert a brittle rigid plastic into a soft and extensible elastomer. Polymers are based on linking molecules that have carbon-carbon bonded structure. They can be classified according to their physical and chemical properties (configuration, molar mass, thermoplastic, crystalline and condensation properties etc.) [1].

Polymers are formed by polymerization which is a process of linking monomer molecules together via chemical reactions. For example polyethylene, which is a typical polymer containing 50000 carbon atoms linked together, is formed by the polymerization of ethylene monomer units. This long chain makes polymers different from other materials and gives them characteristic properties [3]. Common polymers with their monomer units and chemical structures are given in *Table 2.1*.

Table 2.1 Polymers with their monomer units and chemical structures [1]

Monomer	Structure	Polymer	Structure
Ethylene (Ethane)		Polyethylene	
Vinyl chloride (Chloroethane)		Polyvinylchloride	
Propylene (Propene)		Polypropylene	
Styrene (Phenylethene)		Polystyrene	
Methacrylate		Polymethacrylate	

Polymers are utilized in a wide range of applications. The usage area of the polymers in the world industry can be seen in *Table 2.2*. They are mostly used in packaging [1].

Table 2.2 Usage area of polymers in the world industry **[1]**

Product area	Use %	Product area	Use %
Packaging	35	Footwear	1
Medical	2	Toys & sport	3
Building & construction	23	Electronics	8
Transport	8	Agriculture	7
Engineering	2	Other	11

Commonly used plastic materials are polyethylene (PE), polypropylene (PP), polystyrene (PS), polyvinyl chloride (PVC), polycarbonate, and nylon. PE is the most common polymer over all plastic materials. Plastic merchandises annual consumption of polyethylene in industrialized countries currently exceeds 100 kg/person **[2, 6]**.

2.3 Polyethylene

Polyethylene is a polymer formed by the polymerization of ethylene monomer units **[1]**. It is a thermoplastic polymer which softens and flows when it is heated and which hardens when it is cooled **[7]**. It has a very simple chemical structure which is $-(CH_2 - CH_2)_n -$. The backbone of the polymer is made up of carbon atoms connected in a linear fashion and it resembles a piece of string **[1]**.

2.3.1 Structure and Properties of Polyethylene

The ethylene has a sigma (σ) or single bond which connects the hydrogen atoms to the carbon atoms and the two carbon atoms each other. The sigma bond is a very strong bond so it is required to heat up the molecule to several hundred temperature degrees in order to break this bond **[1]**.

Polymerization process simply has three steps: Initiation step is the generation of free radicals, propogation is the growth of the polymer chains by addition of monomers to the free radical active centre and termination is the process where free radical centre is destroyed and converted into a stable entity **[1]**. Schematic diagram for polymerization process of ethylene can be seen in *Figure 2.1*.
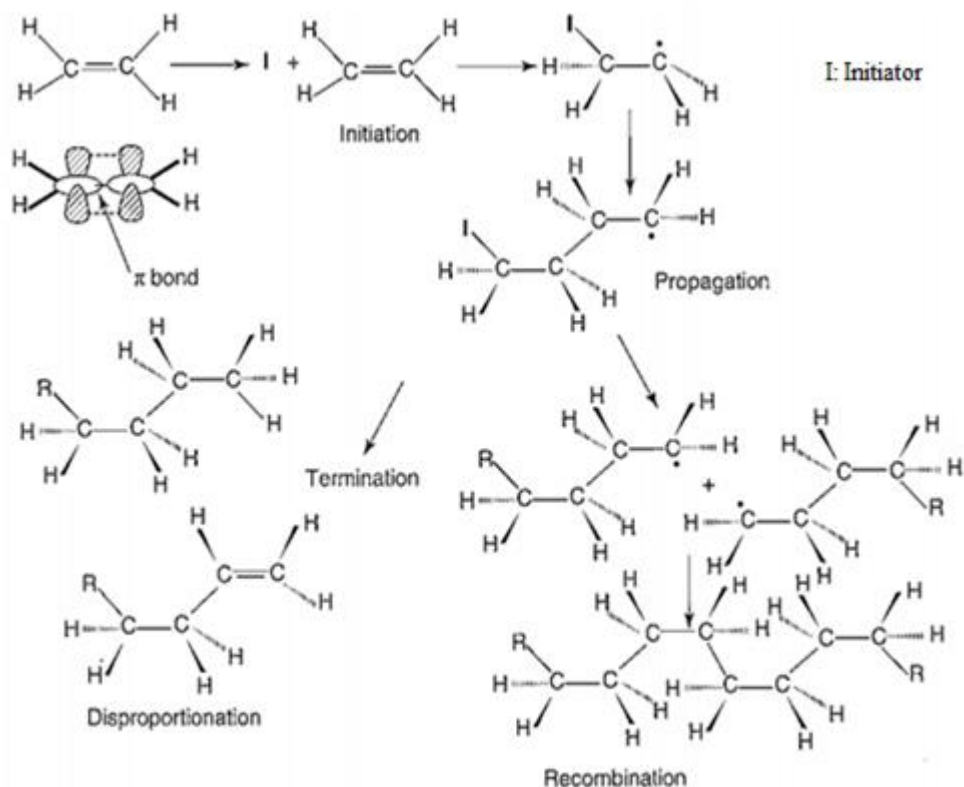
Figure 2.1 Schematic diagram for polymerization process of polyethylene [1]

It is desirable to be able to control the structure of a polymer and hence instead of allowing the polymerization to produce side chains in a random manner, it may be appropriate to add monomers such as 1-butene, 1-hexene or higher 1-alkenes to the reaction mixture and hence produce a more controlled polymer. Other than stereochemical control, the length of the chain, molar mass and block copolymer coordination can be controlled [1, 2].

Ethylene (boiling point; -104 °C) can be obtained from the dehydration of ethanol or by the hydrogenation of acetylene. In places where supplies of natural or petroleum gas are available, monomer is produced by cracking ethane or propane followed by purification process. Polyethylene containing high number of ethylene monomer units is commercially made at pressures between 1000 and 3000 atm or even higher pressures and temperatures at 250 °C [2].

2.3.2 Classification of Polyethylene Structure

Polyethylene is classified according to its density, brancing, and molecular weight. The types of polyethylene are listed below [1, 2]:

- High density (HDPE)
- Linear low density (LLDPE)
- Low density (LDPE)
- Medium density (MDPE)

- Very low density (VLDPE)
- Cross linked (PEX or XLPE)
- High density cross linked (HDXLPE)
- Ultra high molecular weight (UHMWPE)
- High molecular weight (HMWPE)
- Ultra low molecular weight (ULMWPE or PEWAX)
- Chlorinated polyethylene (CPE)

Low density and high density polyethylene has the highest demand over all plastics consumed in the world, which is 34 % of total plastics [4].

2.3.2.1 High density polyethylene (HDPE)

It is a type of polyethylene having high linear content, high degree of crystallinity and density, so it is known as high density polyethylene. As the branched chain content is increased, the density of the polymer is decreased and the product is termed as low density polyethylene [1].

Melting point of HDPE is typically about 135 °C and its density range is 0.95-0.97 g/cm^3. Most of the differences in properties between branced and linear polyethylenes can be related to the higher crystallinity feature of the linear polyethylene. Linear PE has a higher crystalline melting point, greater tensile strength and hardness [2].

40 % of the HDPE is utilized in the production of bottles and other containers. 20 % of it is utilized in housewares and toys and the rest is used in various applications such as film and sheet, wire and cable insulation, extrusion coating and pipe [2].

2.3.2.2 Linear low density polyethylene (LLDPE)

The density of LLDPE is between 0.915-0.925 g/cm^3. It is a linear polymer with a number of short branches which are created by copolymerization of ethylene with short chain alpha olefins. The tensile strength of LLDPE is higher compared to LDPE. Also it exhibits higher films compared to multilayer and composite films [1].

2.3.2.3 Low density polyethylene (LDPE)

Low density (branced) PE was the first commercial polymer of ethylene. LDPE is a partially crystalline solid which melts at about 115 °C and its density is between 0.91-0.94 g/cm^3. It is soluble in a wide range of solvents at temperatures higher than 100 °C. Low density polyethylene contains branched chains. This branching has an observable effect on the solution viscosity of the polymer and can be detected by comparing the viscosity of a branched polyethylene with that of a linear polymer with the same molecular weight [2].

There are various areas that LDPE is applied in industry. Almost half of the LDPE produced is used in film and sheeting applications, 13 % of it is utilized in the production of housewares, 10 % of it is used in wire and cable insulation, 10 % of it is utilized in coating and the rest is used in different areas [2].

2.4 Polypropylene

Polypropylene (PP) is the lightest plastic with a density of 0.905 g/cm^3. It has high crystalline structure, tensile strength, stiffness and hardness. Its high melting point allows polymer to retain its high tensile strength at elevated temperatures. To overcome its brittleness problem, polypropylene is commonly formed with both random and block copolymers of propylene and ethylene. To retain transparency, random copolymers are used in film applications while homopolymer is almost exclusively utilized for filaments. It has very good electrical properties, moisture resistance and chemical inertness. It is completely free from environmental stress cracking [2].

Half of the polypropylene is used in automotive and its appliance fields. Rest of it is used as a filament in rope, cordage, webbing and carpeting [2].

2.5 Polystyrene

Polystyrene (PS) is a clear, transparent, easily colored and fabricated thermoplastic. It has good mechanical and thermal properties, but it is brittle and it softens below 100 °C. It is a linear polymer in amorphous structure. It is outstandingly easy to process and it is a good electrical insulator.

60 % of it is used in packaging including films, foams and appliances, 10 % of it is utilized in housewares and toys, 5% of it is used in home furnishing, construction materials and the rest is applied in other similar areas [2].

CHAPTER 3

PYROLYSIS OF POLYMERS

Common usage of plastics leaves severe amount of plastic waste behind which brings the environmental pollution problem, so disposal of waste plastics becomes an important issue. However disposal of waste plastics constitutes a critical problem in nature because of the reason that most plastics are not biodegradable. In order to overcome this problem, several methods for the disposal of plastic waste have been developed **[8, 9]**.

3.1 Disposal Methods of Polymer Waste

There is a deficiency for the effective control of plastic waste accumulation in nature because of several reasons mentioned previously. In order to overcome the plastic waste accumulation problem, some solution methods are generated. They can be listed as incineration, landfilling and recycling **[10]**.

Incineration is a waste treatment process. It involves the combustion of organic materials present in the waste. With this process the waste plastics are converted into ash and flue gas. Incineration process of plastic waste does not have much acceptance for the disposal of plastic waste because of the emissions of greenhouse gases, discharges of ashes etc. Also population generally has negative opinion for construction of incinerators near residental areas. This approach just converts the solid waste problem to the air pollution problem. Also this is an expensive process **[10-12]**.

The other solution method is landfilling of plastic waste. Landfilling means burying the plastic waste into the soil. It is the oldest form of waste treatment. By this method plastic waste can be destroyed but it is not a good solution method because of the decrease in landfilling site availability. Also the energy content of the plastic is lost with landfilling method. This situation also creates a huge economic waste [**11-13**].

Recycling of plastic material can be done either chemically or mechanically. Mechanical recycling of plastic material is done by mechanical reprocessing method. Mechanical reprocessing is the simplest and relatively cheap method. By this method the waste material undergoes some mechanical processes in order to convert the waste material to the other products. This is generally not a preferred method because of the low quality of the new products **[13]**. Chemical recycling of plastic material is done using pyrolysis method which is mentioned in detail in Section 3.3.

3.2 Biodegradable Plastics

The concept of a plastic which disappears as a consequence of biodegradation process is very attractive. Most hydrocarbon-based polymers, polyethylene, polystyrene, etc. are not subject to biological attack. According to The American Society for Testing of Materials (ASTM) and The International Standards Organisation (ISO) definition, degradable plastics are the plastics that exhibit important difference in chemical structures when specific environmental conditions are provided. Biodegradable plastics are kind of plastics which are

degraded by the action of natural microorganisms like bacteria, fungi etc. The polymer matrix of biodegradable plastics is extracted from natural sources like starch. Microorganisms are capable of consuming these materials up to inorganic materials like carbondioxide and water [1, 5].

Microbial action, photodegradation or chemical degradation are the methods for breakdown of polymer materials. Microbial breakdown of biopolymers involves growing microorganisms for the purpose of digesting polymer materials. Those are targeted microorganisms which specifically degrade petroleum based plastics. Photodegradable polymers undergo degradation by sunlight. Polymers are attacked by the effect of sunlight and broken down into small pieces. In order to achieve a fully degradation, microbial degradation must follow photodegradation. Some biodegradable polymers undergo a rapid dissolution when they are exposed to chemical based particular aqueous solutions. As in photodegradation case, fully biodegradation is provided by further microbial digestion [1, 5].

According to a 2010 US Environmental Protection Agency (EPA) report, the amount of municipal solid waste was 12.4 % or 31 million tons of plastics in US. Only 8.2 % of this ratio or 2.55 million tons of it was recovered. This value was very low compared to that of the total average recovery percentage of all kind of waste which was 34.1 [8].

There are concerns about the use of biodegradable plastics. One of the major concerns is that these plastics only degrade if they are exposed to light, hence burial in landfill sites, where there is no light, does not represent an acceptable method of disposal. The other major concern is that the anaerobic biodegradation will lead to methane production which is a greenhouse and potentially explosive gas [1, 8].

3.3 Pyrolysis

Pyrolysis is the thermochemically decomposition of materials by applying heat without participation of oxygen under inert atmospheric conditions. It is a method for obtaining energy from plastic wastes which is based on the principle that most of the organic materials are thermally unstable and they can be decomposed in an atmosphere free from oxygen. So this method, pyrolysis, has drawn much attention because of the reason that it has been accepted as an environmentally sensitive and friendly method compared to the ordinary solution methods. Moreover, waste plastics can be turned into valuable solid, liquid and gas products by pyrolysis [12, 14]. Plastics are also transformed into fuel like products by this method. It is an endothermic process requiring high amount of energy but it is also a suitable process for waste plastic treatment, because fuel like products which are obtained from plastic wastes have high energy content [14]. In pyrolysis, the selectivity of the product can be controlled using catalysts with controlled temperature, pressure and atmospheric conditions [15].

Pyrolysis process can be done catalytically or non-catalytically. Heat is both used in the non-catalytic and catalytic pyrolysis. The non-catalytic and catalytic pyrolysis of plastic waste gives gas and liquid products. These products can be used as fuel oils or other advanced chemicals with further applications [13].

The non-catalytic or catalytic pyrolysis of waste plastics has drawn much attention as a favorable technique for waste substance utilization. It is also appraised as an additional source of clean fuels [13].

3.3.1 The Non-Catalytic Pyrolysis

The non-catalytic pyrolysis is a type of pyrolysis in which no catalyst is used in the process. In this process, pyrolysis of polymer is carried out by applying heat. The type of the plastic plays an important role for this process which determines the recycled material. Polymers like PET and nylon, which are classified as the condensation polymers, can be turned into their monomer units by using various depolymerization techniques. However, for polyethylene and polypropylene, which are classified as the vinyl polymers, it is very difficult to be degrade up to their monomer units because of random splitting of carbon bonds in the long polymer chains. This process outcomes a wide product variety, requiring high operating temperatures, such as from 500 ºC and even up to 900 ºC. This means high energy input and low selectivity of product. Further processing is required for their quality to be upgraded **[11, 13]**.

Main steps in polyethylene pyrolysis reactions are initiation, propagation and termination. In initiation step, free radicals and molecules are generated in order to react with each other. These radicals can be generated either by the abstraction of a hydrogen atom attached to the backbone or by cleavage of backbone, which are called as random or chain end reactions. In propagation step, intermediate reactions which are scission of free radicals produced in initiation reactions take place. The products of propagation reactions are mainly alkene molecules and smaller free radicals. In termination step, polymer chain is fully unzipped and free radicals are converted to the monomers **[1]**. The pyrolysis scheme of polyethylene is shown in *Figure 3.1*.
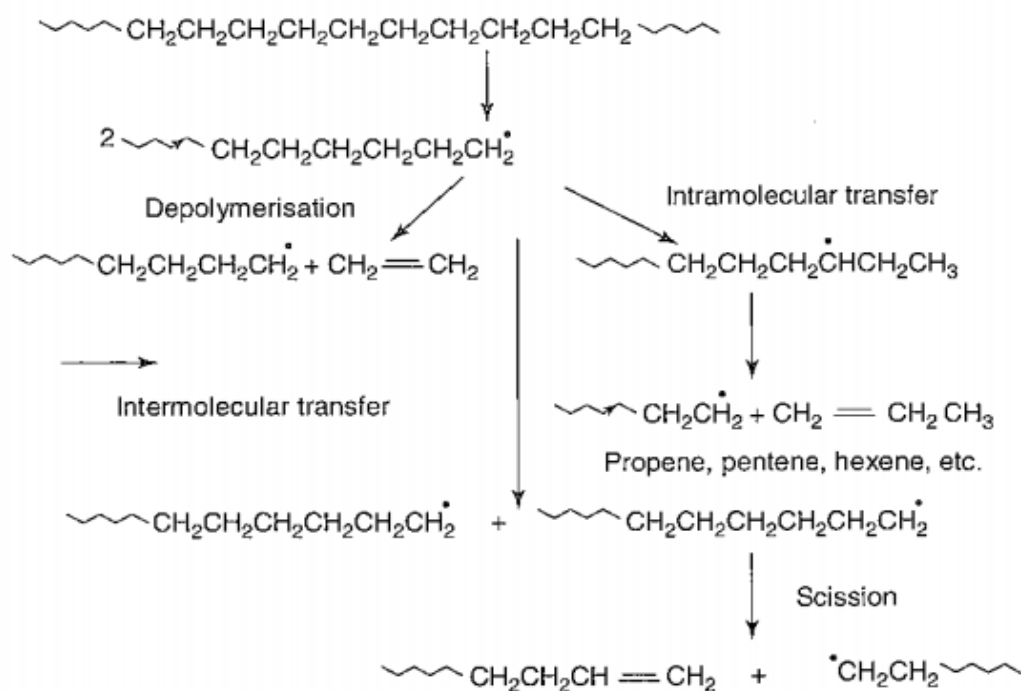
Figure 3.1 Pyrolysis steps of polyethylene

3.3.2 The Catalytic Pyrolysis

The catalytic pyrolysis is the decomposition of the polymeric material using suitable catalyst in the reaction. It is possible to enhance the product selectivity of the process and to decrease its energy input in the catalytic pyrolysis [12]. The non-catalytic pyrolysis usually gives liquid products as a mixture of hydrocarbons with a wide range of carbon number (C6–C25) while the use of catalyst narrows the range of carbon numbers which eliminates the necessity of further processing [10, 16]. Gaseous products are also useful because burning of gas products may supply the energy need of an endothermic cracking process. On the other hand, production of excess gas is undesired. Gaseous products are qualified as low value products due to the transportation costs. As a result, the aim of a commercially significant recycling process is considered as the enhancement in the liquid product yield. Commonly, zeolite based catalysts like silica alumina, clay based materials and MCM type catalysts have been used for these kind of reactions [16]. Lower energy is consumed in the catalytic pyrolysis of plastics (T from 350 °C to 550 °C) compared to the non-catalytic pyrolysis. Also, the chemical distribution of the products in catalytic pyrolysis has a narrower carbon number range compared to the non-catalytic pyrolysis. This means production of more valuable products or higher possibility of attaining desired products [17].

In the catalytic pyrolysis process, generally solid acid catalysts are used. Pore size of solid catalyst can be microporous, mesoporous or macroporous. For the catalytic pyrolysis of plastic materials, due to being more advantageous compared to microporous and macroporous materials, mesoporous catalysts generally have been used.

CHAPTER 4

MESOPOROUS CATALYSTS AND HETEROPOLY ACIDS

Pore diameters of solid materials are classified in three categories according International Union of Pure and Applied Chemistry (IUPAC) classification. Materials having pore diameters larger than 50 nm are categorized as macroporous, the ones having pore diameters between 2 nm to 50 nm are classified as mesoporous and the ones with pore diameters less than 2 nm are called as microporous materials [10]. Pore size distribution scheme for some materials can be seen in *Figure 4.1*.
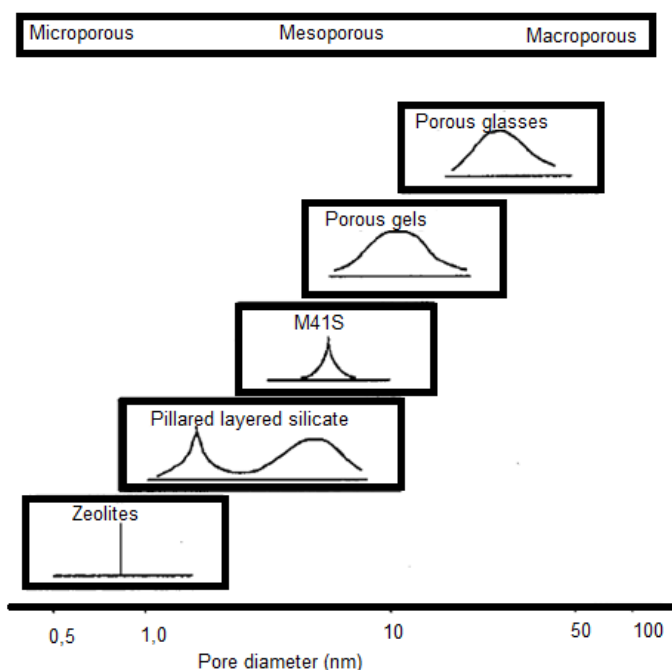
Figure 4.1 Pore size distributions for different types of porous silica materials [18]

The structural property of a catalyst affects the performance and functionality of the catalyst. For that reason, the size and shape of the catalyst are very important parameters. For example, suitable catalysts should be used for polymer reactions, because polymers are huge molecules and when they interact with catalyst they have to access the active sites of the catalyst. It is difficult for large molecules to access into the micropores of catalysts like zeolites. Although zeolites have highly attractive catalytical properties, they have some restrictions because of their pore diameter range. Small pore diameter of them limits the activity of catalyst in some applications because molecules having large sizes loose efficiency when passing inside the active sites of the zeolites. Furthermore, there are some cations inside the structure of the zeolites which may hinder the pore openings in some cases and restricts the rate of reactions [19]. Also because of coke formation, which is deposited

inside the small pores of the zeolite, the normal diffusion rate of reactants and products from the catalyst may decrease [20, 21]. So zeolites can not be applied to reactions where the size of the reactants is greater than the dimensions of the microporous zeolites. Therefore, as an optimum approach in order to overcome the limitation of zeolites, the porous structure of them would stay as the same and the diameter of them would increase towards to the mesoporous region. Most of the organic templates which are used for synthesizing zeolites involve gel formation and they function as gap fillers in the enlarging porous solids. As a result, scientists attempt to find out larger organic templates to attain larger voids in the synthesized molecular sieves. Larger molecules can be catalyzed with the presence of mesopores in these types of materials [22].

Amorphous silica alumina has a mesoporous pore size distribution as it is addressed in the literature. It has a narrow pore size distribution and its catalytic properties are also similar with zeolites. However, this material doesn't have a uniform pore size distribution which affects the selectivity of the catalyst. Consequently, some researchers attempted to synthesize mesoporous materials having a uniform pore size distribution [22, 23].

Mesoporous materials are very likely to be appropriate catalysts especially for waste polymer degradation due to their large pore diameters compared to microporous ones. On the other hand, these materials have very low acidity properties. One of the most important parameters for a cracking process is the presence of the acidic centres in the catalyst. Protonic acidic undertake the role of catalyse the hydrocarbon cracking reaction.[10].

High silica modified (HSM) and molecular sieve ultrastable (MSU) family catalysts have also been classified as mesoporous. These catalysts possess randomly distributed mesopores. They are synthesized at highly acidic and highly basic media conditions. A mesoporous structure is also synthesized by folding kanemite layers and merging them together to form a hexagonal structure. This structure is called as folded sheet mesoporous silica (FSM-16) and because of the advantage of its high surface area, a lot of studies have been done on this catalyst [24-26].

A novel family of mesoporous silica molecular sieves by liquid crystal templates is considered as a significant discovery by Mobil Researchers which is named as M41S. The materials in this family are mesoporous and have uniform channels [27]. This family has three main members which are abbreviated as MCM (Mobil Composition of Matter). One of them is MCM-41, having one dimensional hexagonal array of uniform mesopores, another one is MCM-48, having three dimensional cubic channels, the third one is MCM-50, having uniform lamellar phases [22, 24, 28]. The name of the MCM catalyst changes according to its dimensional structure. These mesoporous materials have high surface area values, above 700 m^2/g, which makes them have a high potential in catalytic applications [23].

Other than the M41S family, mesoporous structures in Santa Barbara Amorphous (SBA) family are synthesized in acidic media which are named as SBA-1, SBA-2, SBA-3, SBA-11, SBA-15 and SBA-16 [24-26]. The most studied catalyst among this family is SBA-15. Similar to the MCM-41 structure, SBA-15 basically has a unidirectional hexagonal pore system. The major difference is due to the dimensions of the pores and pore walls. A typical SBA-15 structure has an average pore diameter of 6 nm and amorphous pore walls of 3 nm thickness. There are micropores in the pore walls of SBA-15 materials which makes this class of material having an interesting feature [24, 25, 29].

4.1 MCM-41

Due to its consistent and promising structural properties, MCM-41 is one of the most studied structures throughout the literature. It consists of an amorphous silica structure, forming hexagonal pores. MCM-41 structure has a unidirectional honeycomb structure [24, 28]. MCM-41 structure can be seen in *Figure 4.2*.
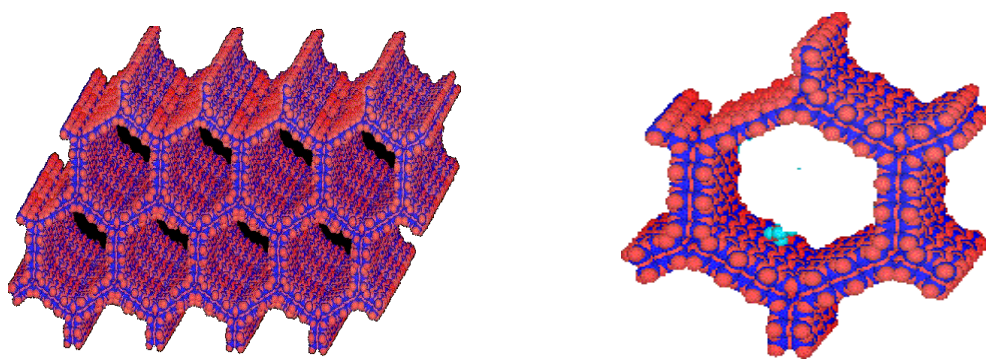
Figure 4.2 MCM-41 structural view [30, 31]

In the hexagonal MCM-41 structure, there are siloxane bridges in the corners of the pores. These bridges assist to constitute hydrophobic portions on the pore surface. On the other hand, the flat areas of the pore surface have hydrophilic properties because of the hydroxyl groups present in this part [25].

Selecting optimum conditions, the channel dimension of the catalyst can be arranged in the range of 15-100 Å or even larger. But this time, the uniformity of the structure can be counterly affected. The BET surface area of this catalyst can be attained at high values, over 1000 m^2/g [27]. It also has a high adsorption capacity which is more than 50 wt % for cyclohexane and 67 wt % for benzene at 40 and 50 Torr, respectively. Moreover, the thermal and hydrothermal stability of MCM-41 is very high which can go up to 800 °C. At acidic medium (for pH around 2), it shows relatively stable characteristics compared to basic medium [32, 33]. It can also be synthesized in basic media; however its structure can be destroyed for pH values greater than 12. The silica framework of MCM-41itself shows catalytically low activity. So, the acidic properties of it are enhanced by different methods. One of them is the isomorphous substitution of silicon with different metals like Al, Ga, Fe [34]. Another one is to incorporate suitable heteropoly acids into the structure of the catalyst, like STA, TPA, and MPA.

4.1.1 Formation Mechanisms of MCM-41

For the synthesis of the mesoporous materials, a silica source around an organic template in an aqueous solvent is polymerized. The organic template is removed by calcination which is necessary for clearing the pores. However, synthesis parameters affect the interaction between the organic template molecules and the silica framework. Also Mobil researchers claimed that the final pore structure of the catalyst is influenced by the concentrations of the

components in the synthesis solution **[27]**.In order to obtain the desired structure, those parameters are needed to be understood well and controlled accordingly **[22, 25]**.

The electrostatic interaction between surfactants and silica species has the role of being a basis for the formation of the organic-inorganic composite material. The surfactant has positive charge and silica species have negative charge on it, constituting a high level of electrostatic interaction. The first mechanism proposed in the literature for the MCM-41 synthesis was defined by Beck et al. The name of the MCM-41 formation mechanism was liquid crystal templating mechanism (LCT). Beck et al. suggested that the the liquid crystals acted as templates for the MCM-41 formation mechanism and in this process, the surfactant molecules were coordinated into these liquid crystals. According to the suggested mechanism, first of all inorganic silica species condensed with organic surfactant which lead to the formation of micellar rods. After that, micellar rods were encapsulated into 2-3 monolayers of silica. Subsequently hexagonal arrays of rods were formed by the incorporation of inorganic array of silica around the rod-like structures. Finally, mesoporous MCM-41 was obtained through the removal of surfactant from the structure. This might proceed via calcination or via solvent extraction **[23, 27, 35]**. Formation mechanism of this catalyst is given in *Figure 4.3*.
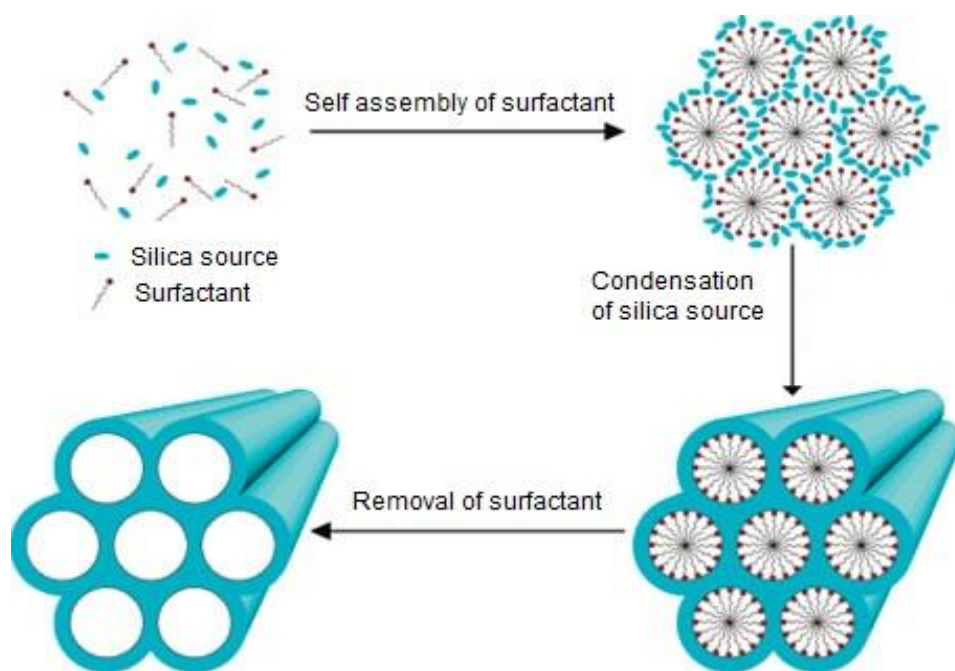
Figure 4.3 Formation mechanism of MCM-41 **[36]**

Beck et al. also proposed an alternative pathway for the formation of MCM-41. It is called silica anion initiated mechanism and in this mechanism cationic surfactant molecules combine with anionic silica species to form a supermolecular structure **[27].**

4.1.2 Components of the MCM-41 Synthesis

There are four main components in the synthesis of MCM-41 which are silica source, surfactant, solvent and mineralizing agent (acid or base) [22].

Commonly used silica sources in the synthesis of mesoporous materials are sodium silica (Na_4O_4Si), sodium meta-silica (Na_2SiO_3), fumed silica, ludox, silica gel and tetraethyl orthosilicate (TEOS). For the acidic media, TEOS is generally used whereas for the basic media, the other silica sources are commonly used [22].

The surfactant term is derived from the expression "surface active agent". The surfactant molecules have polar and non polar parts. The polar part (hydrophilic) is expressed as the dipole or charged group and the non polar part (hydrophobic) generally has a halocarbon or hydrocarbon chain [37]. Ionic surfactants such as cetyltrimethylammonium chloride (CTMACl) and cetyltrimethylammonium bromide (CTMABr) are the most commonly used templating agents for the synthesis of MCM-41. In general, low-molecular weight amphiphiles having the formula $C_nH_{2n+1}(CH_3)_3N^+$ (n=8-22) or $C_nH_{2n+1}C_5H_5N^+$ (n=12 or 16) are used in the formation of MCM-41. Poly (ethylene oxide) is also used as a surfactant for the synthesis of ordered mesoporous materials in literature [37].

In the synthesis of MCM-41, water is used as the solvent. The amount of water used in the synthesis mixture is a critical parameter because it determines the properties of the surfactant and silica mixture formed during synthesis procedure. If the amount of water is very high, it makes difficult to produce a gel during synthesis because of the weak interaction between surfactant and silica molecules, whereas if the amount of water is very low, precipitation of the MCM-41crystals becomes difficult because of the low motion capability of the molecules [37].

The mineralizing agent, which can be acid or base, transforms the silica sources into soluble species with suitable morphologies. For example sodium hydroxide, tetramethylammonium hydroxide or tetraethylammonium hydroxide can be used as basic agent and HCl, HF or HNO_3 can be used as acidic agent [22, 37].

4.2 SBA-15

SBA-15 is a highly ordered, hexagonal structure belonging to Santa Barbara Amorphous type materials family. It is a mesostructured material whose pore wall size changes from 30 to 60 Å and pore diameter from 5 to 9 nm. It is a polymer templated silica structure having thick pore walls which provide high thermal and hydrothermal stability. Also it has interconnecting microporous channels which help binding hexagonal mesopores together. These microporous interconnecting channel provide effective diffusion properties for the reactions compared to the most of mesoporous catalysts [38, 39].

The synthesis of this catalyst was carried out using a triblock copolymer polyethylene oxide-polypropylene oxide-polyethylene oxide. It is a templating agent for the acidic media [39]. If the copolymer weight ratio is higher than 6 %, the final product consists of silica gel, whereas if the copolymer weight ratio is lower than 0.5%, the final product becomes amorphous silica [38]. The synthesis solution of SBA-15 was generally prepared between temperatures of 35 °C to 100 °C. It is not possible to produce SBA-15 below and above this temperature range. Below this range at room temperature amorphous silica powder or poorly

ordered materials could be obtained. Above this range, only silica gel could be produced. A typical SBA-15 was synthesized at 100 °C and calcined at 550 °C. Also type of silica source affected the final product. For SBA-15 synthesis, tetraethoxysilane (TEOS), tetramethoxysilane (TMOS) and tetrapropoxysilane (TPOS) could be used as silica sources [38, 40, 41].

The pH of the synthesis solution is another critical parameter to be adjusted because a highly acidic media is required for the synthesis. To obtain a suitable pH value which is lower than 1 to maintain an acidic medium, strong acids like HCl, HBr, HI, HNO_3, H_2SO_4, H_3PO_3 can be used [41].

Formation mechanism of SBA-15 material can be seen from *Figure 4.4.* Its mechanism is similar to MCM-41 formation mechanism.
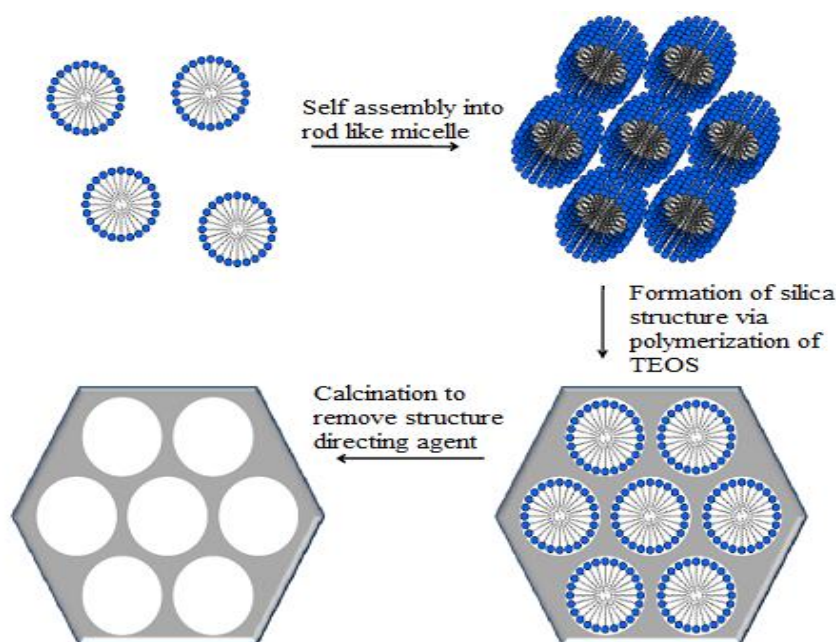
Figure 4.4 Formation mechanism of SBA-15 [42]

4.3 Catalyst Preparation Steps

For solid catalyst preparation, the main aim is to be able to synthesize active and selective catalysts having high porosity, durability, reproducibility, and stability. In catalyst preparation the process parameters are; starting materials, temperature, pressure, time, pH, concentration etc. Catalyst preparation steps are affected from these parameters. By changing these parameters even one by one, it is possible to obtain in an extended variety of different catalyst processes and different catalysts. For this reason optimization is required for the parameters to achieve the main aim of catalyst preparation.

Hydrothermal Synthesis: The hydrothermal synthesis has been used in various applications such as synthesis of molecular sieves and single phase crystalline solids. In this method, the active phase is distributed uniformly in the structure [43].

Temperature, pressure, pH of the solution, concentration, and time are also important parameters that affect the characteristics of the final product of hydrothermal synthesis [44].

Washing: In washing process, the aims are to remove some of the surfactant, to clean the product from the materials that do not enter into the structure and to clean the product from impurities. This process is easy for crystalline precipitates and it is difficult for flocculates. It is not useful for hydrogels [43].

The other aim of washing step is to exchange the unwanted ions. For this application, water at high temperature (100 °C) can be used in order to increase the ion exchange rate [45].

Drying: Removal of solvent from pores of the solid product is known as drying process. This is a traditional and useful treatment for crystalline solids. However, it can cause structural deformation for hydrogels having 90% water in its structure. Drying process can be proceeded under vacuum at low temperatures for the conservation of the amorphous or glassy structure of the solids having low melting temperatures [44].

Calcination: Further heat treatment after drying process is known as calcination. Calcination can be done in the flow of different gases but usually dry air is used. In the calcination step, various chemical, physical and structural modifications occur. Some of them are like that: elimination of chemically bonded water or carbon dioxide, changes in the morphology of the catalyst (small crystals or particles transform into bigger ones), changes in the structure of the catalyst (change in the calcination temperature affects the pore size distribution), generation of active phases and stabilization of mechanical properties [44].

Calcination is performed at a low temperature that the material doesn't degrade so it is a fundamental method to determine the degradation temperature of the material and to have an idea about the thermal stability of the material.

4.4 Characterization Methods for Catalysts

Some specific characterization methods are used to identify catalyst properties. They are mainly X-ray diffraction, Transmission electron microscope, Scanning electron microscope, Nitrogen physisorption technique, Energy dispersive spectroscopy and Thermogravimetric analysis.

4.4.1 X-Ray Diffraction (XRD)

X-ray diffraction technique gives information about the architecture of the solid materials. The diffraction patterns of MCM-41 and SBA-15 materials only give peaks at the low angle range (2θ value is less than 10°). At higher angles, generally no reflection peaks are observed which means that pore walls of the mesoporous materials are mainly amorphous. However, the surfaces of the pore walls show crystalline-like behavior. The XRD peaks do not result from crystal structure in the atomic range, but from the ordered channel walls of the mesoporous material [26].

In the literature, it is indicated that a typical MCM-41 material should have a sharp reflection peak in (100) plane and three reflection peaks in 110, 200 and 210 planes corresponding to Bragg angle degrees of 2.49^o, 4.27^o, 4.93^o and 6.50^o [28]. A typical XRD pattern of MCM-41 is given in *Figure 4.5* which shows the characteristic peaks of this material.
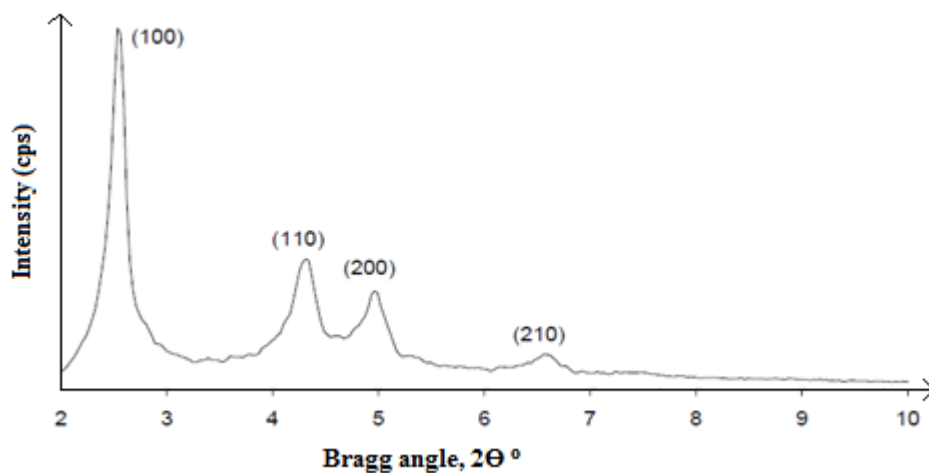
Figure 4.5 XRD pattern of MCM-41 [28]

4.4.2 Transmission Electron Microscope (TEM)

TEM is used to visualize different pore arrangements of the materials. Using TEM characterization technique, dislocations and other crystallographic defect character can be determined. The high-energy electron beam transmits the sample grids and captures an image of the structure of the channels, pores and the hexagonal structure of the material [22].

TEM images of MCM-41 and SBA-15 materials can be seen in *Figure 4.6* and *Figure 4.7* respectively. As seen from the figure, MCM-41 has a hexagonal, honey comb like and cylindrical structure with a uniform pore size distribution and SBA-15 has a cylindrical structure with a uniform pore size distribution.
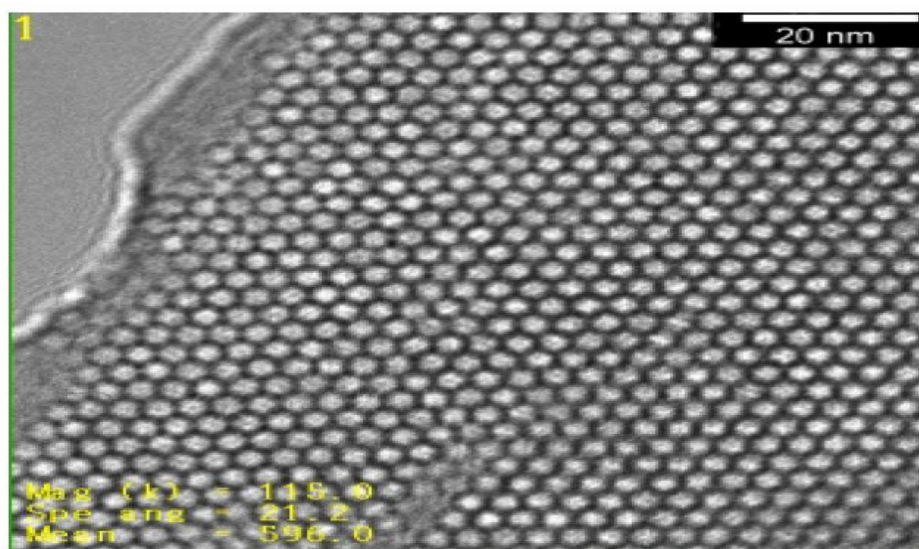
Figure 4.6 TEM image of MCM-41 material **[46]**
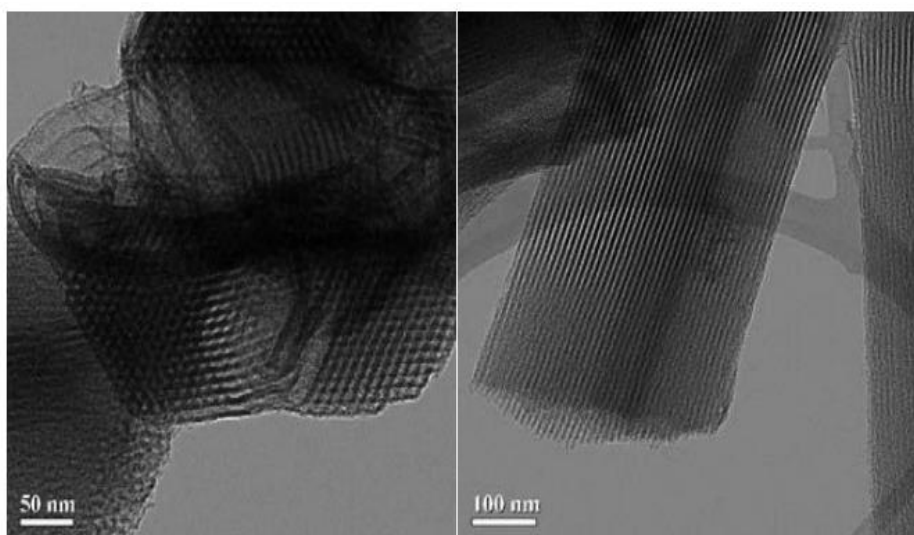
Figure 4.7 TEM image of SBA-15 material **[42]**

4.4.3 Scanning Electron Microscope (SEM) and Energy Dispersive Spectroscopy (EDS)

Scanning Electron Microscopy (SEM) is a useful analysis technique for the examination of the particle shapes, properties, and arrangements **[37]**. SEM image of MCM-41 material is given in *Figure 4.8* showing an agglomerated structure.

Figure 4.8 SEM image of MCM-41 (magnified 10000 times) **[26]**

Energy dispersive spectroscopy (EDS) is an analytical technique used for the elemental analysis or chemical characterization of a sample. In this technique, the number and energy of the X-rays emitted from the material are measured and using this data, elements present in the materials are investigated **[49]**. EDS and SEM analysis are held in the same equipment simultaneously.

4.4.4 Nitrogen Physisorption

Nitrogen physisorption technique is used to detect the porosity and specific surface area properties of a material. According to the IUPAC classification, mesoporous materials reflect typical Type IV adsorption-desorption isotherms **[44]**. The characteristic MCM-41 nitrogen adsorption-desorption isotherm has a sharp curve in the mesoporous range of P/Po= 0.2 to 0.5 depending on the pore size of the catalyst **[47]**. *In Figure 4.9*, nitrogen adsorption-desorption isotherm of pure MCM-41 synthesized using hydrothermal synthesis method is given.
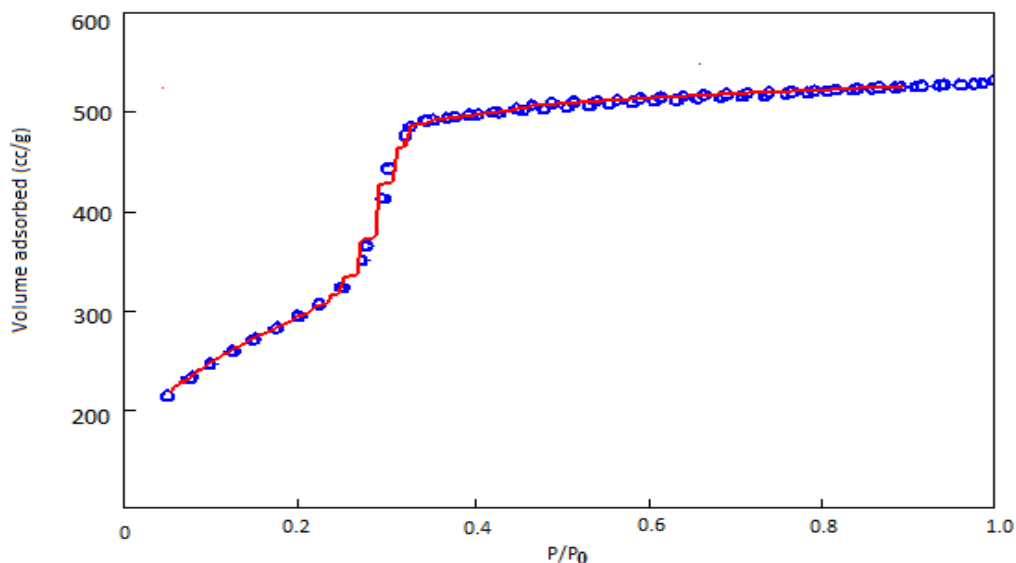
Figure 4.9 Nitrogen adsorption-desorption isotherms **[48]**

4.4.5 Thermogravimetric Analysis (TGA)

The simplest and most common method of assesing polymer pyrolysis is the thermogravimetric analysis (TGA). TGA is a thermal analysis technique which analyzes the physical and chemical property changes of materials by increasing temperature or providing constant heating rate, temperature or mass loss **[1]**.

A TGA curve of the material can be drawn as weight of the material versus temperature. In such a graph, it is understood that heat is applied to the material under some specific conditions. The weight of the material decreases depending on the effect of heat. The rate of weight loss in the material differs according to the structure of the material. For the regions where significant degradation takes place, the decline in weight loss curve becomes significant. At the end the curve becomes a constant straight line which means that the degradation of the material is completed and further heating makes no effect on weight loss.

The TGA apparatus is shown in *Figure 4.10.* It consists of a very sensitive microbalance from which a small pan containing the sample to be analyzed is suspended. The analysis is done typically in ramped heating conditions. Ramped heating gives an idea about the onset of degradation.
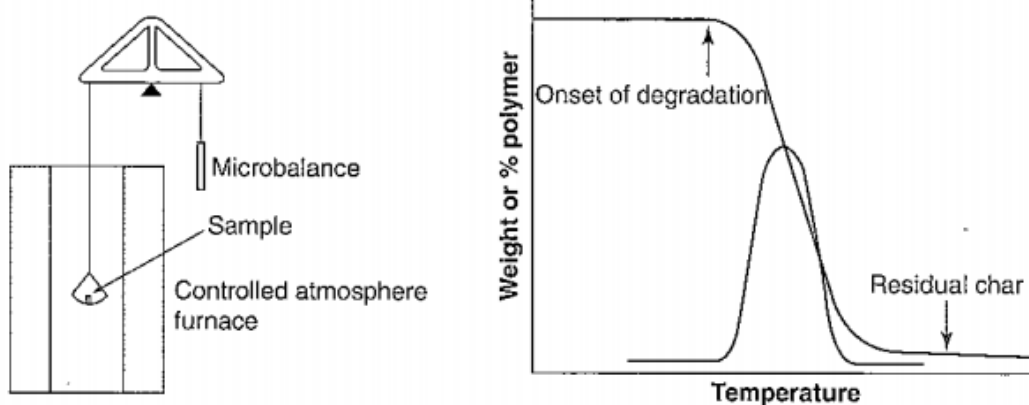
Figure 4.10 Thermogravimetric analyser [1]

4.5 Heteropoly Acid Catalysts

A heteropoly acid is a group of acids composed of a specific combination of hydrogen, oxygen, certain metals and non-metals. Heteropoly acid catalysts are fundamental catalysts which can be used in various reaction media like solid catalysts in homogeneous two phase solution systems [50].

4.5.1 Structure and Properties of Heteropoly Acid Catalysts

Heterogeneous and homogeneous system reactions can be catalyzed by heteropoly acid catalysts. Catalytic purpose of heteropoly compounds in the solid and aquous phase has drawn attention recently since their acidic and redox properties can be controlled and maintained at atomic and molecular levels. Because of their strong acidity property and oxidizing functions, they enable a lot of studies on the heterogeneous and homogeneous catalysis. The property of soft basicity of the polyanion may provide high catalytic activity in some reactions. The other critical properties of the heteropoly acids are high oxidative stability and high possibility of introduction of different elements with polyanions and countercations [51].

In order to define a compound as heteropoly acid, it must contain:

- A metal such as tungsten, molybdenium or vanadium, called as the metal atom,
- Oxygen,
- An element, usually belonging to the p-block of the periodic table, like silicon, phosporus or arsenic, which is called as the central atom,
- Acidic hydrogen atoms.

Since the possibility of different combinations of metal atoms and various kinds of hetero atoms coming together is high, there are many kinds of heteropoly acids. The two best known heteropoly acids are Keggin ($H_nXM_{12}O_{40}$) and Dawson ($H_nX_2M_{18}O_{62}$) structures [52]. Keggin and Dawson structures of heteropoly acids are shown in *Figure 4.11*.
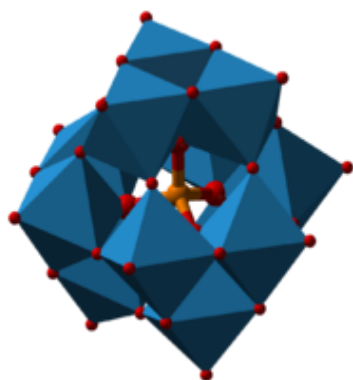
Keggin structure ($XM_{12}O_{40}{}^{x-}$) Dawson structure ($X_2M_{18}O_{62}{}^{x-}$)
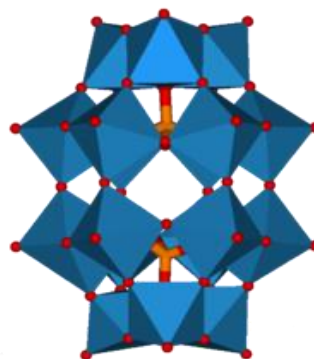
Figure 4.11 Keggin and Dawson structures **[53]**

Keggin type of heteropoly acid is indicated by the formula $XM_{12}O_{40}{}^{x-}$. In the mentioned formula X represents the central atom, which is typically Si^{4+} or P^{5+}; x is the oxidation state and M is used for the metal ion, which can be Mo^{6+}, W^{6+}, V^{5+}, Co^{2+}, Zn^{2+}, etc. Among a wide variety of heteropoly acids, the Keggin heteropoly acids are the most important for catalysis because of the fact that they are the most stable and more easily available **[54, 55]**.

Heteropoly acids are very soluble in polar solvents such as alcohols, water, ethers and esters but they are insoluble in nonpolar solvents such as hydrocarbons. The dissociation constant of heteropoly acids, which is named as the Hammett acidity function can be used for describing the acid features of heteropoly acids in solutions like the hardness of the acid or the softness of the corresponding base. The acidity of heteropoly acid solutions depends on their compositions. Heteropoly acids in solutions are stronger than the common mineral acids like H_2SO_4, HCl, HNO_3 and throughout the heteropoly acids, the tungsten acids are stronger than molybdenum ones. Solid heteropoly acids have very strong Bronsted acidity exceeding that of solid acids like H_3PO_4/SiO_2, $SiO_{26}Al_2O_3$, HX and HY zeolites **[55]**.

Heteropoly acids have mobile ionic structures. Water and different polar organic molecules can enter and leave the structure, therefore, they can absorb high amount of polar molecules in the catalyst bulk. Due to this property, polar molecules not only give reactions on the surface of the heteropoly acid, but also in the heteropoly acid crystalline bulk. This situation is called as 'pseudoliquid phase'. Nearly all proton sites present in the structure of the heteropoly acid participate in the reaction of polar substances. In nonpolar molecules situation, they are not absorbed in the bulk of the heteropoly acid because interaction just occurs on the surface of the heteropoly acid. Based on the pseudoliquid phase behavior which is not a common case for heterogeneous acid catalysis, high catalytic activities are obtained for the reaction of polar molecules at relatively low temperatures. Increase in the surface area for non polar molecules is important and improvement in the surface area can be attained by supporting heteropoly acid on solids having high surface area. Since heteropoly acids are very soluble in several organics and water, it is a crucial matter to establish supported heteropoly acid catalysts that does not leach in liquid or vapor phase **[54, 55]**.

The important criteria for the acidity, stability and catalytic activity of supported heteropoly acids can be listed with the parameters like heteropoly acid type, distribution of heteropoly

acid protons, surface area, particle dimension, pore structure, support features, pretreatment conditions, catalyst preparation conditions, pH, concentration of solution and interaction of the heteropoly acid [55, 56]. The limited neutralization of the acid, the dispersion on various supports and selecting suitable HPA building components are important factors to control the acidity of the heteropoly acid [57].

Solid heteropoly acids have a very high level of proton mobility. Usually, the proton conductivities of solids are correlated with their acid-base catalytic activities [55].

4.5.2 Studies on Heteropoly Acid Catalysts

Studies on heteropoly acids catalysts have exceeded the ones on homogenous acid catalysts, both Bronsted and Lewis types, because of their environmental and safe handling features. Furthermore, because of their flexible redox property, their oxidative dehydrogenation potential is high. Acidic or neutral substances such as silica, activated carbon, aluminosilicate, mesoporous moleculer sieves like MCM-41, SBA-3, SBA-15 which are members of mesoporous silica materials, γ-alumina and zeolites such as HZSM-5 are suitable supports for heteropoly acids. Silica has been considered most popular support due to its low production cost, modification of physiochemical properties and ease of availableness. The interaction of heteropoly acids is related to the type and surface characteristics of the silica [52].

Mesoporous siliceous material MCM-41 has attracted researchers since it has a very high surface area as well as regular hexagonal array of uniform pore size within the mesoporous region [58]. The property of material with larger pore size makes novel mesoporous pure silica moleculer sieve MCM-41 superior compared to zeolites [55]. Tungstophosphoric acid supported MCM-41 catalyst decreased the stability of the heteropoly acid and destroyed the crystallinity of the catalyst. The study related with the impregnation of tungstophosphoric acid into MCM-41 showed that the activity of the catalyst was decreased by heating even at 200 ^{o}C due to surface structural damage of the acid molecules. Also, some tungsten oxides formation was reported due to decomposition of tungstophosphoric acid at 400 ^{o}C [59]. Deactivation of catalyst can be observed during the organic reactions due to formation of coke, which is a carbonaceous deposit on the catalyst surface. For zeolites and aluminosilicates, the regenaration of material can be done by burning coke at 500-550 ^{o}C but the thermal stability of heteropoly acids is not sufficient to implement this conventional process [60].

Tungstophosphoric acid impregnated silica was found to be more active and selective than bulky solid form in liquid phase alkylation and transalkylation reactions. It was reported that this new catalyst had both Bronsted and Lewis acids while bulky tungstophosphoric acid had only stong Bronsted acid sites. The Bronsted acid sites were incremented by increasing HPA loading [61].

The acid strength of heteropoly acids can be determined by microcalorimetry and temperature programmed desorption methods. According to microcalorimetry data which was obtained by the sorption of NH_3 at a temperature of 50 ^{o}C after pretreatment of solids at 150 ^{o}C, the order of acid strengths of some important heteropoly acids was reported as; $H_3PW_{12}O_{40} \geq H_4SiW_{12}O_{40} >> H_3PMo_{12}O_{40} \geq H_4SiMo_{12}O_{40}$ which are tungstophosphoric acid, silicotungstic acid, molybdophosphoric acid and silicomolybdic acid [55].

It was reported that at low loadings, $H_3PW_{12}O_{40}$ and $H_4SiW_{12}O_{40}$ formed finely dispersed species on the SiO_2 surface [55]. Higher solubility of heteropoly acids (HPA) caused the physically adsorbed HPA to be leached out on the surface of the support which prevented the recovery of the catalyst [56]. It was found that leaching of heteropoly acids from modified sample limits their usage in liquid phase reactions. Amine groups were introduced on MCM-41 surface by aminosililation in order to build strong link with the protons of heteropoly acids [62]. It was reported that among MCM-41, silica gel and fumed silica, the functionalized MCM-41 showed the least tendency for anchoring with heteropoly acids [56]. If the catalyst is leached with the solvents having low polarity such as chloroform or toluene instead of ethanol or water, the synthesized catalyst preserves the adsorbed heteropoly acids because HPA is insoluble in these solvents [57].

Staiti et al. worked on phosphotungstic acid and silicotungstic acid (STA) on silica to be used as solid electrolytes by sol gel process. The interaction between the heteropoly acid (HPA) and the support was stronger for samples prepared with silicotungstic acid with respect to sample prepared with phosphotungstic acid. Silicotungstic acid molecule had four protons and at the same HPA loadings, which was 15 and 30 wt % HPA, samples prepared with STA showed higher proton conductivity [63]. Among the heteropoly acids, tungstophosphoric acid and silicotungstic acid were supported on the activated carbon by using their concentrated aqueous solutions. Their Keggin structures were maintained. In the case of low heteropoly acid contents partial decomposition of the tungstophosphoric acid took place [64].

Some heteropoly acids have high thermal stability. When they are thermally decomposed, they lose their acidity. The decomposition temperature of silicotungstic acid is found to be 445 ^{o}C [55]. Değirmenci et al. investigated vapor phase ethyl tertiary butyl ether (ETBE) synthesis using heat treated heteropoly acid catalysts of tungstophosphoric acid (TPA) and silicotungstic acid (STA) by comparing the results of this study with the results of untreated catalysts. The results of ETBE synthesis experiments reflected that heat treatment of TPA at temperatures over 473 K had an important on the reduction of the catalytic activity. On the other hand, the deactivation of STA by heat treatment was observed at 673 K and above temperatures which was more stable against temperature compared to TPA . Heat treatment at elevated temperatures caused loss of constitutional water of these heteropoly acid catalysts. Further increase at the temperature was a reason for the loss of protons and the loss of acidity of the catalysts which resulted the deactivation of the catalysts [65].

Keggin type TPA shows high acid strengths and it is used in different acid catalyzed reaction types. On the other hand, TPA has some significant disadvantages one of which is having low surface area around 5 m^2/g. This property makes it difficult to access into the strong acidic sites. In order to overcome the low surface area problem of this heteropoly acid, some solution techniques were applied. The protons were partially neutralized by different cations and also TPA was supported on high surface area oxides. Different high surface area materials have been supported on heteropoly acids in order to enhance their efficiency. Recently, some studies have been carried on mesoporous silica and ordered pore structures. For very high loadings, highly dispersed materials have been attained and materials have showed good stability towards high temperature treatments. A comparative study of a series of mesoporous materials (MCM-41 and SBA-15) modified with anchoring phase of TPA structures has been held. The results have clearly indicated that the catalytic activity and stability of TPA could be adjusted by modifying the anchoring phase of TPA. The advanced support materials for HPA have consisted of similar monolayer coatings of titania, alumina

and zirconia on MCM-41 and SBA-15 and the stability of the HPA on these supports is confirmed. Consequently, the catalyst having Bronsted acid sites in its structure showed good activity in reactions **[66]**.

CHAPTER 5

LITERATURE SURVEY

The recycling of polymer waste is a critical issue for the conservation of natural resources and the environment. In the literature, there are a number of studies related with the recycling of polymer waste related with the catalyst synthesis.

Garfortha et al. (1997) made an evaluation of catalysts having different pore sizes using thermal analysis method for HDPE pyrolysis. The catalysts that were used in this study were silica alumina, silica and alumina incorporated MCM-41 and HY, HUSY, HZSM-5 zeolites. In TGA experiments, isothermal runs were performed at different temperatures and heating rates. It was found that in the presence of catalysts the activation energy of pyrolysis reaction decreased. Among these catalysts it was observed that silica alumina did not lower activation energy of the reaction whereas zeolite Y and ZSM-5 lowered the activation energy of the reaction significantly. In polymer degradation over these catalysts, limited access to the active catalytic sites was observed due to very small diameters of zeolite Y and ZSM-5. It was suggested that the novel porous material MCM-41 with pore larger openings between 2-20 nm offered more possibilities for accessing into the active sites [67].

In another study, HDPE was degraded over different catalysts using a fluidised bed reactor with isothermal temperature and ambient pressure conditions. HZSM-5 zeolite was used as a pyrolysis catalyst combined with non-zeolitic catalysts which were MCM-41 and amorphous silica alumina (SAHA). Using HZSM-5 catalyst resulted in more volatile hydrocarbons compared to over non-zeolitic catalysts. Both MCM-41 and SAHA resulted a saturate rich product stream with wide range of carbon number distribution and significant coke levels. HZSM-5 was used as a coadditive catalyst and as a result, some valuable hydrocarbons like olefins and i-olefins were produced. Unlike the smaller pore structure of HZSM-5, the larger pore structure of MCM- 41 and SAHA catalysts deactivated. In order to reduce the net disposal cost considerably, waste polymers were converted into feedstock or fuels which was considered as an ideal approach. As a result, provided that convenient reaction conditions and suitable catalysts were implemented, it was possible to adjust both the product yield and product distribution in the polymer pyrolysis reaction [11].

In the study of Zhou et al., the catalytic pyrolysis of PP and LDPE was investigated using ZSM-5 zeolite catalyst and the results were compared with USY (Ultrastable Y). The degradation manner of PP and LDPE using modified ZSM-5 zeolite (DeLaZSM-5) was considerably different from those observed in the thermal degradation reaction of USY catalysts. PP showed lower degradation activity in the presence of DeLaZSM-5 catalyst than LDPE did at comperatively lower temperature values. It was concluded that pore structure and unique acid properties of the DeLaZSM-5 affected degradation reaction. LDPE degraded faster compared to PP with the DeLaZSM-5 catalyst. Also higher conversion at low temperature (330 °C) narrower and lighter carbon number distribution indicated that DeLaZSM-5 had shape selective impact in pyrolysis of PP and LDPE. The narrow pore structure of the DeLaZSM-5 zeolite permitted the LDPE molecules to disperse into the voids of the zeolite to contact with the interior acid sites, while PP was prevented. The reason of this was that side chain methyl groups increased the effective cross section of the PP

molecules, which enabled LDPE to access to more acid sites. Related to this situation, suitable reaction temperature at which no thermal degradation affected the heterogeneous catalytic degradation entirely exploited the shape selective effect of the DeLaZSM-5 zeolite. Moreover, the acidic features of the DeLaZSM-5 which allowed the catalytic pyrolysis carry on relatively at low temperature was found to be important to show the shape selective effect of the DeLaZSM-5 zeolite. It was also concluded that the cooperative actions of polymers, catalysts and reaction conditions were crucial parameters having effect on the catalytic pyrolysis of the polyolefin. This would be a reference point for selecting and adjusting optimum catalysts and reaction conditions for the catalytic pyrolysis of various polymers [38].

In one study, ZSM-11 zeolite and modified MCM-41 catalysts were used in polymer cracking reactions. Zn, H and Mo were used as the supports to these catalysts. At the end of the reactions, a mixture of lower and higher hydrocarbons of HDPE was obtained. Benzene, xylene and toluene were the main liquid products. It was observed that H supported zeolite yielded gaseous hydrocarbons (C1–C4) at higher ratios than Mo and Zn supported zeolites. From the Zn supported MCM-41 reactions, mainly C5–C16 products were obtained. It was concluded that the catalytic conversion of temperature of polyolefin was lower compared to the thermal decomposition temperature of pure HDPE. Using microporous and mesoporous catalysts with Zn, H or Mo, it was possible to use HDPE as gaseous and liquid hydrocarbon source at a temperature range of 410–500 °C. Due to the high proportion of Lewis sites, the selectivity to xylene obtained with Zn supported ZSM-11 was higher than value given in the literature [13].

In another study, Akpanudoh et al. performed the pyrolysis of PE using 20 % and 40 % USY zeolite as catalysts in a semi-batch reactor. In this research the effect of the polymer to catalyst ratio was studied on the formation of liquid hydrocarbons. It was reported that the liquid yield was inversely proportional to the acidity content of the catalyst. This indicated acidity content around 7 % for USY. Related to the boiling point distribution of the catalyst, there was a shift towards to the lighter outputs. Liquid hydrocarbon formation was increased depending on the increase in the acidity content of the commercial degradation catalysts. For the fully conversion of the polymer, the number of acid sites was inadequate at low acidity values, while at high acidity values fully cracking was performed and more gaseous products were obtained [16].

Catalytic pyrolysis of HDPE was performed in a fluidised bed reactor for obtaining gas fractions at high yield. The reactions were held at 350 °C and 550 °C and HZSM-5 zeolite was used as catalyst. Butenes composed of olefins with high yield at 25 % were obtained as gas products. The resulted waxes were fully composed of paraffins having carbons from C_{10} to C_{20}. The temperature was an important factor to affect the gas and wax yields. As the temperature increased, gas production increased. However, for the temperatures higher than 500 °C, some HDPE was cracked, which increased the wax yield. At very low reaction temperatures around 350-400 °C, the polymer was not degraded completely and in parallel with this, a solid residue was formed at the end of the reaction. Olefins were the main gas product. It was concluded that the non-catalytic pyrolysis gave lower amount of gas product yield most of which was consisted of (C_5-C_7) compared to the catalytic pyrolysis. The waxes were compositionally differed and the composition was increased the olefinic and cyclic contents as the polyethylene to catalyst ratio increased. In conclusion, the optimum temperature and HDPE/Catalyst ratio for this reaction were 450 °C and 1.41, respectively, without resulting any solid residue. Also, the wax was free from operationally and

environmentally hazardous cyclics and olefins. The catalytic pyrolysis of HDPE was considered as a promising and low cost process with respect to the other polymer recycling technologies. At milder temperatures, gas products were obtained at higher yields and selectivity compared to the non-catalytic pyrolysis [68].

In a study of Kim et al., pyrolysis of HDPE was performed using Al-MCM-4l-P which was synthesized by post-synthetic grafting method and Al-MCM-41-D which was synthesized by direct sol-gel method. Thermogravimetric analysis under static conditions was also carried out to estimate the activation energies of the catalytic decomposition reactions of HDPE. Higher catalytic activities and lower activation energies of the decomposition reaction of HDPE was observed when AI-MCM-41-P was used. It was put forward that this result might be due to the fact that Al-MCM-41-P had more acid sites compared to Al-MCM-41-D. Even with high aluminum content, unfavorable hydrothermal deterioration was seen in both catalysts with the effect of Bronsted acid sites [12].

In a study, two different metal loading techniques were used in order to synthesize Fe-MCM-41 catalysts. In the first method, Fe was inserted to the catalyst during hydrothermal synthesis and in the second one, MCM-41 catalyst was impregnated to the iron nitrate. In order to recover the waste polymeric material both catalysts were used in polymer pyrolysis reactions. The polymers of the reaction were polyethylene, polymethylmetacrylate (PMMA) and polystyrene. X-ray photoelectron spectroscopy (XPS) technique was used in order to determine the iron and carbon chemical states atomic concentrations. There were some differences in the iron chemical states between the two Fe loaded MCM-41 catalysts before and after the reaction. The product analysis of two catalysts also showed differences depending on the type of tested polymer. The Fe loaded MCM-41 sample which was synthesized during hydrothermal synthesis was designated as a good catalyst for polyethylene and PMMA taking account of no carbon deposition at the end of the reaction. The electronic spectra of this catalyst showed that bulk structure of the catalyst was partially destroyed during the reaction and iron oxides were agglomerated [69].

In another study, six solid catalysts having different acidic and structural properties were examined for their catalytic activity of the polymer degradation reaction using TGA method. The polymers used in pyrolysis reactions were pure LDPE, pure HDPE and recycled PE from agricultural and urban origins. The catalysts of the reactions were standard ZSM-5, nanocrystalline n-ZSM-5, beta as zeolitic catalysts and solgel Al-MCM-41 (sg), hydrothermal Al-MCM-41 (hy) and Al-SBA-15 as mesoporous structures. The ability of shifting the pyrolysis reaction temperature to lower values was a significant indicator determining the catalytic activity of these catalysts. Standard ZSM-5 zeolite showed very low catalytic activity despite showing strong acid properties among the other catalyst. This situation was related to the diffusional limitations that significantly affected the access of the bulky polymer molecules into the internal active sites. The catalysts beta zeolite and nanocrystalline n-ZSM-5 showed the strongest catalytic activity among the other catalysts and these catalysts partly eliminated the diffusional limitations due to both having strong acid properties and high surface area. Mesostructured solid catalysts exhibited weaker acid properties compared to the zeolitic catalyst due to their non-crystalline nature. Having larger pores partly eliminated the disadvantage of diffusional limitations. Al-MCM-41 (hy) showed one of the best catalytic activities by exceeding the performance of crystalline solids due to having stronger acid properties [4].

In a study conducted by Gaca et al., pyrolysis of polyethylene was carried out over MCM-41 molecular sieves modified with TPA (TPA/MCM-41) and its insoluble nonstoichiometric cesium salt (CsTPA/MCM-41). For comparison, high silica zeolite ZSM-5 was used as pyrolysis catalyst as well. These catalysts (TPA/MCM-41, CsTPA/MCM-41 and ZSM-5) caused to decrease HDPE degradation temperature with respect to the non-catalytic degradation. Using catalyst also affected the final product distribution of the cracking reaction. TPA/MCM-41 catalyst yielded low amount of gas products and 80 wt % of liquid products while ZSM-5 catalyst resulted in gas products about 50 wt % of with selectivity. Only aliphatic hydrocarbons like olefins and paraffins were the products of the catalytic degradation of high density polyethylene in the presence of TPA/MCM-41 and CsTPA/MCM-41 while in the presence of ZSM-5 zeolite, liquid products contained aromatic compounds. It was concluded that PE pyrolysis over ZSM-5 zeolite produced liquid contained mainly aromatic hydrocarbons, while high yield gas product mostly contained C_3 and C_4 hydrocarbons [10].

In the study of Aydemir, Al incorporated MCM-41 and TPA loaded SBA-15 catalysts were synthesized to be utilized in the catalytic pyrolysis reactions of PE. The non-catalytic and catalytic pyrolysis reactions of PE were carried on. Gas and liquid hydrocarbons were obtained as final products. In the catalytic degradation reactions performed with TPA loaded SBA-15 catalysts, gas yields were higher and the liquid yields were lower compared to the non-catalytic degradation reaction product yield values. It was observed that liquid product yield increased with an increase in reaction temperature in the reactions performed with SBA-15 catalysts. Due to the increase in the acidity degree, liquid product yield increased with respect to the increase in TPA loading. Catalytic pyrolysis reactions performed using Al loaded MCM-41 catalysts resulted in higher yield of gas products and lower yield of liquid product which reflected similarity with the results of TPA loaded SBA-15 catalysts. The analysis of gas products indicated that in the non-catalytic pyrolysis of PE, C3 and C4 hydrocarbons were obtained at very high selectivity values. In catalytic degradation reactions, Al incorporated MCM-41 catalysts were selective to higher molecular weight gas products which were propylene, n-butane and iso-butane. On the other hand, the selectivities of the lower molecular weight gas products like ethylene and n-butane were very high in the catalytic pyrolysis reactions of TPA loaded SBA-15 catalyst [70, 76].

In another study, catalytic pyrolysis of HDPE was investigated using silica alumina as the catalyst by TGA method. It was proposed that both the non-catalytic and catalytic degradation occurred simultaneously, one of which was degradation of the huge polymer molecules using the catalyst with an activation energy value of 174 kJ/mol. On the other hand the non-catalytic cracking took place with an activation energy value of 256 kJ/mol. The non-catalytic degradation was especially responsible for over cracking and formation of gas products. It was also concluded that as the production of liquid fuels had the industrial importance because of their economically attractive situation for industry, using suitable catalysts would allow predicting the required reaction time for a specific product distribution [71].

In one study, mesoporous MCM-41 was synthesized by leaching of sepiolite. A highly ordered MCM-41 catalyst was synthesized at 100 °C in 24 h in a synthesis solution pH value of 12 using a hydrothermal synthesis process and with post Mg sepiolite extraction. Its BET surface area, pore size and pore volume were 1036 m^2/g, 2.98 nm and 1.06 cm^3/g, respectively. It was seen from these results that the crystallinity and pore size of MCM-41 increased with increase of crystallization time, ratios of surfactant to SiO_2 and decrease of

Mg content. The experimental results of the catalytic pyrolysis of PS waste indicated that MgO incorporated MCM-41 had higher catalytic activity and selectivity compared to styrene for the catalytic pyrolysis of PS. Ethylbenzene, isopropylbenzene, isopropenylbenzene were formed by side reactions. The Mg content was found to be the key factor for determining the degree of a long range of mesostructure. For the catalytic pyrolysis of polystyrene, decrease of Mg content lead to high crystallinity of MCM-41. MCM-41 showed good selectivity and high catalytic activity between C_5–C_{12} aromatic hydrocarbons. The styrene yield was 50.7 % when polystyrene was catalytically degraded over MCM-41 from sepiolite [72].

In a study, the non-catalytic and catalytic degradations of PE wastes were performed in order to obtain energy and valuable chemical compounds to be used in the chemical industry. Catalysts used in this study were silica gel, 5A molecular sieve and activated carbon. The pyrolysis was done in a batch reactor at 450, 500 and 700 °C during 2 h for each catalyst. The ratio of catalyst/PE was 10% w/w. The optimum operation temperature for pyrolysis with silica gel and activated carbon was 450 °C and for 5A molecular sieve it was 700 °C. It was concluded that degradation products of the reaction were dependent on the temperature conditions and catalyst type [14].

Throughout the literature survey, it was observed that there were a lot of studies related to the synthesis of mesoporous materials (MCM-41 and SBA-15) and pyrolysis of polymers. However, limited studies were carried out related to the incorporation of STA into MCM-41 structure and no study was carried out in the literature up to now related to the pyrolysis of polyethylene in the presence of STA loaded MCM-41 and STA incorporated SBA-15. So the aim of this study is:

- ✓ To synthesize and characterize STA incorporated MCM-41 and SBA-15 materials using hydrothermal synthesis method.
- ✓ To test the performance of the synthesized catalysts in the PE pyrolysis reaction by TGA method.
- ✓ To determine the kinetic parameters for the PE pyrolysis reaction.

CHAPTER 6

EXPERIMENTAL STUDY

The experimental part of this study is handled in three sections. The first section is the synthesis of STA incorporated catalysts, the second one is the characterization of the synthesized catalysts and the last one is the determination of kinetic parameters and activity test of the catalyst using thermogravimetric analyser.

6.1 Catalyst Preparation

STA loaded MCM-41 (25 % n/n) and SBA-15 catalysts (10 % n/n) were synthesized following a direct hydrothermal synthesis method.

6.1.1 Preparation of STA Incorporated MCM-41 Catalysts

The reagents for the preparation of STA incorporated MCM-41 catalyst were tetraethylorthosilicate (TEOS, $C_8H_{20}O_4Si$, Merck) as the silica source, cetyltrimethylammonium bromide (CTMABr, $C_{16}H_{33}(CH_3)_3NBr$, Merck) as the surfactant source, sulphuric acid (H_2SO_4, 98 %, Merck) as the acid source, deionized water (Milli-Q H_2O) as the solvent source and silicotungstic acid (STA, Sigma-Aldrich).

The procedure used in the synthesis of STA incorporated MCM-41 catalyst was a modified version of the procedure described by Obalı et al [73]. 13.2 g of CTMABr was dissolved in 87 ml of deionized water and this solution was continuously stirred at 500 rpm for about half an hour until a clear solution was obtained. The temperature of the solution was kept at 30 ºC using temperature controlled stirrer. The pH value of this surfactant solution was around 6.5. Then, 15.64 ml of TEOS was added to this solution dropwise with a continuous stirring. After that predetermined amount of STA which was dissolved in small amount of deionized water, was added dropwise. Calculation of the STA amount to be added into the MCM-41 structure according to W/Si molar ratio was given in *Appendix A.1*. The pH value of the synthesis solution was adjusted to a desired value with a few drops of 4 N H_2SO_4 solution. This solution was mixed for 1 hour under the same temperature and stirring rate conditions. The resulting solution was transferred into a Teflon lined stainless steel autoclave which was at 120 ºC for hydrothermal synthesis to take place for 96 hours. Then, the material was taken from the autoclave and suspended in 300 ml of deionized water. This material was filtered and washed with the deionized water. Filtering and washing procedure was repeated until the pH value of the residual water of the filtering and washing procedure became constant. After washing and filtering, the material was taken into oven at 40 ºC and left for drying about 2 days. The calcination temperature of the uncalcined sample was determined according to thermogravimetric analysis results which were given in *Appendix B.1*. The dried material was calcined at 400 ºC in tubular quartz tube reactor for 8 hours. The catalysts were obtained in a powder form.

In TGA curve, for silicotungstic acid (STA) loaded catalyst, weight loss at low temperatures corresponds to the seperation of structural water, weight loss at medium temperatures corresponds to proton loss and weight loss at high temperatures corresponds to acidity loss

meaning the deactivation of catalyst [65]. So this is a fundamental method for determining the calcination temperature of material. The synthesis procedure for STA loaded MCM-41 material can be seen in *Figure 6.1.*
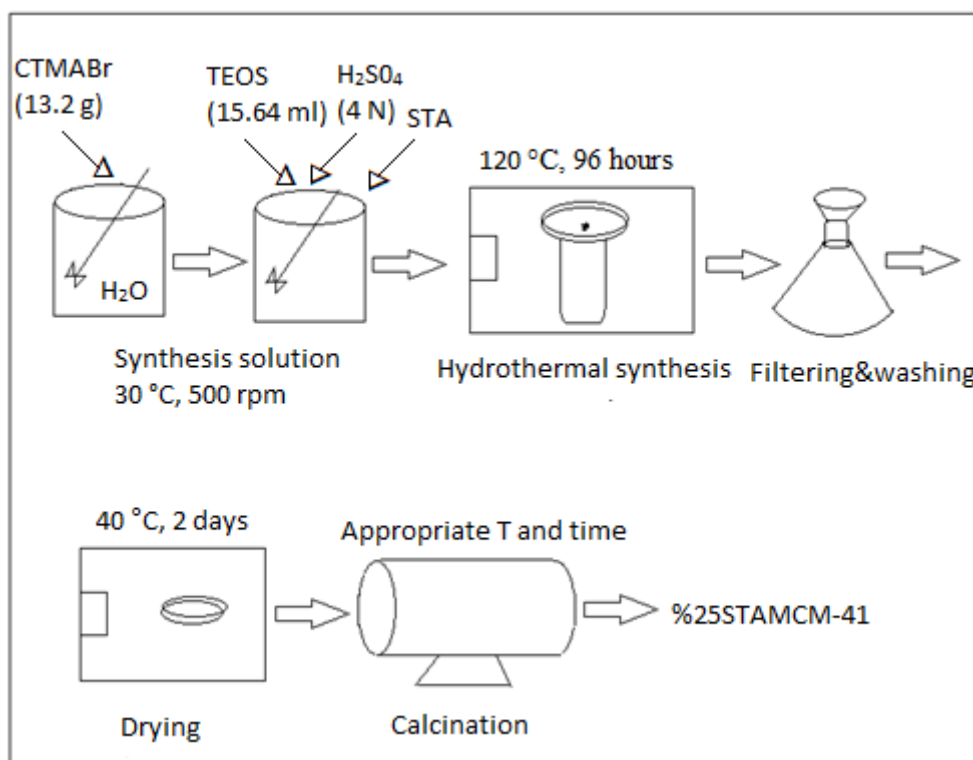

Figure 6.1 Synthesis steps for STA incorporated MCM-41 catalyst

6.1.2 Preparation of STA Incorporated SBA-15 Catalyst

The reagents for the synthesis of STA incorporated SBA-15 catalyst were poly (ethylene glycol)-block-poly (propylene glycol)-block-poly (ethylene glycol) (P-123, Sigma-Aldrich) as the surfactant source, tetraethyl orthosilicate (TEOS, $C_8H_{20}O_4Si$, Merck) as the silica source, hydrochloric acid (HCl, 37 %, Merck) as the solvent source and silicotungstic acid (STA, Sigma-Aldrich).

The procedure used in the synthesis of STA incorporated SBA-15 catalyst was a modified version of the procedure described by Obalı et al [74, 76]. For the synthesis of STA incorporated SBA-15 catalyst, 4 g of surfactant was dissolved in 120 ml of 2 M HCl solution with a continuous stirring rate of 350 rpm at 40 °C for 4 h. Then, 8 g of silica source was added dropwise to the solution with a continuous stirring for half an hour. After that predetermined amount of STA was dissolved in small amount of deionized water and added to this solution dropwise. Calculation of the STA amount to be added into the SBA-15 structure according to W/Si molar ratios are shown in *Appendix A.2.* The synthesis solution was stirred totally 1 day with the same temperature and stirring rate from the beginning of

synthesis procedure. The resulting solution was transferred into a teflon lined stainless steel autoclave for the hydrothermal synthesis taking place at 100°C for 48 hours. The obtained mixture was filtered and washed with the deionized water. The solid product was then dried in the oven at 80 °C for one day. If the material in the oven was not dried completely, it was left in the oven for another one day at 60 °C. The dried material was calcined at 250 °C in tubular quartz tube reactor for 8 hours. The catalyst was obtained in a powder form. Synthesis steps for the STA loaded SBA-15 catalyst can be seen in *Figure 6.2.*
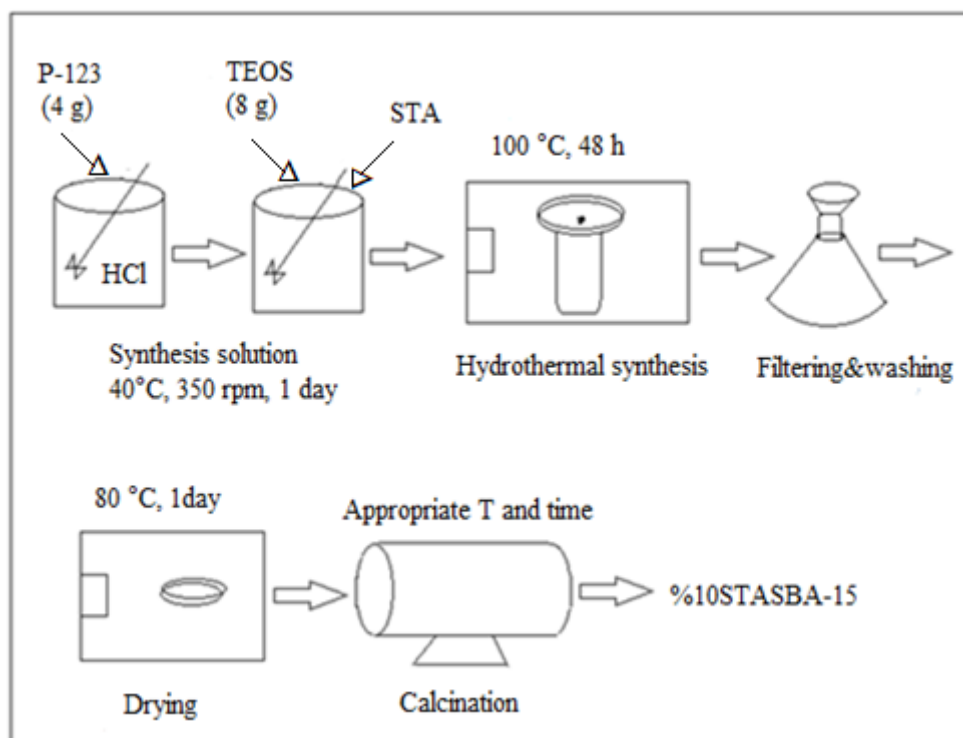

Figure 6.2 Synthesis steps for the STA incorporated SBA-15 catalyst

6.2 Characterization Techniques for the Synthesized Catalysts

In order to determine the physical and structural properties of the synthesized catalysts, the characterization techniques of XRD, Nitrogen adsorption-desorption, SEM, EDS and DRIFTS were used.

6.2.1 X-Ray Diffraction (XRD)

XRD analysis of the synthesized catalysts was performed using Rigaku Ultima IV In-Plane Diffractometer in Central Laboratory and Rigaku D/MAX2200 diffractometer in Metallurgical and Materials Engineering Laboratory at METU. The Bragg angle values were in the range of 1°-10° for low angle diffraction with a step size of 0.02 for MCM-41 and SBA-15 materials. For wide angle diffraction, the Bragg angle values were in the range of 1-

50 ° with the same step size value. The analysis was held at conditions of 40 kV and 40 mA using parallel beam method.

6.2.2 Nitrogen Adsorption-Desorption

N_2 adsorption-desorption analysis of the synthesized catalysts was done using Micromeritics Tristar II 3020 analyser at METU Chemical Engineering Laboratory. The samples were degassed at 80 °C overnight before the analyis. The analysis was carried out at a relative pressure of 0.05 to 0.99 at liquid nitrogen atmosphere of 77 K.

6.2.3 Scanning Electron Microscope (SEM) and Electron Dispersive Spectroscopy (EDS)

SEM and EDS analysis of the synthesized catalysts was performed using Quanta 400 F Field Emission SEM instrument which had a resolution value of 1.2 at METU Central Laboratory. The samples were coated with gold in order to provide proper electrical conductivity to the samples before the analysis.

6.2.4 Diffuse Reflectance Infrared Fourier Transform Spectroscopy (DRIFTS)

In order to determine the Bronsted and Lewis acidity structure of the catalysts, DRIFTS spectra were carried out using a Perkin Elmer Spectrum One instrument in METU Chemical Engineering Kinetic Laboratory with pyridine adsorption method. Before the analysis, the samples were dried at 110 °C for 12 hours. 1 ml of pyridine was added dropwise onto the samples and pyridine adsorbed samples were dried at 40°C for 2 hours. KBr was used as the background material in order to constitute a baseline to the spectra. The spectrum of fresh catalysts and the spectrum of pyridine adsorbed catalysts were analyzed in the instrument with number of 50 scans for one sample and at the wave number range of 1390-1690 cm^{-1}. In Spectrum V.5.0.1 program, the spectrum of fresh catalysts was substracted from the spectrum of pyridine adsorbed catalysts and Bronsted and Lewis acid sites of the catalysts were determined.

6.3 Thermogravimetric Analysis

Thermogravimetric analysis is a technique for monitoring the weight loss of a sample while heating the sample up to a desired temperature. In order to test the performance of the synthesized catalysts in the polyethylene pyrolysis reaction, thermogravimetric analysis was performed using Shimadzu Simultaneous DTA-TGA analyser with Shimadzu DTG-60H detector in METU Chemical Engineering Thermogravimetric Analysis Laboratory. In order to obtain an optimum $w_{catalyst}/w_{polymer}$ ratio, the catalyst and polymer were weighed at ratios of 1/2, 1/5 and 1/10. As catalyst and polymer were in powder form, in order to enhance mixing of catalyst and polymer, the catalyst was crushed finely and mixed with the polymer thoroughly. For STA loaded MCM-41 catalysts, total maximum amount of the material to be loaded into the instrument was adjusted to 12 mg and all the weighed material was put into the analyser in order to maintain the $w_{catalyst}/w_{polymer}$ ratio.

Thermogravimetric analysis consisted of a gas tank, furnace, temperature controller and analytical balance. Flow rate of the gas was adjusted to the desired value and the furnace was turned on. Then the sample was put onto the analytical balance. Starting from the room temperature conditions, the temperature of the system was increased by suitable temperature

intervals up to a desired temperature while the weight of the sample was recorded. After reaching to the desired temperature, the gas was shut off and the furnace was turned off. Thermogravimetric analysis parameters are listed in *Table 6.1*.

Table 6.1 Thermogravimetric analysis parameters

Parameter	Value
Gas flow rate (Nitrogen)	60 cc/min
Temperature range	30-550 °C
Heating rate	5 °C/min

CHAPTER 7

RESULTS AND DISCUSSION

In this study, STA incorporated MCM-41 and SBA-15 catalysts were synthesized using a direct hydrothermal synthesis method. Main parameters that affected the synthesis of the catalysts were STA loading amount, calcination temperature and the pH value of the synthesis solution. The synthesized catalysts were characterized using several techniques and their performances were tested using a thermogravimetric analyser.

7.1 Characterization Results of STA Loaded MCM-41 Materials

STA loaded MCM-41 materials were prepared at the calcination temperature of 400 °C with the W to Si molar ratio of 0.25 and the solution pH values of 1.2 and 1.4.

7.1.1 X-Ray Diffraction Results of STA Loaded MCM-41 Materials

Low angle XRD patterns of the synthesized STA loaded MCM-41 catalysts are given in *Figure 7.1*. According to this figure, both samples had a wide peak. STA loaded MCM-41 catalyst having pH value of 1.2 had the most intense peak at 2Θ value of 2.26^{o} and the one having pH value of 1.4 had the most intense peak at 2Θ value of 2.51^{o}. In the literature, it was indicated that a typical MCM-41 material should have a sharp main peak in (100) plane and three reflection peaks in 110, 200 and 210 planes corresponding to 2.49^{o}, 4.27^{o}, 4.93^{o} and 6.50^{o} [28]. This was an indication that major peaks of STA loaded MCM-41 materials were mostly preserved and an MCM-like structure was obtained. This indicated that STA loading might cause some deformation in the ordered structure of the mesoporous material.
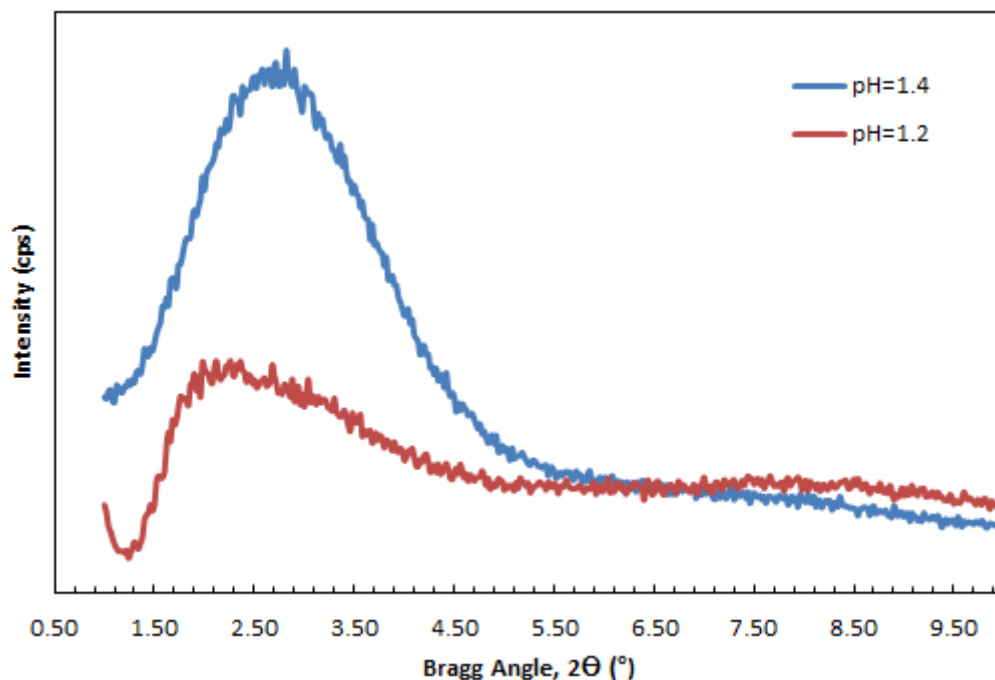
Figure 7.1 Low angle XRD patterns of STA loaded MCM-41 catalysts synthesized at pH values of 1.2 and 1.4

Figure 7.2 shows the wide angle XRD pattern of STA loaded MCM-41(pH=1.2) catalyst. According to this figure, this catalyst had peaks at 2Θ values of 24.1 $^\circ$, 26.58 $^\circ$, 28.1 $^\circ$ and 35.1 $^\circ$. The main peak at 2Θ value of 24.1 $^\circ$ corresponded to the amorphous silica structure of this catalyst. Pure STA characteristic peaks were given in *Appendix C.1*. Comparing the wide angle XRD pattern of this catalyst with pure STA XRD pattern, it was observed that the first and major peaks of pure STA which were at 2Θ values of 26.58 $^\circ$ and 35.1 $^\circ$ were preserved in the synthesized catalyst. STA species weren't well dispersed in the lattice of this catalyst.
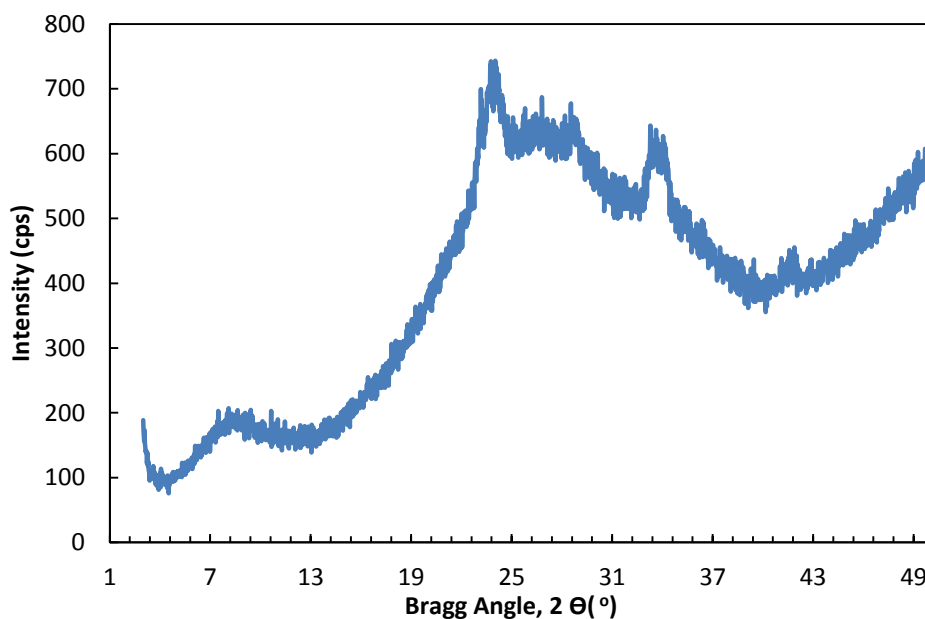
Figure 7.2 Wide angle XRD pattern of STA loaded MCM-41 catalyst (pH=1.2)

Figure 7.3 shows the wide angle XRD pattern of STA loaded MCM-41 (pH=1.4) catalyst. In this figure it was seen that this sample had a broad main peak around 23° which corresponded to the amorphous silica structure of the synthesized catalyst and most of the other characteristic pure STA peaks were not observed so this catalyst had a different structure. STA species were well dispersed in the lattice of the synthesized material.
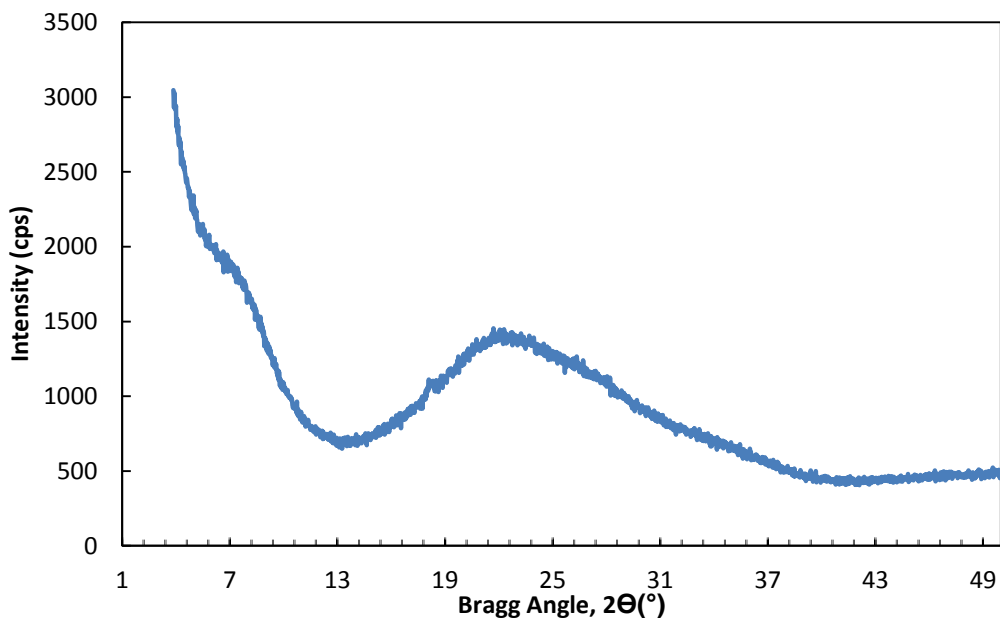

Figure 7.3 Wide angle XRD pattern of STA loaded MCM-41 catalyst (pH=1.4)

7.1.2 Nitrogen Adsorption-Desorption Results of STA Loaded MCM-41 Materials

Figure 7.4 shows adsorption-desorption isotherms of the STA incorporated MCM-41 catalysts. According to this graph both catalysts had Type IV isotherms indicating the mesoporous structure of these catalysts. The sample having pH value of 1.4 had a nitrogen capillary condensation at relative pressures between 0.45 and 0.80 which had a sharp increase in the adsorbed volume. This behaviour indicated a narrow pore size distribution. It showed an H2 type of hysteresis which resulted from the differences betweeen adsorption and desorption mechanisms. The sample having pH value of 1.2 had a nitrogen capillary condensation at relative pressures between 0.62 and 0.95. As capillary condensation of nitrogen started at a higher relative pressure compared to the other sample, it caused an enlargement in the mesopores of this sample. The sample having pH value of 1.2 had an H1 type of hysteresis which indicated a parallel tendency in the adsorption and desorption behaviours.
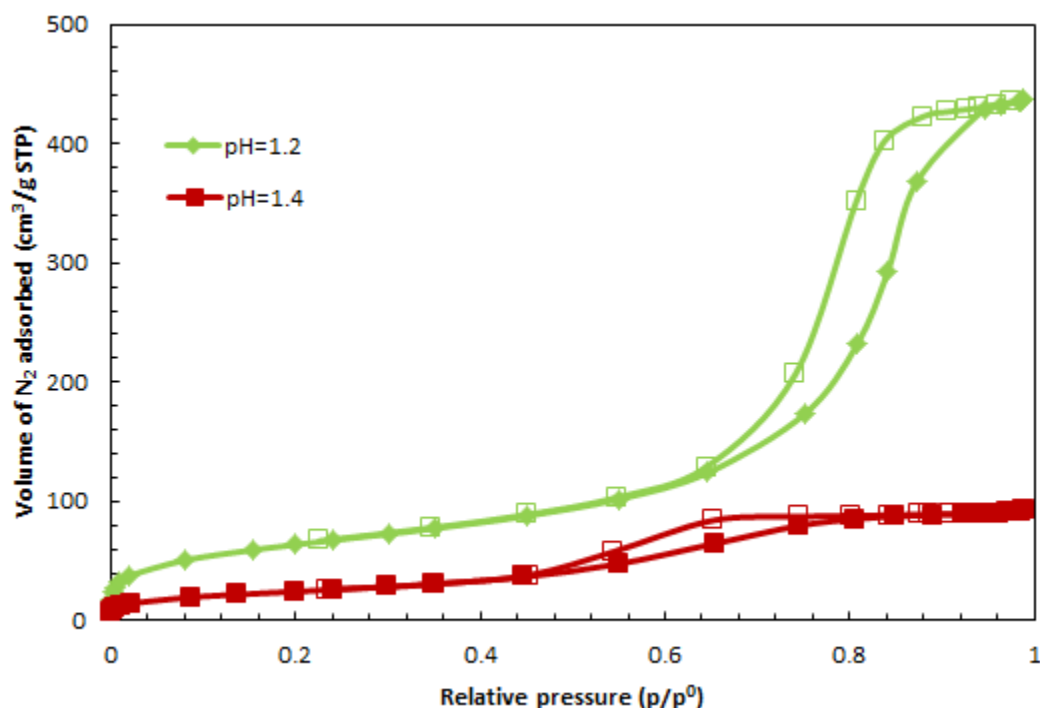

Figure 7.4 N_2 adsorption-desorption isotherms of STA loaded MCM-41 catalysts
(Filled symbols: adsorption; empty symbols: desorption)

Physical properties of these samples related to pore sizes which were obtained from nitrogen adsorption-desorption analyses are given in *Table 7.1*. BET surface areas of the samples having pH values of 1.2 and 1.4 were 234.1 m^2/g and 90.3 m^2/g, respectively. Also BJH desorption cumulative pore volumes of these samples were 0.68 cm^3/g and 0.15 cm^3/g, respectively. As seen in this table microporosity percent of the former sample is smaller than the latter sample.

Table 7.1 The physical properties of STA loaded MCM-41 catalysts

Property	pH=1.2	pH=1.4
Surface area (BET)	234.1 m^2/g	90.3 m^2/g
Desorption cumulative pore volume (BJH)	0.68 cm^3/g	0.15 cm^3/g
Desorption average pore diameter (4V/A) (BJH)	8.2 nm	4.3 nm
Average pore diameter (4V/A) (BET)	11 nm	6.5 nm
Microporosity	10.7 %	19.1 %

Pore size distribution of the STA loaded MCM-41 samples is given in *Figure 7.5*. According to this figure, the sample having the pH value of 1.2 had a broader pore size distribution and larger pores whereas the sample having the pH value of 1.4 had a narrower pore size distribution and smaller pores.
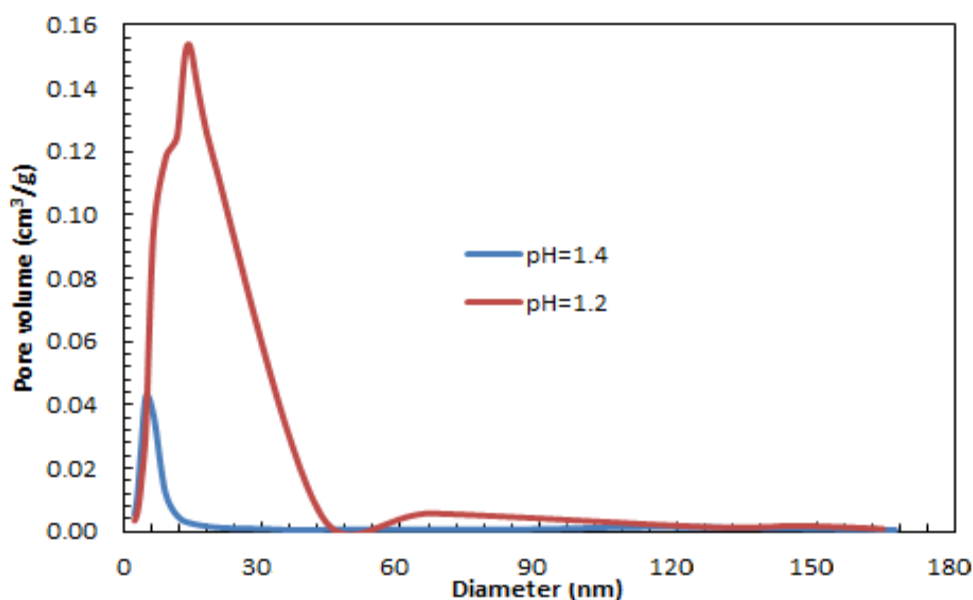

Figure 7.5 Pore size distribution of STA loaded MCM-41 catalysts

7.1.3 SEM Analysis of STA Loaded MCM-41 Samples

Figure 7.6 belongs to the SEM images of the sample having pH value of 1.2. The SEM images were different from the ones given in the literature for MCM-41. The particles of the synthesized material did not have well defined shapes. This was probably because of the reason that STA addition affected the morphology of MCM-41.
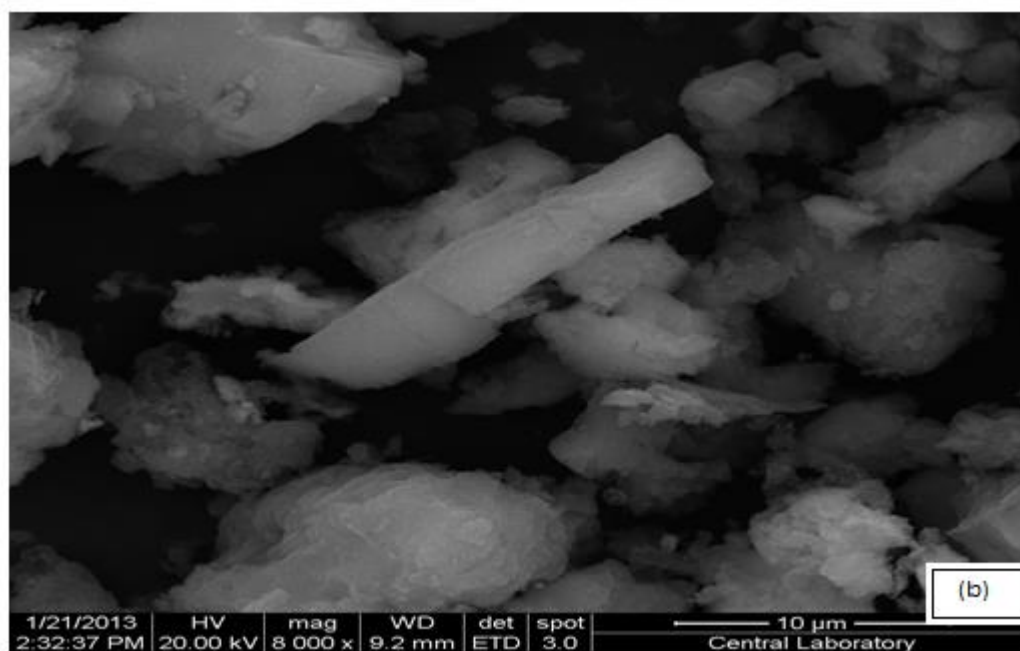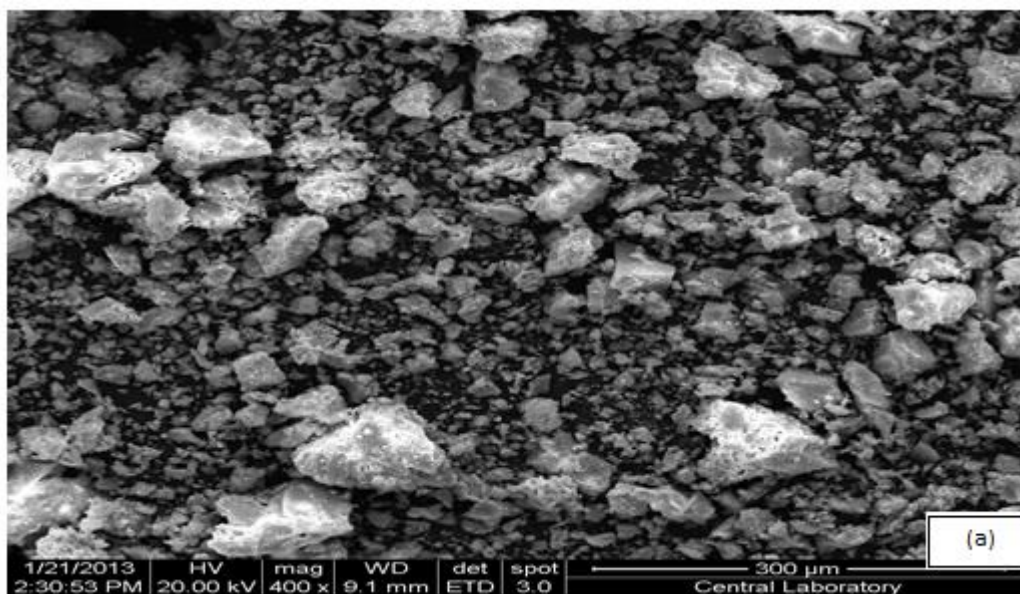
Figure 7.6 SEM images of STA loaded MCM-41 (pH=1.2) catalyst; (a) magnified 400 times and (b) magnified 8000 times

7.1.4 EDS Result of STA Loaded MCM-41 Samples

Figure 7.7 shows the EDS result of STA loaded MCM-41 sample having pH value of 1.2. According to this figure, the W/Si molar ratio of this sample was calculated as 0.17 whereas initial W/Si molar ratio was 0.25 which indicated that the most of the STA was incorporated

46

into the structure. Oxygen in the structure came from the formation of SiO_2 during the synthesis of the catalyst.
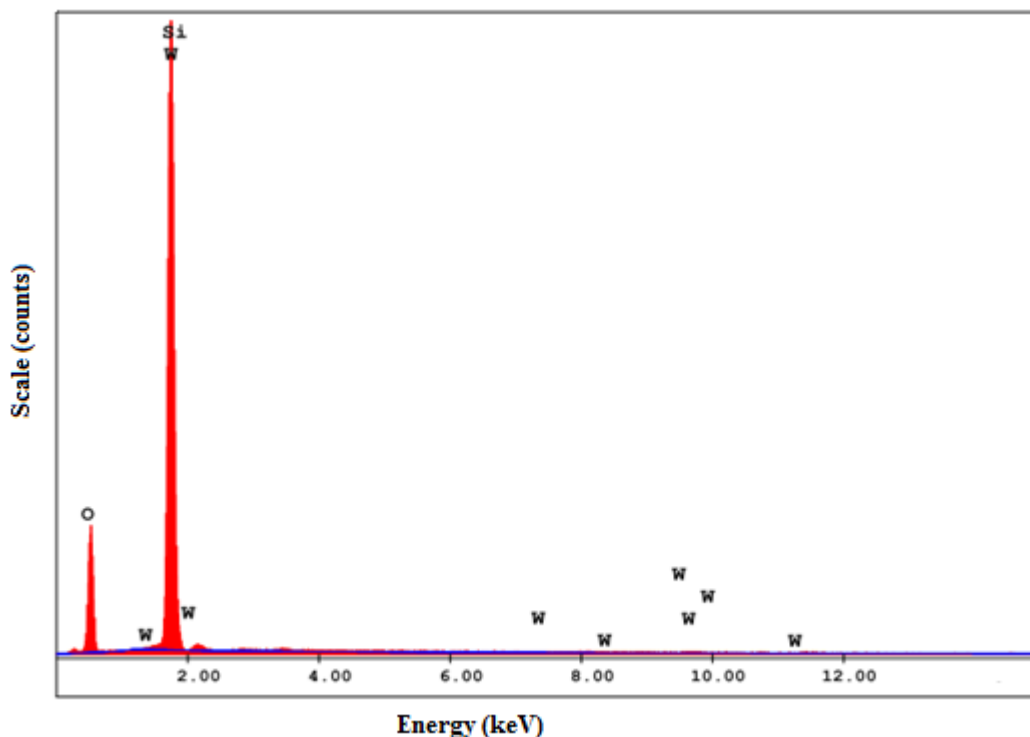

Figure 7.7 EDS result of STA loaded MCM-41 (pH=1.2) catalyst

7.1.5 DRIFTS Analysis of STA Loaded MCM-41 Catalysts

According to the DRIFTS spectra, the bands obtained at 1447 cm^{-1} and 1598 cm^{-1} correspond to the existence of Lewis acid sites, the bands obtained at 1540 cm^{-1} and 1640 cm^{-1} correspond to the existence of Bronsted acid sites and the bands obtained at 1489 cm^{-1} correspond to the existence of both Bronsted and Lewis acid sites [70]. *Figure 7.8* shows the DRIFTS analysis of the syntesized STA loaded MCM-41 catalysts. According to this figure, the sample having pH value of 1.2 showed all the Bronsted and Lewis acidic sites significantly in its structure whereas the sample having pH value of 1.4 had small peaks corresponding to the Bronsted and Lewis acidic sites. It indicated that the sample having pH value of 1.2 had strong Bronsted acid sites in its structure which was important for the pyrolysis reactions.
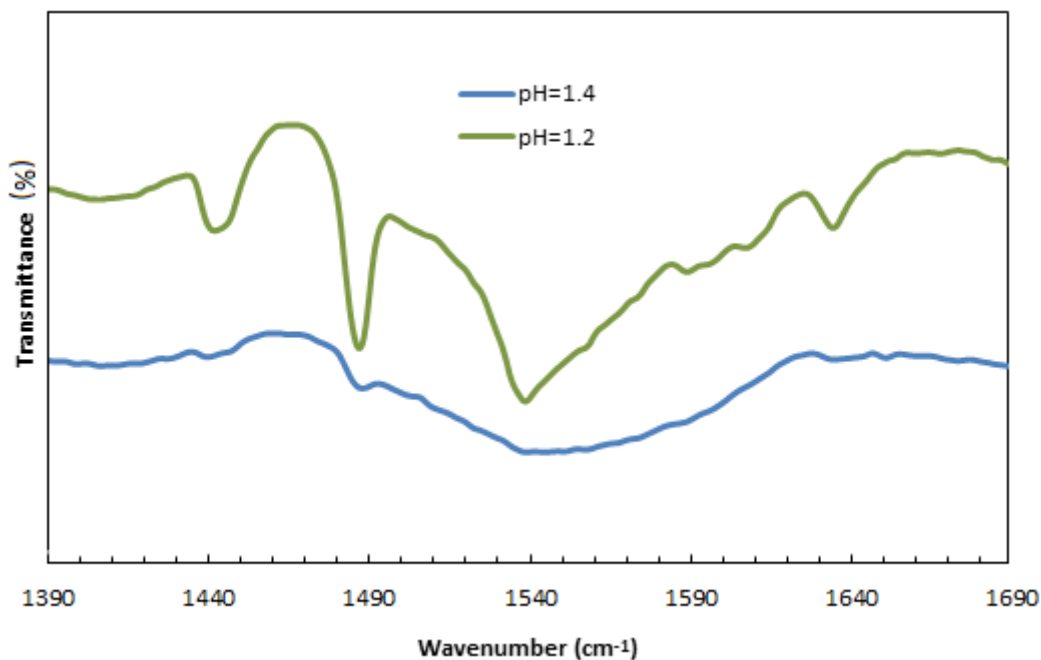
Figure 7.8 DRIFTS spectra of the STA loaded MCM-41 Catalysts

7.2 Characterization Results of STA Loaded SBA-15 Catalyst

STA loaded SBA-15 catalyst was prepared with the W to Si molar ratio of 0.1 and at a calcination temperature of 250 °C.

7.2.1 X-Ray Diffraction Result of STA Loaded SBA-15 Materials

Figure 7.9 illustrates the low angle XRD pattern of the synthesized STA loaded SBA-15 catalyst. A typical SBA-15 material had three peaks corresponding to Bragg angle degrees of 0.92 °, 1.60 ° and 1.85 ° **[29]**. The synthesized STA loaded SBA-15 material had a sharp peak at 1.37 ° and a reflection peak at 2.25 °. This was an indication that STA loading caused some deformation in the ordered structure of SBA-15.

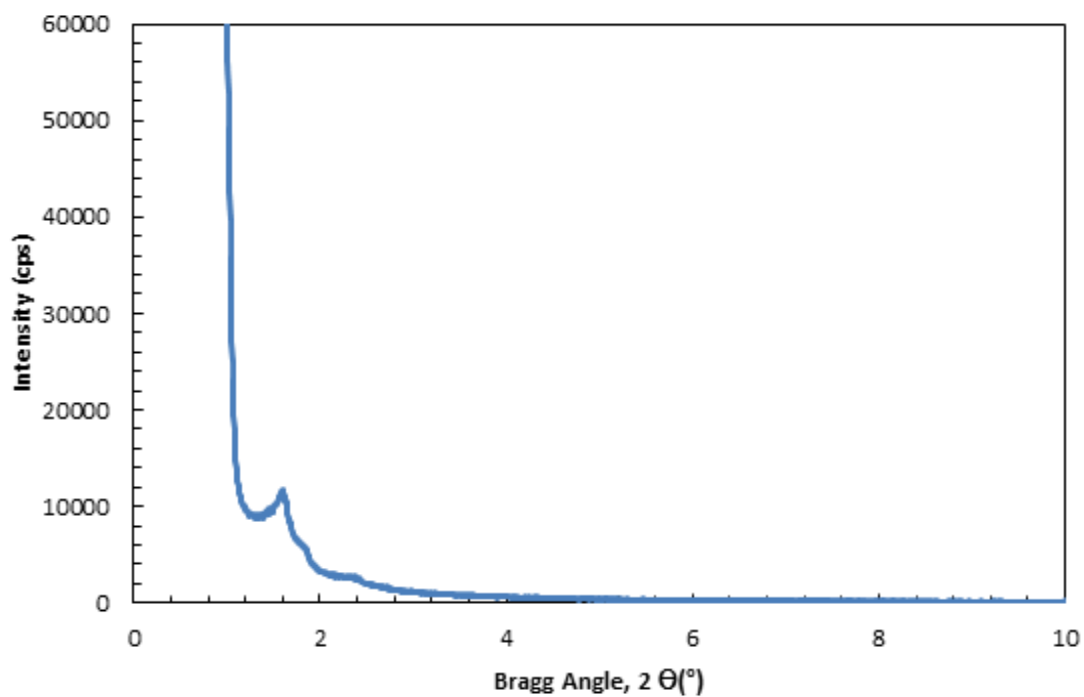**Figure 7.9** Low angle XRD pattern of STA loaded SBA-15 catalyst

Figure 7.10 illustrates the wide angle XRD pattern of STA loaded SBA-15 catalyst. According to the figure, it had a broad peak at 2Ө value of 23.7 ° which indicated the amorphous silica structure of the synthesized catalyst and no characteristic STA peak was observed in the wide angle XRD pattern of STA loaded SBA-15 catalyst.
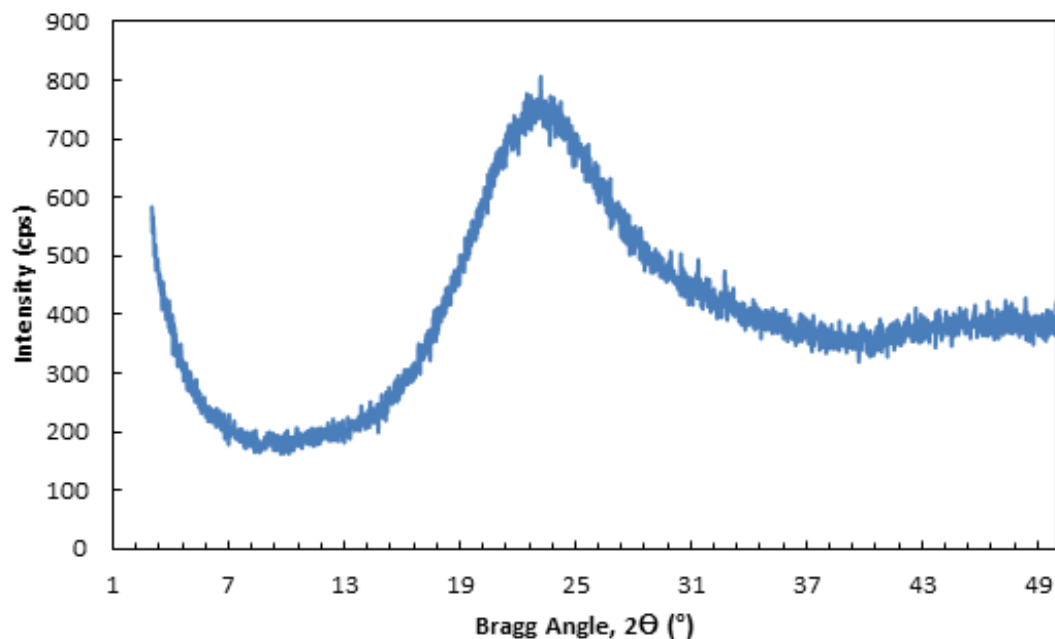
Figure 7.10 Wide angle XRD pattern of STA loaded SBA-15 catalyst

7.2.2 Nitrogen Adsorption-Desorption Results of STA Loaded SBA-15 Materials

Figure 7.11 illustrates the N_2 adsorption-desorption isotherms of the synthesized STA loaded SBA-15 sample. According to this graph, Type IV isotherm of SBA-15 structure was seen which reflected the mesoporous structure of this catalyst. Nitrogen capillary condensation was about relative pressures of 0.62 - 0.82. Adsorption and desorption branches were parallel to each other which indicated a narrow pore size distribution having H1 type of hysteresis.
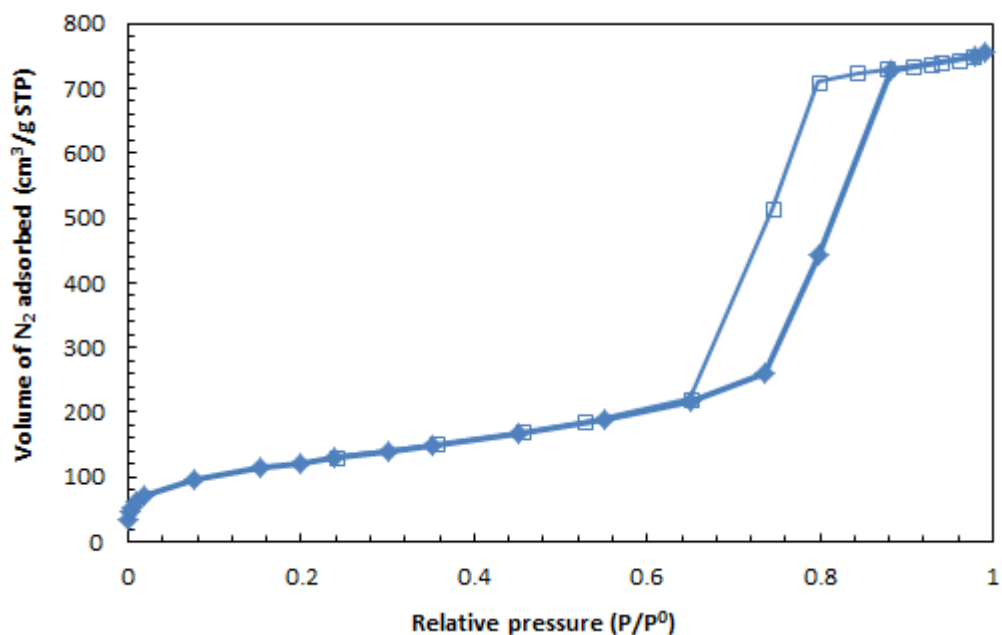
Figure 7.11 N_2 adsorption-desorption isotherms of STA loaded SBA-15 catalyst
(Filled symbols: adsorption, empty symbols: desorption)

Physical properties related to the pore size of this sample obtained from nitrogen adsorption-desorption analysis can be seen in *Table 7.2*. Its BET surface area was 448.49 m^2/g which was the highest surface area value among the other synthesized STA loaded catalysts in this study. Its BET average pore diameter was 10 nm.

Table 7.2 The physical properties of STA loaded SBA-15 catalyst

Property	Value
Surface area (BET)	448.49 m^2/g
Desorption cumulative pore volume (BJH)	1.72 cm^3/g
Desorption average pore diameter (4V/A) (BJH)	7.4 nm
Average pore diameter (4V/A) (BET)	10 nm
Microporosity	12 %

Pore size distribution of this sample is given in *Figure 7.12*. It had a narrow pore size distribution. This result was in good agreement with the nitrogen adsorption-desorption isotherm results.
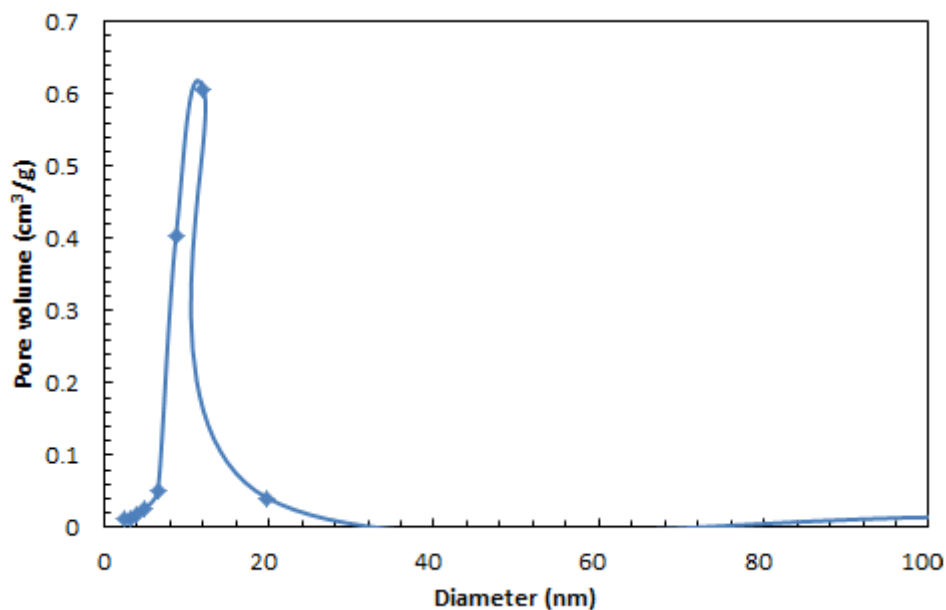
Figure 7.12 Pore size distribution of STA loaded SBA-15 catalyst

7.2.3 SEM Analysis of STA Loaded SBA-15 Catalyst

Figure 7.13 belongs to the SEM images of STA loaded SBA-15 catalyst. The particles of the synthesized material did not have a homogeneous distribution. Also, agglomeration of the catalyst could be seen very clearly which might stem from the preparation steps of the catalyst.

Figure 7.13 SEM images of STA loaded SBA-15 catalyst; (a) magnified 400 times and (b) magnified 8000 times

7.2.4 EDS Result of STA Loaded SBA-15 Catalyst

Figure 7.14 shows the EDS result of STA loaded SBA-15 catalyst. According to this figure, the W/Si molar ratio of this sample was calculated as 0.001 whereas initial W/Si molar ratio was 0.10 which indicated that most of the STA was lost during the synthesis of the catalyst and it didn't incorporate into the structure of the catalyst. Oxygen in the structure came from the formation of SiO_2.
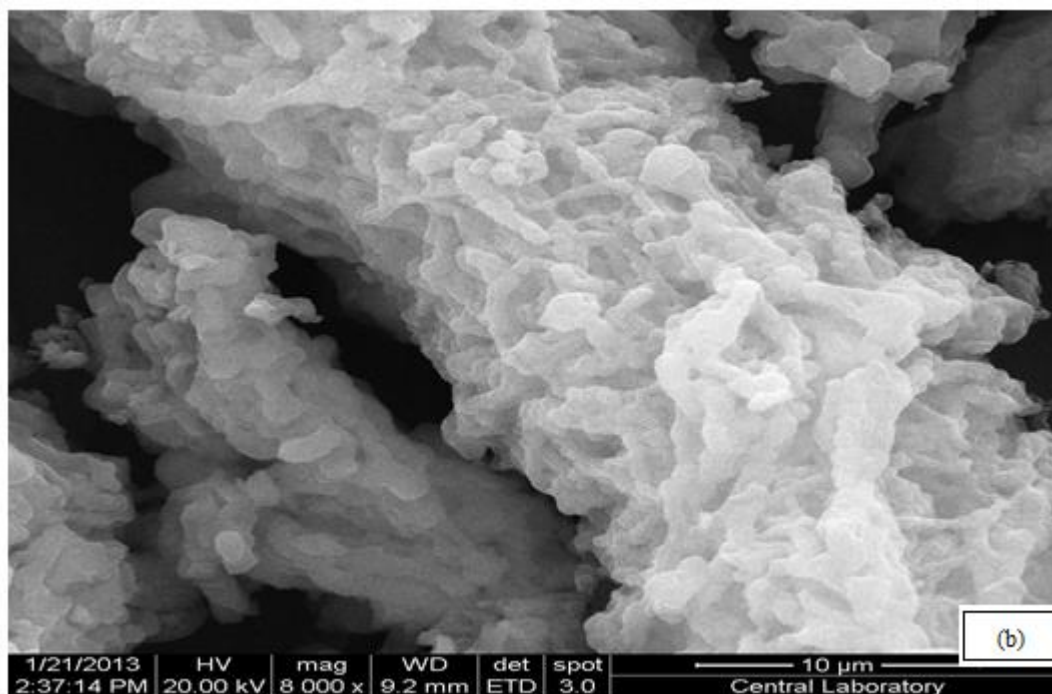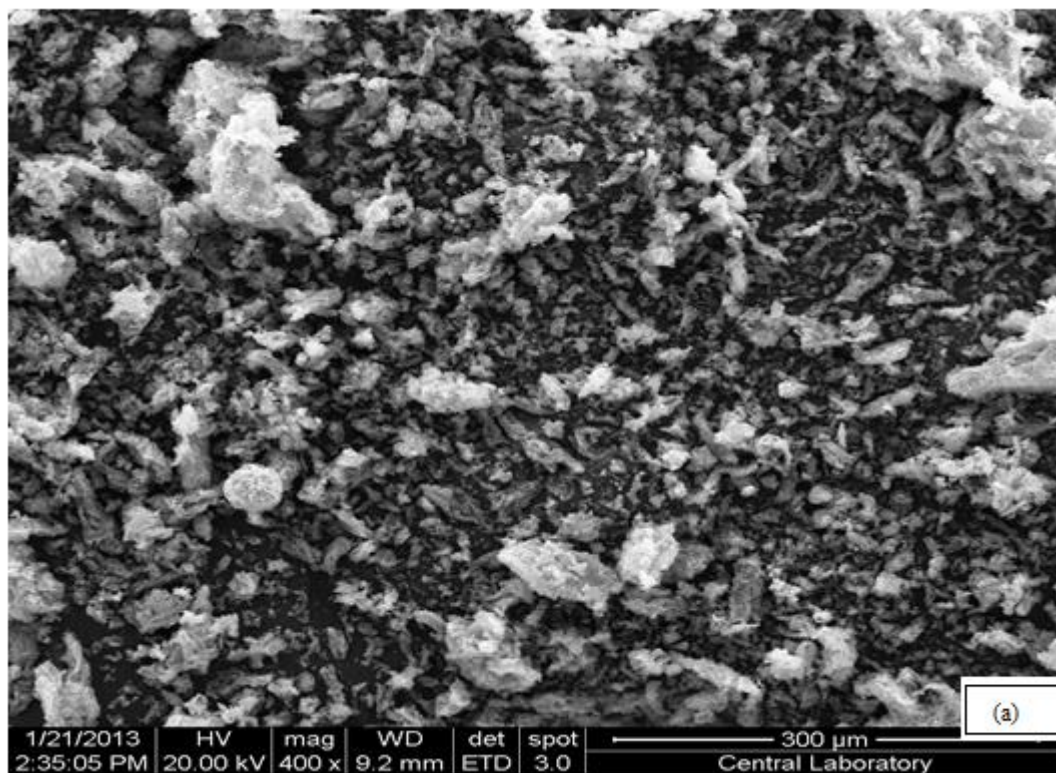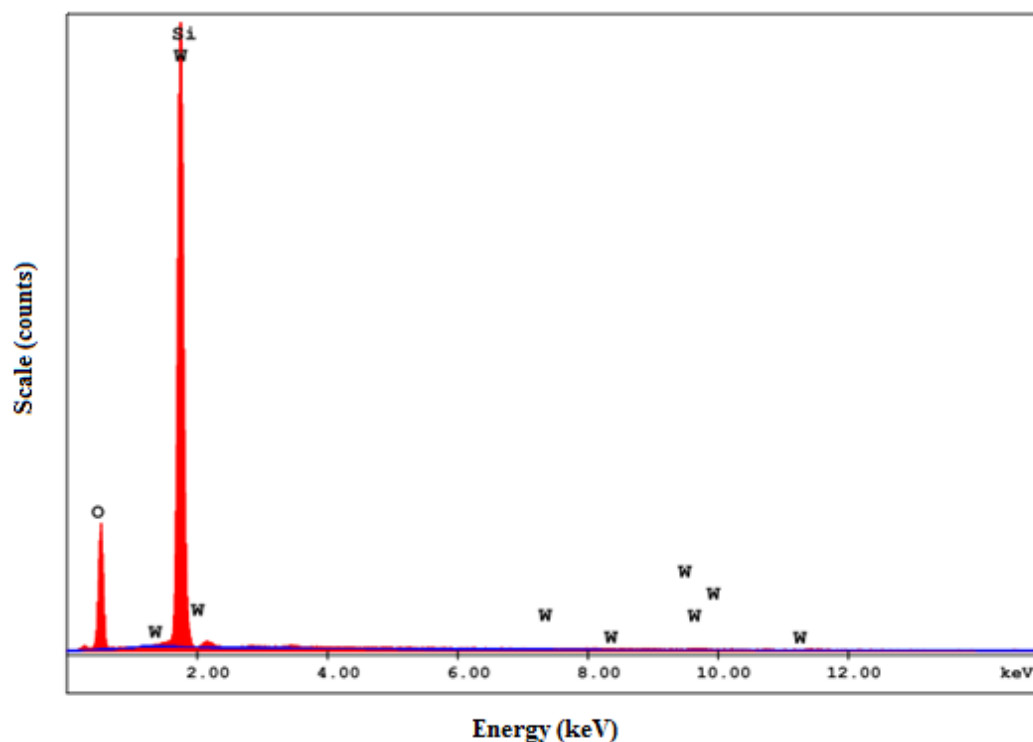

Figure 7.14 EDS result of STA loaded SBA-15 catalyst

7.2.5 DRIFTS Analysis Result of STA Loaded SBA-15 Catalyst

Figure 7.15 shows the DRIFTS spectrum of the synthesized STA loaded SBA-15 catalyst. According to this figure, the sample had a small band at 1447 cm^{-1} indicating the Lewis acidity, a broad band and 1575 cm^{-1} and another small band at 1680 cm^{-1} which might indicate Bronsted acidity including some shifts in the specific Bronsted acidity bands.

Figure 7.15 DRIFTS spectrum of STA loaded SBA-15 catalyst

7.3 Thermogravimetric Analysis Results

Figure 7.16 shows the thermogravimetric analysis trends for STA loaded MCM-41 sample (pH=1.2) using different catalyst to polymer weight ratios (1/2, 1/5 and 1/10). As the weight ratios of catalyst and polymer were different, the remaining catalyst amounts were different for the mixed catalyst polymer samples. The remaining catalyst amount was the maximum for the catalyst to polymer weight ratio of 1/2 and it was the minimum for the catalyst to po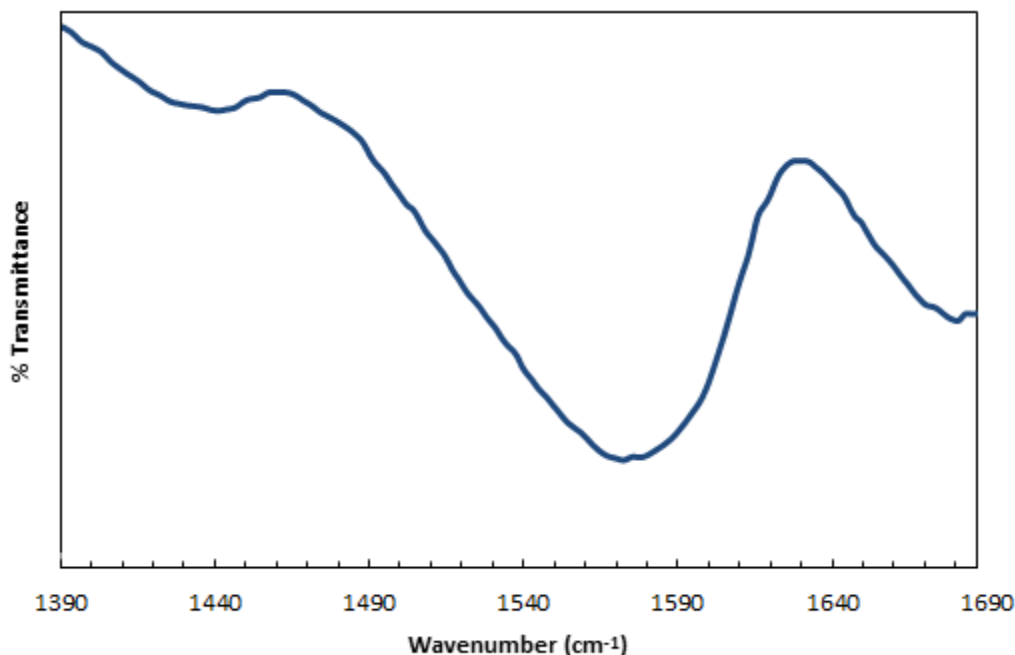lymer weight ratio of 1/10 which was the expected situation. As seen from this figure, at low catalyst ratio (1/5, 1/10), there wasn't a significant shift to the left side in the weight % curve, which indicated that there wasn't a significant decrease in degradation temperature of the pyrolysis reaction. At high catalyst ratio (1/2) there was a significant shift to the left side in the weight % curve, which indicated that there was a significant decrease in the degradation temperature of the pyrolysis reaction.

In thermogravimetric analysis, for a regular proceeding reaction, the entering amount of the catalyst into the reaction had to be the same with the exiting amount of the catalyst from the reaction and all the polymer that was put into the reaction had to be used up at the end of the reaction. Because the amount of the catalyst at the beginning of reaction was same with the catalyst amount at the end of reaction, no carbon deposition on the surface of the catalyst was observed for MCM-41 catalyst having pH value of 1.2.
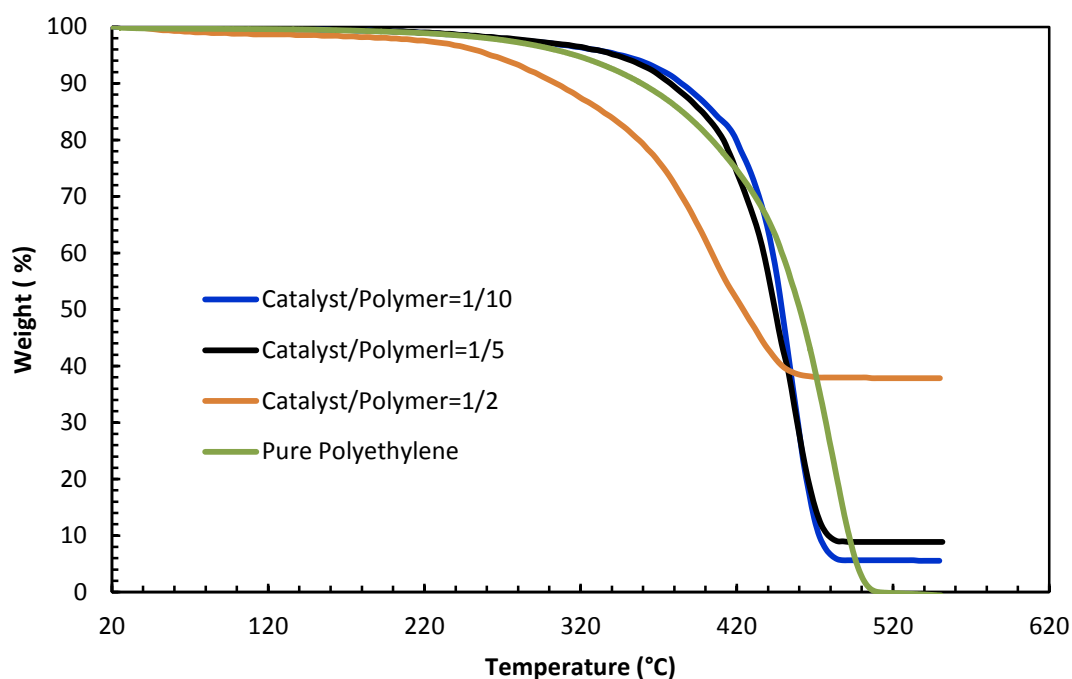
Figure 7.16 TGA graph of STA loaded MCM-41 (pH=1.2) catalyst for different $w_{catalyst}/w_{polymer}$ ratios

Figure 7.17 shows the TGA trends of synthesized STA incorporated MCM-41 and SBA-15 catalysts. According to this graph STA loaded MCM-41 catalyst having pH value of 1.2 and STA loaded SBA-15 catalyst had a good TGA trend for decreasing the polymer decomposition temperature by shifting the weight loss curve to left side due to the presence of the Bronsted acid sites in the catalyst structure.

Thermogravimetric analysis trends for STA loaded SBA-15 catalyst using different $w_{catalyst}/w_{polymer}$ ratios (1/2, 1/5 and 1/10) were illustrated in *Appendix B.2*. It reflected a similar thermogravimetric analysis trend with the synthesized STA loaded MCM-41 catalyst having pH value of 1.2.

Figure 7.17 TGA graph of STA loaded MCM-41 and SBA-15 catalysts
(for $w_{catalyst}/w_{polymer}=1/2$)

7.3.1 Determination of Kinetic Parameters for the Polyetylene Degradation Reaction in the Presence of Catalyst

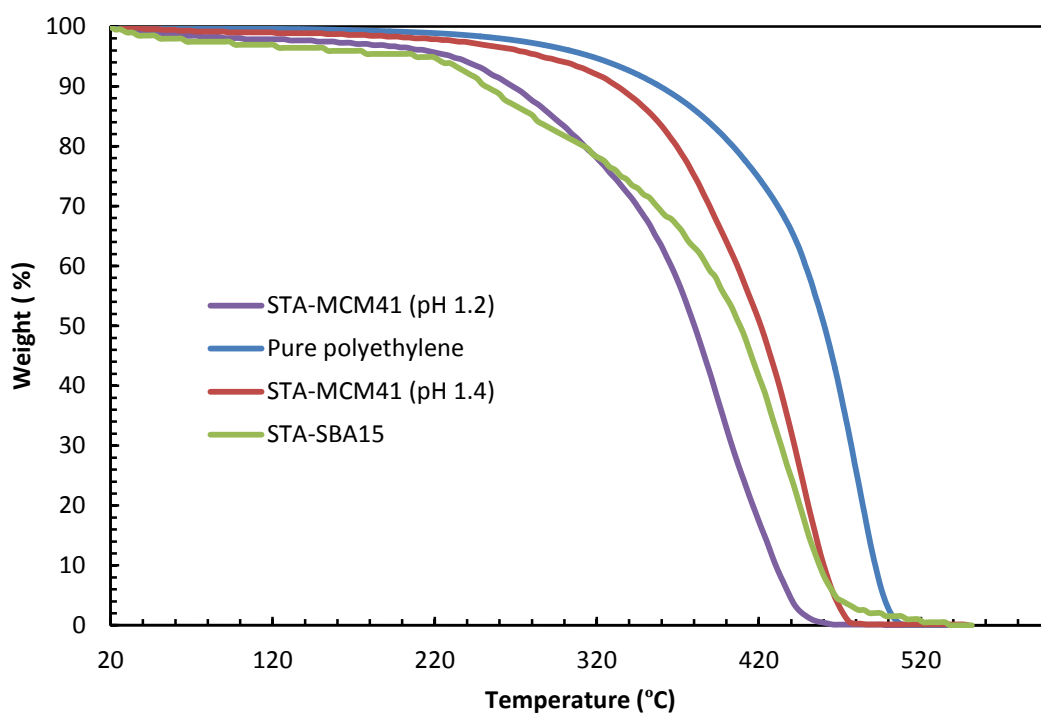Using the TGA data, kinetic parameters for the PE degradation reaction in the presence of catalyst were determined following the procedure reported in the literature studies **[74, 75]**. The activation energy for the polyethylene reaction was found to be 136 kJ/mole. The overall order of the degradation reaction was found to be one. Activation energy values for the polyethylene pyrolysis reaction in the presence of these catalysts were tabulated in *Table 7.3*. A significant decrease in the activation energy of PE degradation reaction was observed in the presence of STA loaded MCM-41 catalyst having pH value of 1.2 and STA loaded SBA-15 catalyst. All the calculations related with the kinetic parameters were given in *Appendix D.*

For STA loaded MCM-41 sample having pH value of 1.4, loading of STA didn't increase the performance of this catalyst significantly and it didn't cause a decrease in activation energy of the pyrolysis reaction. This might be due to the presence of less Bronsted acid sites in the sample having pH value of 1.4 compared to the sample having pH value of 1.2.

Table 7.3 Activation energy values for the polyethylene degradation reaction in the presence of catalysts

Sample name (For $w_{catalyst}/w_{polymer} = 1/2$)	Activation energy, E (kJ/mole)
Pure polyethylene	136.0
STA loaded MCM-41 (pH=1.4)	130.0
STA loaded MCM-41 (pH=1.2)	53.4
STA loaded SBA-15	59.3

Comparing the activation energies with the literature, when Al loaded MCM-41 was used, the activation energy of polyethylene pyrolysis reaction was found as 106 kJ/mole and when TPA loaded SBA-15 was used the activation energy of polyethylene pyrolysis reaction was found as 60.4 kJ/mole **[70],** which had similar effect in decreasing the activation energy of polyethylene pyrolysis reaction compared to the STA loaded MCM-41 (pH=1.2) and SBA-15 samples. So as a result STA loaded MCM-41 sample having pH value of 1.2 and STA loaded SBA-15 catalyst that were synthesized in this study were considered as successful catalysts for the polyethylene degradation reaction.

CHAPTER 8

CONCLUSIONS

In this study STA containing MCM-41 and SBA-15 catalysts were synthesized to observe the performance of these catalysts in pyrolysis reactions of polyethylene.

- XRD pattern of the STA loaded catalyst (pH=1.2) reflected an MCM-like structure and XRD pattern of SBA-15 catalyst exhibited the ordered silica structure of SBA-15.

- All the synthesized STA incorporated catalysts exhibited Type IV isotherms with the H1 and H2 types of hysteresis and their surface areas were in the range of 90.33-448.49 m^2/g. STA incorporated SBA-15 catalyst had the highest surface area among the other synthesized catalysts. The average pore diameters were in the range of 6.5-11 nm which revealed the mesoporosity of these catalysts.

- SEM and EDS results showed that the incorporation of STA into MCM-41 (pH=1.2) was more efficient compared to the STA loaded SBA-15 catalyst. STA loaded SBA-15 catalyst was agglomerated and the particles of STA loaded MCM-41 (pH =1.2) catalyst didn't have well defined shapes.

- DRIFTS analysis of STA loaded MCM-41 (pH=1.2) and SBA-15 catalysts clearly exhibited the existence of Bronsted acid sites in the materials in addition to Lewis acid sites.

- According to thermogravimetric analysis results, STA loaded MCM-41 (pH= 1.2) catalyst reduced the activation energy of the polyethylene pyrolysis reaction from 130 kJ/mole to 53.4 kJ/mole whereas STA loaded SBA-15 catalyst reduced it to 59.3 kJ/mole. Both STA loaded MCM-41 (pH=1.2) and SBA-15 catalysts were active catalysts for PE degradation reaction.

REFERENCES

[1]   Pethrick, R.A., (2010). "*Polymer Science and Technology for Engineers and Scientists*", Whittles publishing, Scotland.

[2]   Aguado, J., Serrano, D.P., San M.G., Escola, J. M., Rodriguez, J.M., (2007). "*Catalytic Activity of Zeolitic and Mesostructured Catalysts in the Cracking of Pure and Waste Polyolefins*", J. Anal. Appl. Pyrolysis **78**, p.153-161.

[3]   Young, R.J., Lovell, P.A., (1991). "*Introduction to Polymers*", Chapman & Hall.

[4]   Billmeyer, F., (1971). "*Polymer Science*", The Science of Large Molecules, Wiley & Sons.

[5]   Kolybaba, M., Tabil, L.G., Panigrahi, S., Crerar, W.J., Powell, T., Wang, B., (2003). "*Biodegradable Polymers: Past, Present and Future*", The American Society of Agricultural Engineers, RRV03-0007.

[6]   Renzini, M.S., Lerici, L.C., Sedran, U., Pierella, L.B., (2011). "*Stability of ZSM-11 and BETA Zeolites During the Catalytic Cracking of Low-Density Polyethylene*, Journal of Analytical and Applied Pyrolysis **92,** 450–455.

[7]   Rudin, A., (1999) "*The Elements of Polymer Science and Engineering, An Introductory Text and Reference for Engineers and Chemists*", Academic Press.

[8]   EPA US Environmental Protection Agency, (2010). http://www.epa.gov/osw/nonhaz/municipal/pubs/msw_2010_rev_factsheet.pdf, Last access date: 30.09.2013.

[9]   Achilias, D.S., (2012). "*Recent Advances in the Chemical Recycling of Polymers PP, PS, LDPE, HDPE, PVC, PC, Nylon, PMMA*", Greece.

[10]   Gaca, P., Drzewiecka, M., Kaleta, W., Kozubek, H., Nowińska K. (2008). "*Catalytic Degradation of Polyethylene over Mesoporous Molecular Sieve MCM–41 Modified with Heteropoly Compounds*", Polish J. of Environ. Stud. **17**, No. 1, 25-31.

[11]   Lin, Y.H., Yangx, M.H., Yeh, T.F., Ger, M.D., (2004). "*Catalytic Degradation of High Density Polyethylene Over Mesoporous and Microporous Catalysts in a Fluidised-Bed Reactor*", Polymer Degradation and Stability **86**, 121-128.

[12]   Kim, S., Jang, E.S., Kim, J.S., Jeon, J.K., Yim, H.J. 4, Kim, J.M., Jung, J., Park, Y.K., (2006). "*Catalytic Degradation of High Density Polyethylene Over Post Grafted MCM-41 Catalyst: Kinetic Study*", Studies in Surface Science and Catalysis **159**, p. 437.

[13]   Pierella, L.B., Renzini, S., Anunziata, O.A., (2005). "*Catalytic Degradation of High Density Polyethylene Over Microporous and Mesoporous Materials*", Microporous and Mesoporous Materials **81**, 155–159.

[14] González, Y.S., Costa, C., Márquez, M.C., Ramos, P. (2011). *"Thermal and Catalytic Degradation of Polyethylene Wastes in the Presence of Silica Gel, 5A Molecular Sieve and Activated Carbon"*, Journal of Hazardous Materials **187,** 101.

[15] Ali, M.F., Qureshi, M. S., (2011). *"Catalyzed Pyrolysis of Plastics: A Thermogravimetric Study"*, African Journal of Pure and Applied Chemistry **5**, 284-292.

[16] Akpanudoh, N.S., Gobin, K., Manos, G., (2005). *"Effect of Polymer to Catalyst Ratio/Acidity Content"*, Journal of Molecular Catalysis A: Chemical **235**, 67–73.

[17] Ali, M.F., Siddiqui M.N., (2005). *"Thermal and Catalytic Decomposition Behavior of PVC Mixed Plastics with Petroleum Residue"*, J. Anal. Appl. Pyrol. **74**, 282-289.

[18] Norvegian Technical University, Chemical Engineering Dept., (2012). http://www.chemeng.ntnu.no. Last access date: 01.09.2013.

[19] Park, M., Shin, S.C., Choi, C.L., Lee, D.H., Lim, W.T., Komarneni, S., Kim, M.C., Choi, J., Heo, N.H., (2001). *"Role of Framework on NH_4NO_3 Occlusion in Zeolite Pores"*, Microporous and Mesoporous Materials **50**, 91-99.

[20] Antunes, A.P., Ribeiro, M.F., Silva, J.M., Ribeiro, F.R., Magnoux, P. and Guisnet, M. (2001). *"Catalytic Oxidation of Toluene Over Cunahy Zeolites Coke Formation and Removal"*, Applied Catalysis B: Environmental **33**, 149-164.

[21] Chua, Y.T. , Stair, P.C., (2003). "A*n Ultraviolet Raman Spectroscopic Study of Coke Formation in Methanol to Hydrocarbons Conversion over Zeolite HMFI"*, Journal of Catalysis **213**, 29.

[22] Øye G., Sjöblom J., Stöcker M., (2001) *"Synthesis, Characterization and Potential Applications of New Materials in the Mesoporous Range"*, Adv. in Coll. and Inter. Sci. **89**, 439-466.

[23] Xu, J., (1999). "S*pectroscopic Studies of Synthesis, Modification and Characterization of Novel Mesoporous Molecular Sieves"*, PhD Thesis, University of Houston.

[24] Taguchi, A., Schüth, F., (2005). *"Ordered Mesoporous Materials in Catalysis"*, Microporous and Mesoporous Materials **77**, p.1-45.

[25] Collart, O., (2003). *"Nanodesign of an Aluminasilicate Framework in Mesoporous MCM-48 Architecture"*, PhD Thesis, University of Antwerpen.

[26] Sener, C., (2006). **"***Synthesis and Characterization Of Pd-MCM-Type Mesoporous Nanocomposite Materials",* MS Thesis, METU.

[27] Beck, J.S., Kresge, C.T., Leonowicz, M.E., Roth, W.J. and Vartuli, J.C., 1992. *"Ordered Mesoporous Molecular Sieves Synthesized by Liquid Crystal Templating Mechanism"*, Nature **359**, p. 710.

[28] Ciesla, U., Schüth, F. (1999). "*Ordered Mesoporous Materials*", Microporous and Mesoporous Materials **27**, p.131-149.

[29] Zhao, D., Feng, J., Huo, Q., Melosh, N., Fredrickson, G.H., Chmelka, B.F., Stucky, G.D., (1998). Science **279**, p. 548.

[30] University of Bristol, School of Chemistry, http://www.chm.bris.ac.uk, Last access date: 01.09.2013.

[31] Malesia University of Technology, Zeolite and Nanostructured Materials Laboratory http://www.zeolite.utm.my, Last access date: 01.09.2013.

[32] Chen, L.Y., Jaenicke, S. (1997). "*Thermal and Hydrothermal Stability of Framework-Substituted MCM-41 Mesoporous Materials*, Microporous Material", **12**, 323-330.

[33] Cheng, C.F., Chou, S.H., Cheng, P.V., Cheng, H.H., (2007). "*Control of Wall Thickness and Extraordinarily High Hydrothermal Stability of Nanoporous MCM-41 Silica",* Journal of Chinese Chemical Society, **54**, 35-40.

[34] Kosslick, H., Lischke, G., Walther, G., Storek, W., Martin, A. and Fricke, R. (1997). "*Physico-Chemical and Catalytic Properties of Al-, Ga-, and Fe- Substituted Mesoporous Materials Related to MCM-41*". Microporous Material, **9**, p. 13-33.

[35] Mohamed, A. B., (2005). "*Synthesis, Characterization and Activity of Al- MCM-41 Catalyst for Hydroxyalkylation of Epoxides*", MS Thesis, Malaysia Teknology University.

[36] University of Strathclyde Science, Department of Pure and Applied Chemistry http://info.chem.strath.ac.uk/people/academic/lorraine_gibson/research/sorbents, Last access date: 01.09.2013

[37] Güçbilmez, Y., (2005). "*Vanadium and Molybdenum Incorporated MCM-41 Catalysts for Selective Oxidation of Ethanol*", PhD Thesis, METU.

[38] Zhou, Q.,Zheng, L., Wang, Y.Z., Zhao, G.M., Wang, B., (2004). "*Catalytic Degradation of Low Density Polyethylene and Polypropylene Using Modified ZSM-5 Zeolites*", Polymer Degradation and Stability **84**, 493-497.

[39] Fulvio, P. F., Pikus, S., Jaroniec, M. (2005). "*Short-Time Synthesis of SBA-15 Using Various Silica Sources*", Journal of Colloid and Interface Science **287**, p.717-720.

[40] Vinu, A., Murugesan, V., Böhlmann, W., Hartmann, M. (2004). "*An Optimized Procedure for the Synthesis of AlSBA-15 with Large Pore Diameter and High Aluminum Content*", J. Phys. Chem. B, **108**, p.11496-11505.

[41] Galarneau, A., Cambon, H., Renzo, F., Ryoo, R., Choi, M., Fajula, F., (2003). "*Microporosity and Connections Between Pores in SBA-15 Mesostructured Silicas as a Function of the Temperature of Synthesis*" , New J. Chem., **27**, p. 73–79.

[42] Fairuz, M., (2010). "*Preparation and Characterization of SBA-15 Supported Co/Zn Catalyst for Fisher Tropsch Synthesis: Effect of Cobalt Loading*", MS Thesis, University of Malaysia

[43] Schwarz J. A., (1995). "*Methods for Preparation of Catalytic Materials*", Chem. Rev. **95**, 477-510.

[44] Arınan, A., (2010). **"*Direct Synthesis Of Dimethyl Ether (DME) from Synthesis Gas Using Novel Catalysts*"**, MS Thesis, METU.

[45] Sun, K., Lu, W., Qiu, F., Liu, S., Xu, X., (2003). "*Direct Synthesis of DME Over Bifunctional Catalyst: Surface Properties and Catalytic Performance*", Applied Catalysis A: General **252**, 243-249.

[46] Utreicht University, April, 2007, http://www.library.uu.nl/digiarchief/dip/diss/2003-0325- 14324/inhoud.htm, Last access date: 30.09.2013.

[47] Gündüz, S., (2011). "*Sorption Enhanced Ethanol Reforming Over Cobalt, Nickel Incorporated MCM-41 for Hydrogen Production*", MS Thesis, METU

[48] Powershow, (2012). http://www.powershow.com/view/62bb3-ZmU0N/Physi-sorption_Methods_and_Techniques_powerpoint_ppt_presentation, Last access date: 01.09.2013.

[49] Özdoğan, E., (2007). "*Steam Reforming of Ethanol for Hydogen Production Using Cu-MCM41 and Ni-MCM-41Type Mesoporous Catalytic Materials*, MS Thesis, METU.

[50] Misono, M. (2000). "*Acid Catalysts for Clean Production: Green Aspects of Heteropoly acid Catalysts*", Surface Chemistry and Catalysis **3**, p.472.

[51] Okuhara, T., Mizuno, N., Misono, M. (2001). "*Catalysis by Heteropoly Compounds: Recent Developments*", Applied Catalysis **222**, p. 63, 72.

[52] Varışlı, D. (2007). "*Kinetic Studies for Dimethyl Ether and Diethyl Ether Production*", PhD Thesis, METU.

[53] Çiftçi, A., (2009). "*Nanocomposite Nafion and Heteropolyacid Incorporated Mesoporous Catalysts for Dimethyl Ether Synthesis from Methanol*", MS Thesis, METU.

[54] Corma, A., (1997). "*From Microporous to Mesoporous Molecular Sieve Materials and Their Use in Catalysis*", Chem. Rev.. **97**, 2373-2419.

[55] Kozhevnikov, I.V., (1998), "*Catalysis by Heteropoly Acids and Multicomponent Polyoxometalates in Liquid-Phase Reactions*", Chem. Rev. **98**, pp.171-198.

[56] Tarlani, A., Abedini, M., Nemati, A., Khabaz, M., Amini, M.M., (2006). "*Immobilization of Keggin and Preyssler Tungsten Heteropolyacids on Various Functionalized Silica*", Journal of Colloid and Interface Science **303**, 32-38.

[57] Haber, J., Pamin, K., Matachowski, L., Mucha, D., (2003). "*Catalytic Performance of the Dodecatungstophosphoric Acid on Different Supports*", Applied Catalysis A: General **256**, pp. 141-152.

[58] Liu, Q.Y., Wu, W.L., Wang, J., Ren, X.Q., Wang, Y.R., (2004). "*Characterization of 12-Tungstophosphoric Acid Impregnatined on Mesoporous Silica SBA-15 and Its Catalytic Performance in Isopropylation of Naphthalene with Isoproponol*", Microporous and Mesoporous Materials **76**, 51-60.

[59] Jalil, P.A., Tabet, N., Faiz, M., Hamdan, N.M., Hussain, Z., (2004). "*Surface Investigation on Thermal Stability of Tungstophosphoric Acid Supported on MCM-41 Using Synchrotron Radiation*", Applied Catalysis A: General **257**, 1-6.

[60] Devassy, B.M., (2005). "*Zirconia-supported heteropolyacids: Characterization and Catalytic Behavior in Liqud-Phase Veratrole Benzoylation*", Journal of Catalysis **236**, p. 313

[61] Zhang, Y., Du, Z., Min, E., (2004). "*Effect of Acidity and Structures of Supported Tungstophosphoric Acid on Its Catalytic Acitivity and Selectivity in the Liquid Phase Synthesis of Ethylbenzene*", Catalysis Today **93**, p. 327-332.

[62] Nowińska, K., Formaniak, R., Kaleta, W., Wącław, A., (2003). "*Heteropoly Compounds Incorporated Into Mesoporous Material Structure*", Applied Catalysis A: General **256**, p. 115-123.

[63] Staiti, P., Freni, S., Hocevar, S., (1999). "*Synthesis and Characterization of Protonconducting Materials Containing Dodecatungstophosphoric and Dodecatungstosilic Acid Supported on Silica*", Journal of Power Sources **79**, p. 250-255.

[64] Pizzio, L.R., Caceres, C.V., Blanco, M.N., (1998). "*Acid Catalysts Prepared by Impregnaton of Tungstophosphoric Acid Solutions on Different Supports*", Applied Catalysis A: General **167**, p.283-294.

[65] Değirmenci, L., Oktar, C., Doğu, G., (2010), "*ETBE Synthesis over Silicotungstic Acid and Tungstophosphoric Acid Catalysts Calcined at Different Temperatures*", Fuel Processing Technology **91**, 737–742.

[66] Herrera, E., Kwak, J., Hu, J., Wang, Y., Peden, C. (2008). "*Effects of Novel Supports on the Physical and Catalytic Properties of Tungstophosphoric Acid for Alcohol Dehydration Reactions*", Top Catal **49**, p. 259, 260, 266.

[67] Garforth, A., Fiddy, S., Lin, Y.-H., Ghanbari Siakhali, A., Sharatt, P.N., Dwyer, J. (1997). "*Catalytic Degradation of High Density Polyethylene: An Evaluation of Mesoporous and Microporous Catalysts Using Thermal Analysis*", Thermochimica Acta **294**, p.65-69.

[68] Mastral, J.F., Berrueco, C., Gea, M., Ceamanos, J., (2006). "*Catalytic Degradation of High Density Polyethylene over Nanocrystalline HZSM-5 Zeolite*", Polymer Degradation and Stability **91**, 3330-3338.

[69] Stefanis A.D., Kaciulis, S., Pandolfi L., (2007). "*Preparation and Characterization of Fe-MCM-41 Catalysts Employed in the Degradation of Plastic Materials*", Microporous and Mesoporous Materials **99**, 140–148.

[70] Aydemir, B. (2010), "*Synthesis of Mesoporous Catalysts and Their Performance in Pyrolysis of Polyethylene*", MS Thesis, METU.

[71] Sarathy, S., Wallis, M.D., Bhatia. S.K., (2010). "*Effect of Catalyst Loading on Kinetics of Catalytic Degradation of High Density Polyethylene: Experiment and Modelling*", Chemical Engineering Science **65**, 796 –806.

[72] Jin, S., Cui, K., Guan, H., Yang, M., Liu, L., Lan, C., (2012). "*Preparation of Mesoporous MCM-41 from Natural Sepiolite and Its Catalytic Activity of Cracking Waste Polystyrene Plastics*", Applied Clay Science **56**, 1-6.

[73] Obalı, Z., Sezgi, N, A., Doğu, T., (2011). "*The Synthesis and Characterization of Aluminum Loaded SBA-Type Materials as Catalyst for Polypropylene Degradation Reaction*", Chemical Engineering Journal **176-177**, p.202-210.

[74] Obalı, Z., (2010). "*Synthesis of Aluminum Incorporated Mesoporous Catalysts for Pyrolysis of Polypropylene*", PhD Thesis, METU.

[75] Aydemir, B., Sezgi, N.A., Doğu, T., (2012). "*Synthesis of TPA Impregnated SBA-15 Catalysts and Their Performance in Polyethylene Degradation Reaction*", AIChE Journal **58**, p.2466-2472.

[76] Obalı, Z., Sezgi, N.A., Doğu, T., (2012). "*Catalytic Degradation of Polypropylene over Alumina Loaded Mesoporous Catalysts*", Chemical Engineering Journal **207-208**, p.421-425.

CALCULATION OF STA AMOUNTS TO BE INCORPORATED INTO CATALYSTS

A.1 Calculation of STA Amounts to Be Incorporated into MCM-41 Catalysts

It was assumed that MCM-41 only consisted of silica.

The reagents used in the synthesis steps were as follows:

> TEOS, $C_8H_{20}O_4Si$ (MW_{TEOS}= 208.33 g/mol, d_{TEOS}=0.94 g/cm^3, V_{TEOS}=15.64 ml used for the synthesis solution)
> STA, $H_4O_{40}SiW_{12}$ (MW_{STA}=2878.17 g/mole)

$$m_{TEOS}=V_{TEOS}*d_{TEOS} \tag{A.1}$$

m_{TEOS}=15.64ml*0.94g/ml
m_{TEOS}=14.70 g

$$n_{TEOS}=m_{TEOS}/MW_{TEOS} \tag{A.2}$$

n_{TEOS}=14.70g/208.33 g/mole
n_{TEOS}=0.07057 mole

As all the silica structure of the catalyst consisted of silica, $n_{TEOS}=n_{Si}$ in the catalyst. For a desired ratio of W/Si, the mole number of W was calculated using equation (A.3):

$$n_W/n_{Si}=D \tag{A.3}$$

where D is the desired ratio of W/Si. When the mole number of W was calculated, it was known that 1 mole of STA had 12 moles of W which indicated that $n_{STA}=n_w/12$

$$m_{STA}=(n_W/12)*MW_{STA} \tag{A.4}$$

For D=0.10, n_{Si}=0.07057
n_W/n_{Si}=0.10
n_W=0.007057

m_{STA}=(0.007057/12)*2878.17
m_{STA}=1.69 g

For D=0.25, n_{Si}=0.07057
n_W/n_{Si}=0.25; n_W=0.0176
m_{STA}=(0.0176/12)*2878.17
m_{STA}=4.23 g STA.

A.2 Calculation of STA Amounts to Be Incorporated into SBA-15 Catalysts

The calculations were done assuming that all SBA-15 silica structure was consisted of silica.

The reagents used in the synthesis steps were as follows:
> TEOS, $C_8H_{20}O_4Si$ (MW$_{TEOS}$= 208.33 g/mol, d$_{TEOS}$=0.94 g/cm^3, m$_{TEOS}$=8 g used for the synthesis solution)
> STA, $H_4O_{40}SiW_{12}$ (mw$_{STA}$=2878.17 g/mole)

$$n_{TEOS}=m_{TEOS}/MW_{TEOS} \tag{A.5}$$

n_{TEOS}=8g/208.33 g.mol^{-1}
n_{TEOS}=0.0384 mole

As all the silica structure of the catalyst consists of silica, $n_{TEOS}=n_{Si}$ in the catalyst. For a desired ratio of W/Si, the mole number of W was calculated using equation A.6:

$$n_W/n_{Si}=D \tag{A.6}$$

where D is the desired ratio of W/Si. When the mole number of W was calculated, it was known that 1 mole of STA had 12 moles of W which indicated that $n_{STA}=n_w/12$

$$m_{STA}=(n_W/12)*MW_{STA} \tag{A.7}$$

For D=0.10, n_{Si}=0.0384 mole
n_W/n_{Si}=0.10
n_W=0.00384

m_{STA}=(0.00384/12)*2878.17
m_{STA}=0.921 g STA.

TGA GRAPHS OF SOME CATALYSTS

B.1 TGA-DTA Graph of Uncalcined STA Loaded MCM-41 Catalyst

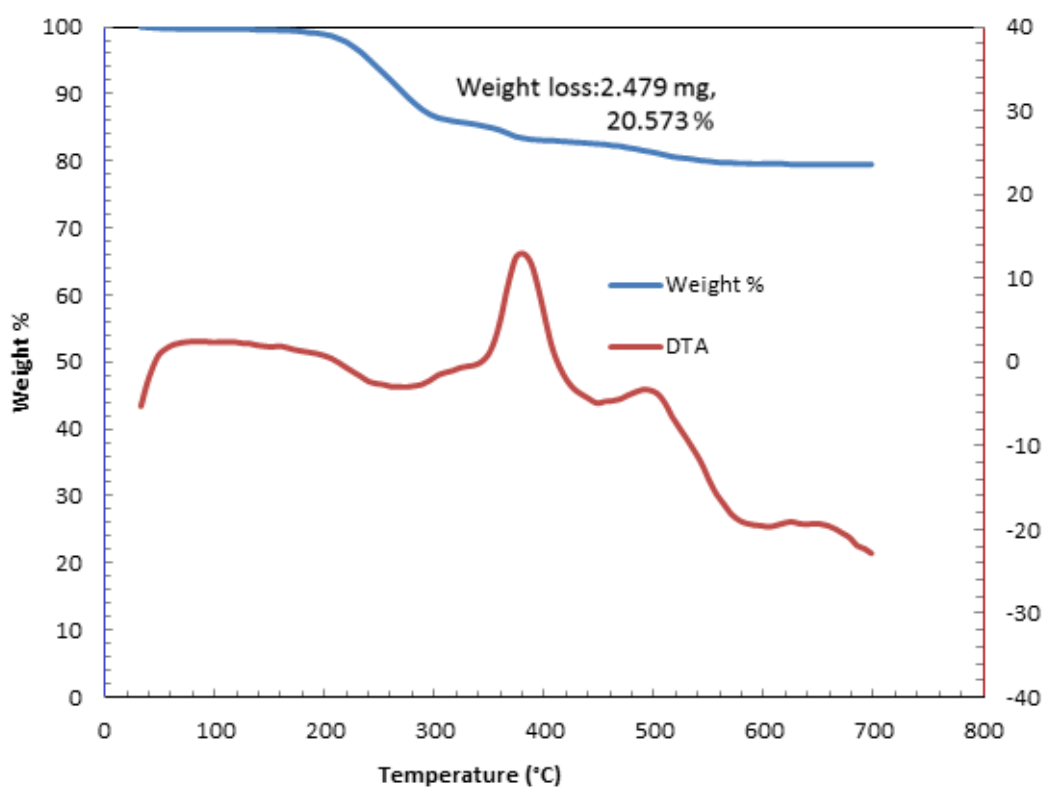**Figure B.1** TGA-DTA graph of uncalcined STA loaded MCM-41 catalyst (pH=1.4)

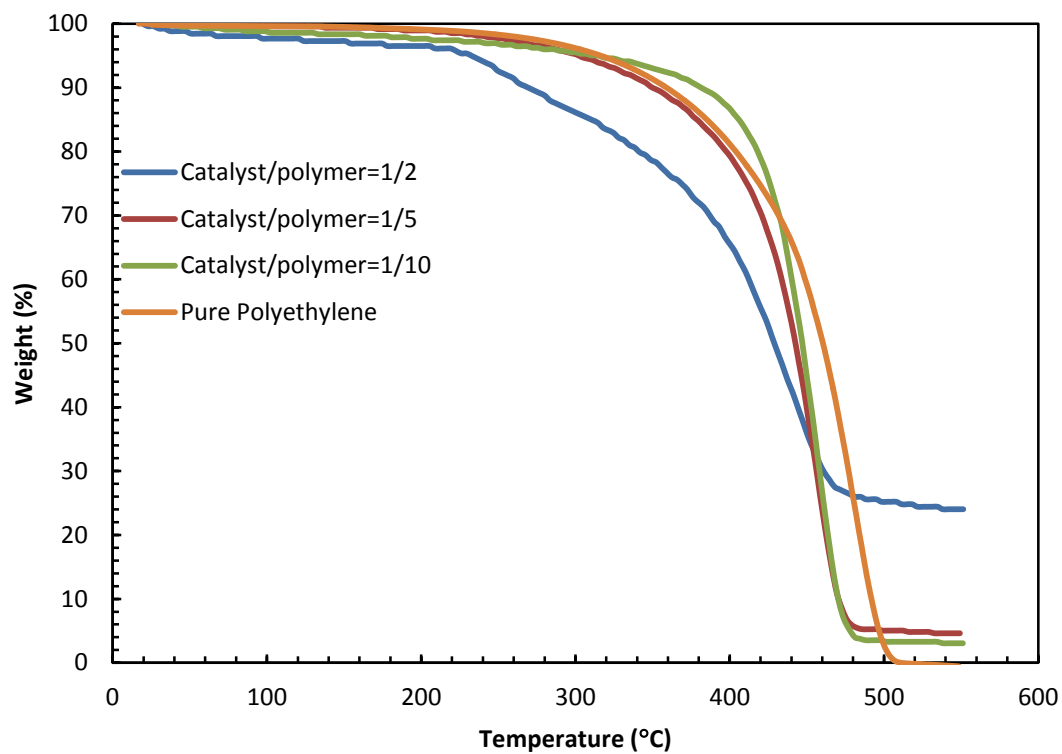**B.2 TGA Graph of STA Loaded SBA-15 Catalyst for Different $W_{Catalyst}/W_{Polymer}$ Ratios**

Figure B.2 TGA graph of STA loaded SBA-15 material for different catalyst to polymer weight ratios

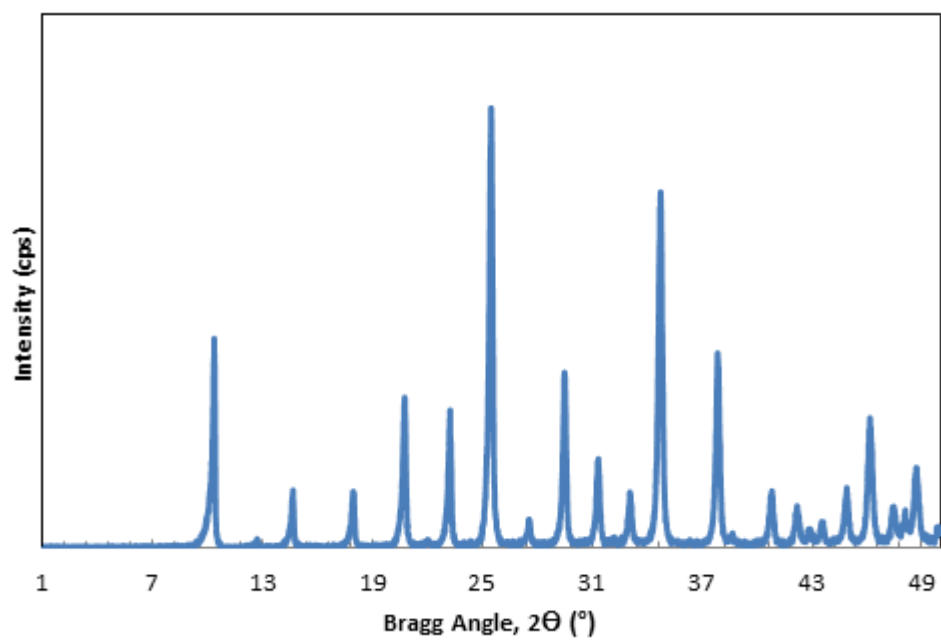# XRD PATTERNS OF SOME MATERIALS

C.1 XRD Pattern of Pure STA

Figure C.1 XRD pattern of pure STA

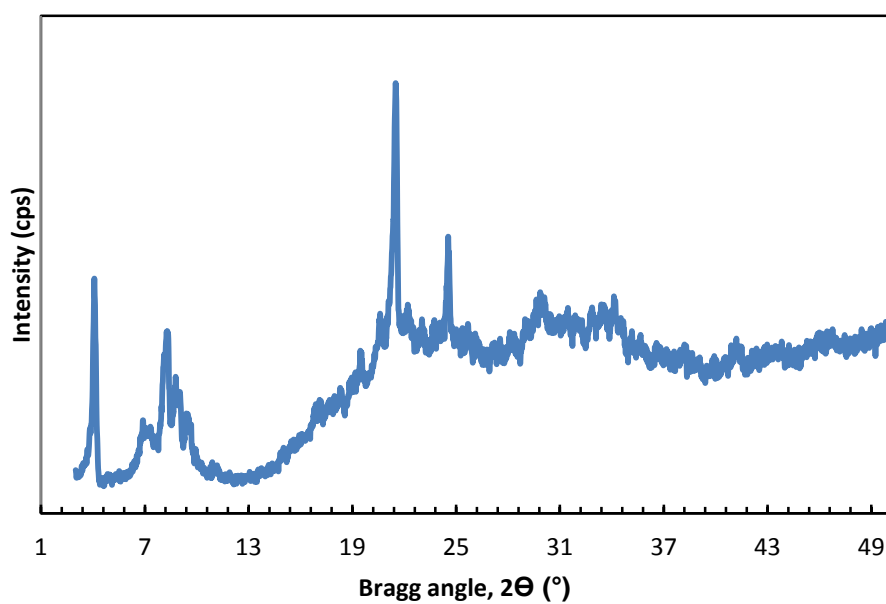**C.2 XRD Pattern of Uncalcined STA Loaded MCM-41 Catalyst (pH=1.2)**

Figure C.2 XRD pattern of uncalcined STA loaded MCM-41 catalyst (pH=1.2)

APPENDIX D

DETERMINATION OF KINETIC PARAMETERS FROM TGA DATA

In a polymer degradation reaction, the solid state reaction can be indicated with the following equation:

$aA_{(s)} \rightarrow bB_{(s)} + cC_{(g)}$ where A is the polymer that enters the pyrolysis reaction.

For the calculation of kinetic parameters from thermogravimetric analysis data, the same method given in the literature **[73, 74]** was applied.

The kinetics of the reaction is expressed with the following equation:

$$\frac{da}{dt} = Ae^{(-E/RT)}(1-a)^n \qquad (D.1)$$

where A represents preexponential factor, E is the activation energy of the reaction, α is the polymer's decomposition fraction at a specified time and R is the gas constant, n is the overall reaction order.

The decomposition fraction at time t can be written as:

$$a = \frac{w_0 - w_t}{w_0 - w_\infty} \qquad (D.2)$$

where w_0 is the initial weight, w_t is the weight at time t and w_∞ is the final weight.

The temperature at any time can be written as:

$$T = T_0 + qt \qquad (D.3)$$

where q is the heating rate, T_o is the initial temperature and t is the time.

By inserting equation (D.3) into equation (D.1) and rearranging, the rate equation becomes as:

$$\frac{da}{(1-a)^n} = \frac{A}{q}\exp(-\frac{E}{RT})dT \qquad (D.4)$$

In order to integrate the equation above, the substitution method $u=E/RT$ is used:

$$\int_{u}^{\infty} e^{-u} u^{-b} du = u^{1-u} \sum_{n=0}^{n=\infty} \frac{(-1)^n (b)_n}{u^{n+1}} \tag{D.5}$$

The boundary conditions of the equation (D.5) are: $a = 0$; $T = T_0$ and $a = a$; $T = T$. The following equations are obtained after integration where $n \neq 1$:

$$\frac{1 - (1-a)^{(1-n)}}{(1-n)T^2} = \frac{AR}{qE} (1 - \frac{2RT}{E)}) \exp(\frac{-E}{RT}) \tag{D.6}$$

Assuming that $\dfrac{2RT}{E} \ll 1$ and taking the natural logaritm of both sides, the below equation is obtained:

$$\ln \frac{1 - (1-a)^{(1-n)}}{(1-n)T^2} = \ln \frac{AR}{qE} - \frac{E}{RT} \tag{D.7}$$

Assuming that it is a first order reaction (n=1), integration of the equation (D.5) gives:

$$\ln \frac{-\ln(1-a)}{T^2} = \ln \frac{AR}{qE} - \frac{E}{RT} \tag{D.8}$$

From thermogravimetric analysis data, a values are found and put into equations above. Using the equation (D.8) $\ln \dfrac{-\ln(1-a)}{T^2}$ versus $\dfrac{1}{T}$ graph gives a straight line. The slope and intercept of this line are equal to $\dfrac{-E}{R}$ and $\ln \dfrac{AR}{qE}$, respectively. From this data, E (activation energy) and A (preexponential factor) values are calculated.

D.1 STA Loaded MCM-41 (pH=1.4) Catalyst

The activation energy graph of STA loaded MCM-41 sample with a pH value of 1.4 for the polyethylene degradation reaction was given in Figure D.1.
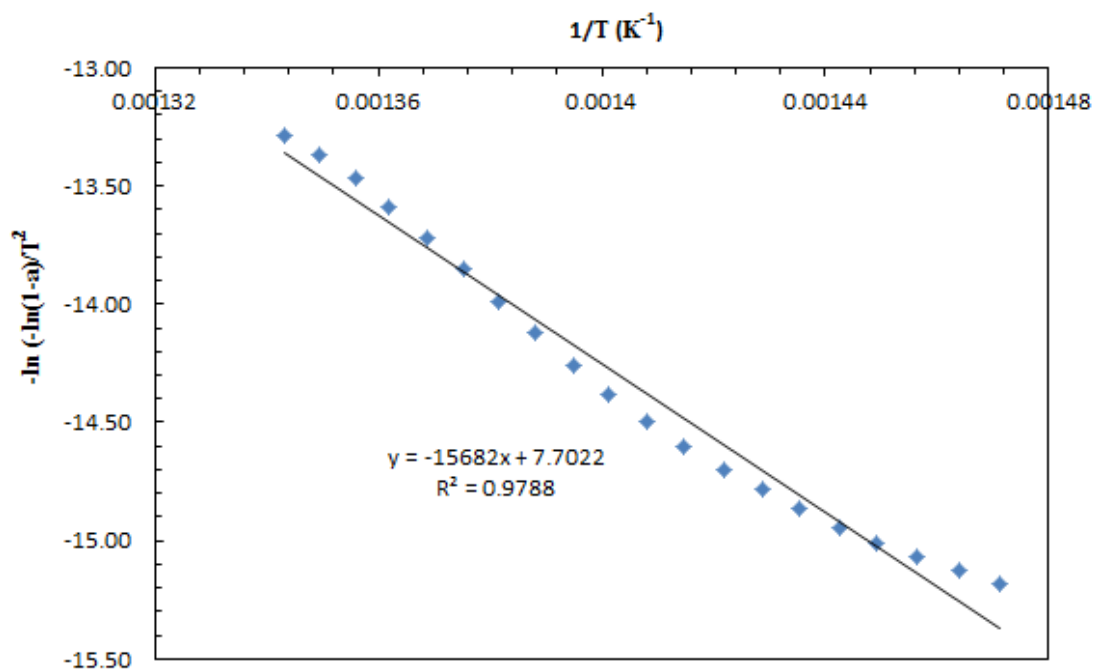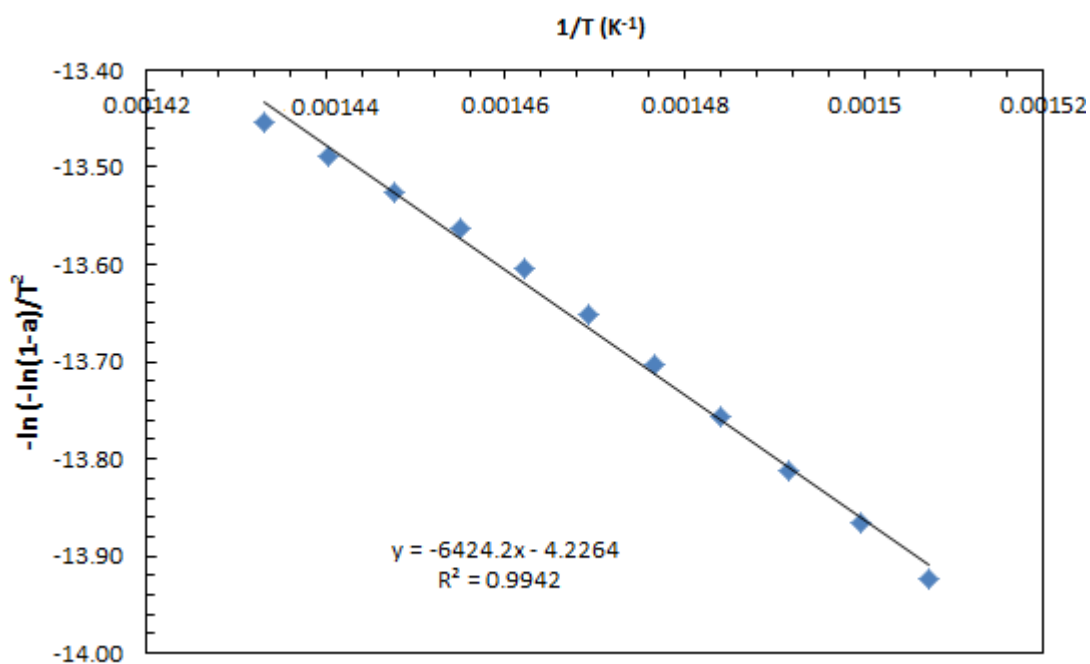

Figure D.1 Activation energy graph of STA loaded MCM-41 catalyst (pH=1.4)

➢ Calculation of activation energy:

$\ln(-\ln(1-a)/T^2)$ vs. 1/T graph,
Slope =-E/R,
slope=-15682, R=8.314 J/mole

E=-slope*R
E=15682*8.314=130380 J/mol=130 kJ/mol

D.2 STA Loaded MCM-41 (pH=1.2) Catalyst

The activation energy graph of STA loaded MCM-41 sample with a pH value of 1.2 for the polyethylene degradation reaction was given in Figure D.2.

Figure D.2 Activation energy graph of STA loaded MCM-41 catalyst (pH=1.2)

➢ Calculation of activation energy:

$\ln(-\ln(1-a)/T^2)$ vs. 1/T graph,
Slope =-E/R,
slope=-6424.2, R=8.314 J/mole

E=-slope*R
E=6424.2*8.314
E=53411 J/mol=53.4 kJ/mol

D.3 STA Loaded SBA-15 Catalyst

The activation energy graph of STA loaded SBA-15 sample for the polyethylene degradation reaction was given in Figure D.3.
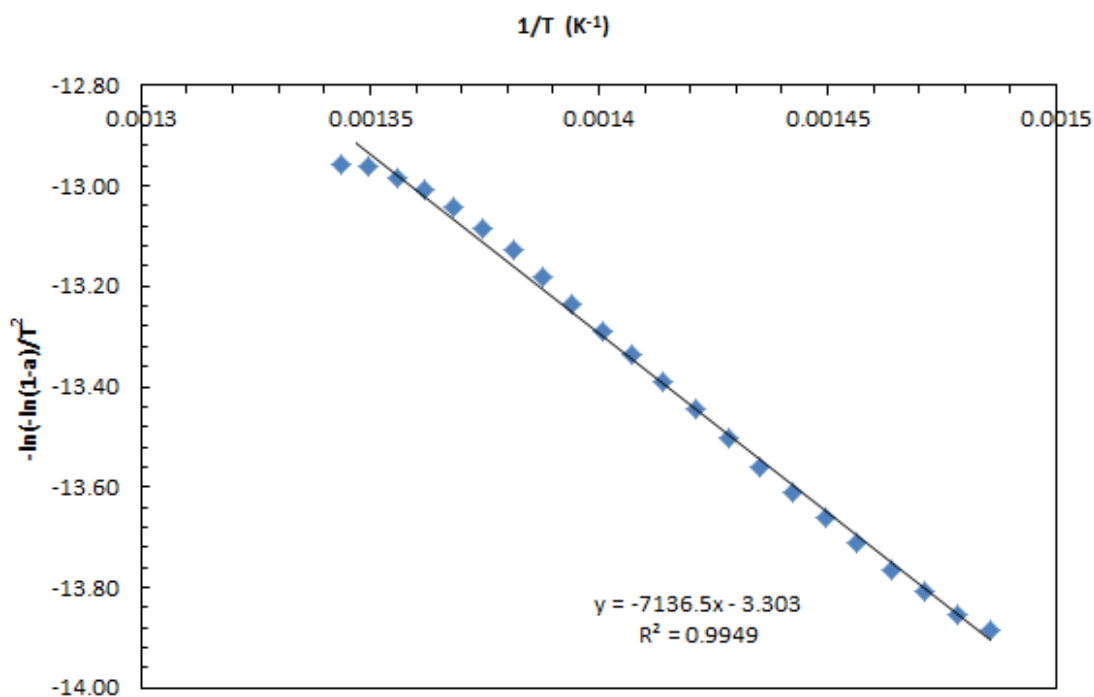

Figure D.3 Activation energy graph of STA loaded SBA-15 catalyst

➢ Calculation of activation energy:

$\ln(-\ln(1-a)/T^2)$ vs. $1/T$ graph,
Slope $=-E/R$,
slope$=-7136.5$, R$=8.314$ J/mole

E$=-$slope*R
E$=7136.5*8.314$
E$=59332$ J/mol$=59.3$ kJ/mol

D.4 Pure Polyethylene

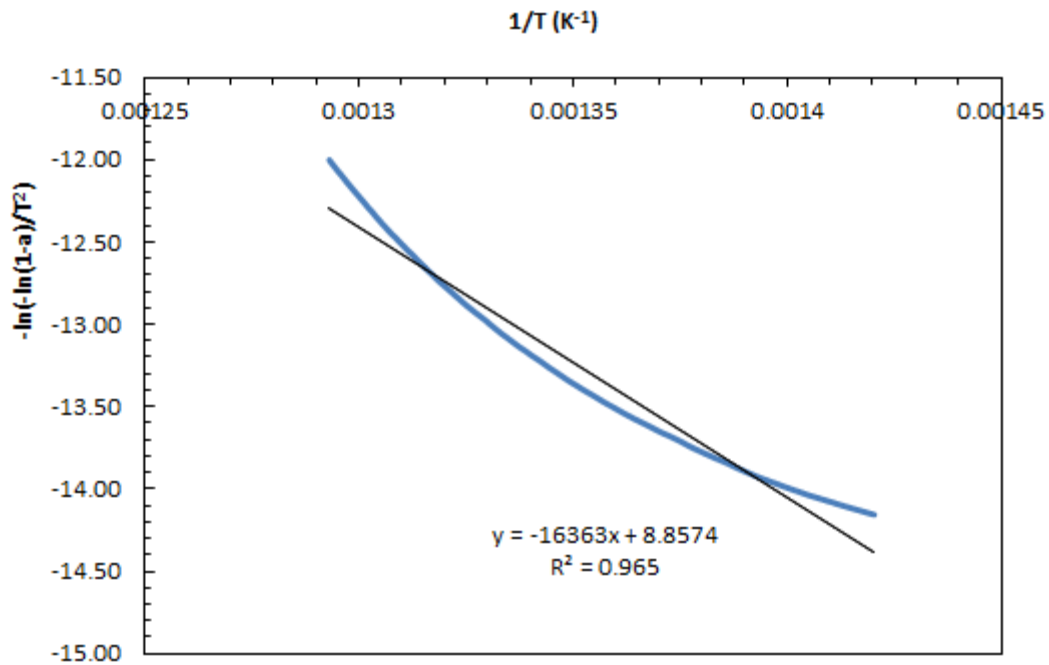The activation energy graph of pure polyethylene was given in Figure D.4.

Figure D.4 Activation energy graph of pure polyethylene

➢ Calculation of activation energy:

$\ln(-\ln(1-a)/T^2)$ vs. 1/T graph,
Slope =-E/R,
slope=-16363, R=8.314 J/mole

E=-slope*R
E=16363*8.314
E=136041 J/mol=136 kJ/mol